PhD degree in Molecular Medicine (curriculum in Molecular Oncology)

European School of Molecular Medicine (SEMM),

University of Milan and University of Naples "Federico II"

Settore disciplinare: Bio/11

RAB5A in the control of mammary epithelial morphogenesis and motility

Chiara Malinverno

IFOM, Milan

Matricola n. R09375

Supervisor: Prof. Giorgio Scita

IFOM, Milan

Anno accademico 2013/2014

To my beloved family.

TABLE OF CONTENTS

LIST OF ABBREVIATIONS

2D	bi-dimensional
3D	three-dimensional
ADP	adenosine diphosphate
AJs	adherens junctions
AKT (PKB)	protein kinase B
AMT	amoeboid to mesenchymal transition
AP2	adaptor protein 2
AREG	amphiregulin
ARF6	ADP-ribosylation factor 6
Avl	avalanche
BIM	BH3-only protein
BSA	bovine serum albumin
c-Met (HFGR)	hepatocyte growth factor receptor
CAT	collective to amoeboid transition
CDC42	cell division control protein 42
ChiP	chromatin immunoprecipitation
CIP4	CDC42-Intercatin Protein 4
CIV	cell image velocimetry
CLICs	clathrin- and dynamin-independent carriers
CME	clathrin mediated endocytosis
CTGF	connective tissue growth factor
DCIS	ductal carcinoma in situ
DIC	differential interference contrast
DMSO	dimethyl sulfoxide
DOX	doxycycline
DPPIV	dipeptidylpeptidase 4

ECL	enhanced chemiluminescence
ECM	extracellular matrix
EEA-1	early endosome antigen 1
EECs	endocytic/exocytic cycles
EGF	epidermal growth factor
EGFR	epidermal growth factor receptor
EMT	epithelial to mesenchymal transion
ER	estrogen receptor
ErbB (HER)	human epidermal growth factor receptor
ERE	estrogen responsive element
ESCRT	endosomal sorting complex required for transport
EV	empty vector
F-BAR	FCH-Bin-Amphiphy-sin-Rvs
FAK	focal adhesion kinase
FAs	focal adhesions
FBP17	formin-binding protein 17
FITC	fluorescein isothiocyanate
FRET	fluorescence resonance energy transfer
GAP	GTPase activating protein
GAPDH	glyceraldehyde-3-phosphate dehydrogenase
GDF	GDI dissociation factor
GDI	GDP dissociation inhibitor
GDP	guanosine diphosphate
GEF	guanine-nucleotide exchange factor
GFP	green fluorescent protein
GGT	geranylgeranyl transferase
GPCRs	G-protein coupled receptors
GTP	guanosine triphosphate
GTPases	guanosine triphosphatase
HGF	hepatocyte growth factor
HIF-2α	hypoxia inducible factor 2 α
HRE	hypoxia responsive element
IB	immunoblot
IC	invasive carcinoma
IDC	invasive ductal carcinoma

IF	immunofluorescence
IgG	immunoglobulin G
IL-2R-β	interleukine-2 receptor β chain
IL6	interleukin 6
JAK	Janus Kinase
JNK	c-Jun NH(2)-terminal kinase
LATS1/2	large tumor suppressor kinase 1/2
LKB1 (PAR4)	partitioning defective protein 4
MAPK	mitogen-activated protein kinase
MAT	mesenchymal to amoeboid transition
MEK1 (MAPKK1)	mitogen-activated protein kinase kinase 1
MHC I	class I major histocompatibility complex molecules
MOB1A/1B	mps one binder 1a/1b
MST1	mammalian Ste20-like kinase 1
MT1-MMP	membrane type 1-matrix metalloproteinase
mTOR	mammalian target of rapamycin
MTT	3-(4,5-dimethylthiazol-2-yl)-2,5-diphenyltetrazolium bromide
MVBs	multivesicular bodies
NCE	non-clathrin mediated endocytosis
NCi	negative control RNAi
Neo	neomycin
nTSG	neoplastic tumor suppressor genes
P	phosphorylated
PBS	phosphate-buffered saline
PDGF	platelet derived growth factor
PFA	paraformaldehyde
PI	propidium iodide
PI(3)Ks	phosphatidylinositol-3-OH kinases
PIV	particle image velocimetry
PLCγ	phospholipase Cγ
PM	plasma membrane
PMA	phorbol 12-myristate 13-acetate
PR	progesteron receptor
PS	phosphatidylserine

PtdIns(3)P	phosphatidylinositol-3-phosphate
Puro	puromycin
qRT-PCR	quantitative RT-PCR
RAB	Ras-related in brain
Rb	retinoblastoma protein
REP	RAB escort protein
rHGF	recombinant HGF
RhoA	Ras homolog gene family, member A
RNAi	RNA interference
ROCK	Rho-associated protein kinase
ROI	region of interest
RTKs	receptor tyrosine kinases
SAV	Salvador
SDS	sodium dodecyl sulfate
SEM	standard error mean
siRNAs	small interfering RNAs
SMA	smooth muscle actin
STAT	signal transducer activator of transcription
TACE (ADAM17)	TNFa converting enzime
TAZ	transcriptional co-activator with PDZ-binding motif
TBS	Tris-buffered saline
TGFβ1	transforming growth factor β 1
TJs	tight junctions
TNF	tumor necrosis factor
TOCA1	transducer of CDC42-dependent actin assembly 1
TRITC	tetramethylrhodamine
uPA	urokinase-type plasminogen activator
uPAR	urokinase-type plasminogen activator receptor
Upd	Unpaired
VEC	vascular endothelial cadherin
WT	wild type
YAP	yes associated protein

FIGURES INDEX

ABSTRACT

Endocytosis has been originally considered as a fundamental mechanism involved in the internalization of nutrients and membrane-bound molecules into the cell. However, recent studies demonstrate that endocytosis is a more complex network that regulates the delivery of specific time- and space-resolved signals to the cell.

The small GTPase RAB5A, a master regulator of endocytosis, is emerging as a key player in tumor progression and metastatic dissemination. Consistently, the expression of RAB5A has been shown to promote a tumor mesenchymal invasive program and to correlate with the metastatic potential of different tumors. In *Drosophila*, however, loss-of-function mutant of RAB5 transforms imaginal disc epithelia into highly proliferative tissues, pointing to a tumor suppressor function of RAB5.

To dissect the complex role of this GTPase in tumor development, we investigated the impact of RAB5A deregulation on MCF-10A, an immortalized non-transformed mammary epithelial cell line that forms hollow acinar-like spheroids recapitulating the morphogenesis of the human mammary gland, when cultured on 3D reconstituted basement membrane.

We generated stable and inducible MCF-10A cells expressing either RAB5A WT or its dominant negative form (RAB5AS34N). We found that the expression of RAB5AS34N is sufficient to sustain MCF-10A cells proliferation in the absence of EGF. We identified Amphiregulin, a known EGFR ligand, as the secreted diffusible factor responsible for EGF-independent proliferation. Conversely, the expression of RAB5A WT delayed cell

cycle progression of cells grown in 2D, albeit it promoted the formation of hyper-proliferative acini when these cells were grown in 3D, without affecting acini morphological architecture or polarity establishment. Thus, RAB5A may either be implicated in growth factor independent growth, or may promote proliferation in 3D.

Both clinical data and *in vitro* studies showed that RAB5A is required for invasion and metastasis formation, suggesting its involvement in tumor progression. In particular, the overexpression of RAB5A has been shown to be predictive of aggressive behavior and metastatic ability in human breast cancer. To further explore this function, we investigated the role of RAB5A in MCF-10A cells motility. We demonstrated that RAB5A expression does not affect single cell migration, but specifically enhances collective locomotion, the typical motility mode frequently observed in invasive cancer of epithelial origin, such as breast carcinoma. Indeed, RAB5A expression promotes increased speed and coordination of the epithelial cell sheet motility, related both to the increase in the area and persistence of migratory protrusions in cells at the leading front, and possibly to a tightening of cell-to-cell contacts, which improves cohesiveness of the migrating epithelial sheet.

In conclusion, our data suggest a temporally distinct dual role of RAB5A in tumor development. On one hand, RAB5A may exploit a tumor suppressor function controlling epithelial tissue morphogenesis and homeostasis, which impairment may induce tumor initiation. On the other hand, RAB5A promotes not only a mesenchymal program of individual cell invasion, as previously shown by our group, but also it enhances coordinated collective epithelial migration, thus promoting cancer progression and dissemination.

INTRODUCTION

1. The endocytic network.

1.1 Endocytic pathways.

Endocytosis has traditionally been regarded as a mechanism exploited by the cell to internalize nutrients and membrane-bound proteins. However, emerging recent evidences point to the notion that the function of endocytosis goes well beyond this canonical view. Indeed, endocytic networks are better described as a highly interconnected infrastructure of various cellular circuitries that is essential for the execution of different cellular programs (Scita and Di Fiore 2010). In general, signaling outputs are rendered interpretable to the cell by the resolution of the signal, in space and time, executed through endocytosis and membrane trafficking (Sorkin and von Zastrow 2009; Scita and Di Fiore 2010; Sigismund, Confalonieri et al. 2012). Accordingly, activated membrane receptors are internalized and transported as cargoes onto endocytic vesicles. Receptor-loaded endosomes may act either as specialized and spatially confined signaling hubs, or as a sorting station for the subsequent recycling of cargos back to the plasma membrane (PM) to initiate a new round of signaling or for directing cargos to lysosomal degradation to extinguish signals (Sorkin and von Zastrow 2009; Scita and Di Fiore 2010; Sigismund, Confalonieri et al. 2012). This process ensures control over signal duration, intensity, and ultimately has a major impact on biological outputs. This concept is summarized by the term “endocytic matrix”, which

was coined a few years ago to indicate the pervasiveness of endocytic control over virtually every aspect of the life of a cell (Scita and Di Fiore 2010). In this framework, it is not surprising that cell migration and invasion might exploit the diffuse interconnectivity of the "matrix" to execute part of its program, with particular regard to the ability of a cell to perceive, transduce and adapt to soluble cues as well as spatial information, ultimately affecting cell polarity, motility and invasiveness.

In the course of more than 3 decades of studying membrane trafficking, a very large number of critical molecular determinants have come into view, betraying the complexity of the process and its pervasive nature as a "hidden matrix" at the core of the cell blueprint. Among these players, the RAB (Ras-related in brain) family of small GTPases (guanosine triphosphatase) exerts a fundamental role by orchestrating virtually every aspect of vesicles trafficking. There are more than 63 members of this family in mammalian, constituting the more numerous group among small G proteins.

The complexity of the endocytic system starts at the plasma membrane, where cargos can be internalized through different entry portals, which can be categorized in two main categories: the clathrin mediated endocytosis (CME) and the non-clathrin mediated endocytosis (NCE), the former being by far the most widely investigated. The best-characterized CME pathway involves the internalization of a wide variety of transmembrane receptors and their ligands in clathrin-coated pits, mediated by the adaptor protein AP-2 that bridges cargos with clathrin in vesicle formation at the plasma membrane. Subsequent vesicle release from the plasma membrane into the cytoplasm is mediated by dynamin, a severing GTPase that promotes the scission of the invaginated pits from the PM to form a coated vesicle (Disanza, Frittoli et al. 2009; Sigismund, Confalonieri et al. 2012). This seemingly simple process is aided and optimally tuned and regulated by a vast *plethora* of endocytic adaptors, which help in sensing membrane curvature as well as in deforming the PM (Itoh, Erdmann et al. 2005). Furthermore, these

adaptor molecules link the invaginated membrane to the underlying actin cytoskeleton that is harnessed to produce sufficient forces to complete internalization (Yarar, Waterman-Storer et al. 2005), or form macromolecular complexes for the recruitment of cargos and accessory molecules not necessarily required in the early endocytic steps, but that will be exploited in the subsequent trafficking events (Scita and Di Fiore 2010).

NCE, on the other hand, includes all entry routes that are insensitive to inhibition of the CME pathway. Among the diverse NCE pathways, it is worth to mention: i) the caveolin-dependent endocytosis, characterized by the invagination of membrane fraction enriched in sphingolipids and cholesterol, coated with members of the caveolin protein family; ii) the RhoA (Ras homolog gene family, member A)-dependent pathway that mediates the internalization of interleukine-2 receptor β chain (IL-2R- β); iii) the ARF6 (Adenosine diphosphate-ribosylation factor 6)-mediated and dynamin-independent endocytosis of several protein such as β1 integrin and class I major histocompatibility complex molecules (MHC I); iv) whereas, fluid phase markers and bulk membranes enter the cells through tubular intermediates, the clathrin- and dynamin-independent carriers (CLICs). Lastly, phagocytosis, the common mechanism mediating pathogens or apoptotic cells elimination, and macropynocytosis for fluid uptake are processes that has been shown to be dependent on and triggered by actin remodeling of the plasma membrane, leading to the formation of large vesicles that internalize relatively large amount of plasma membrane (Mayor and Pagano 2007).

Internalized cargos, either by CME or NCE, are then routed to RAB5-positive early endosomes, which represent the first, nearly obligatory endosomal sorting station. From this compartment, cargos final destiny is decided. Cargo can, indeed, be directed to late endosomes/multivesicular bodies (MVBs), or recycled back to the plasma membrane through a variety of frequently ill-defined, but molecular distinct routes. In the former case, cargo can traffic to a RAB7-dependent lysosomal degradative route and are

subsequently targeted by ubiquitin to degradation in lysosome. In the latter case and in a simplified view, recycling may be executed either through a fast (RAB4-dependent) or a relatively slow (RAB8- and RAB11-dependent) routes (Disanza, Frittoli et al. 2009; Scita and Di Fiore 2010) (Fig.1).

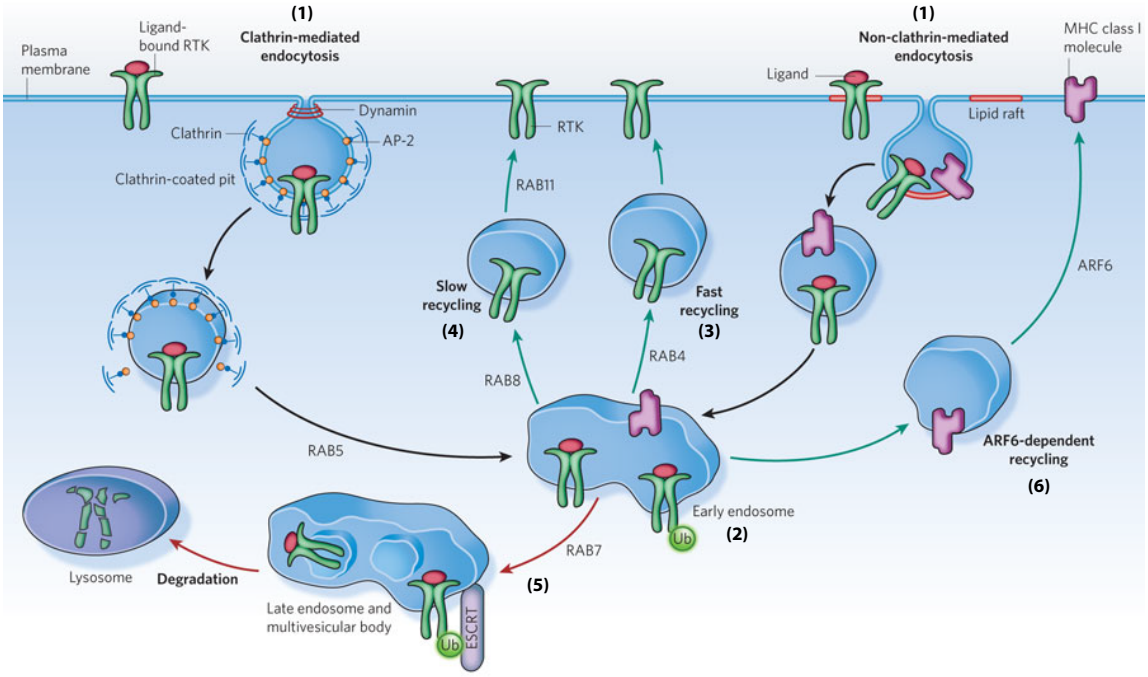

Figure 1. The endocytic circuitry of signaling receptors.

(1) Plasma membrane and ligand-bound receptors (for example RTKs, receptor tyrosine kinases) can be internalized through clathrin-mediated (CME) or non-clathrin-mediated (NCE) endocytosis. **(2)** After internalization, both routes converge into RAB5-positive early endosomes. **(3-4)** From this sorting station, cargos can be recycled to the plasma membrane through a fast (which depends on RAB4), or a slow (which depends on RAB8 and RAB11) recycling routes. **(5)** Alternatively, cargo can be targeted to a RAB7-mediated degradative route, *via* late endosomes and multivescicular bodies, before being degraded into lysosome. Ubiquitylation (ub) and endosomal sorting complex required for transport (ESCRT) play a crucial role in the degradative pathway. **(6)** In addition, cargos such as major histocompatibility complex class I molecules (MHC-I) or the interleukin receptors that do not enter through CME, can be redelivered back to the plasma membrane through ARF6-dependent pathways.
Adapted from (Scita and Di Fiore 2010).

1.2 The family of RAB GTPases.

RAB GTPases is the most numerous family of Ras-like small GTPases. These proteins are invariably found in all eukaryotes, demonstrating their fundamental role in the cell biology of complex organisms. More than 63 members have been identified in mammals, classified in subfamilies depending on the degree of conservation of specific sequence motifs (Zerial and McBride 2001).

The central role exerted by RAB family protein is highlighted by the observation that they have been shown to control each aspect of vesicular trafficking from vesicle biogenesis, fusion and maturation, to actin- or microtubule-dependent vesicle motility, tethering and fusion to the PM (Zerial and McBride 2001). Like all GTPases, they act as molecular switches, cycling between two different conformations, an "inactive" GDP (guanosine diphosphate)- and an "active" GTP (guanosine triphosphate)-bound form. The nucleotide-bound status determines not only their ability to transduce signals but also their location and activity (Stenmark, Parton et al. 1994; Stenmark and Olkkonen 2001; Zerial and McBride 2001). In the GTP-bound "active" conformation, they can recruit a vast set of specific downstream effector proteins, which are invariably necessary to carry out their trafficking functions. Importantly their site of action is confined to membrane organelles and consequently the ability to associate to the lipid bilayer is an essential built-in component in their regulation. As a consequence, RABs are variably post-translationally modified through the appendage of hydrophobic moiety, among which prenylation is key to direct them to various organelles, the identity of which is frequently dictated by the presence of different charge lipids, such as phosphoinositydes.

Newly synthetized RAB-GDP associates with RAB escort protein (REP) that directs it to geranylgeranyl transferase (GGT) and to its target membrane. The delivery of RAB to the membrane is catalyzed by the GDI dissociation factor (GDF) that catalyzes the release of RAB-GDP from the GDP dissociation inhibitor (GDI). The guanine-nucleotide exchange

factor (GEF) is essential to convert the inactive RAB-GDP into its active form GTP-bound, allowing subsequent interaction with specific effectors. RAB GTPase activity is then accelerated by the binding with GTPase activating protein (GAP), that enhance the intrinsic GTPase activity hydrolyzing GTP into GDP, which concomitantly shut off RAB activity, priming it for the subsequent cycle (Stenmark 2009) (Fig.2).

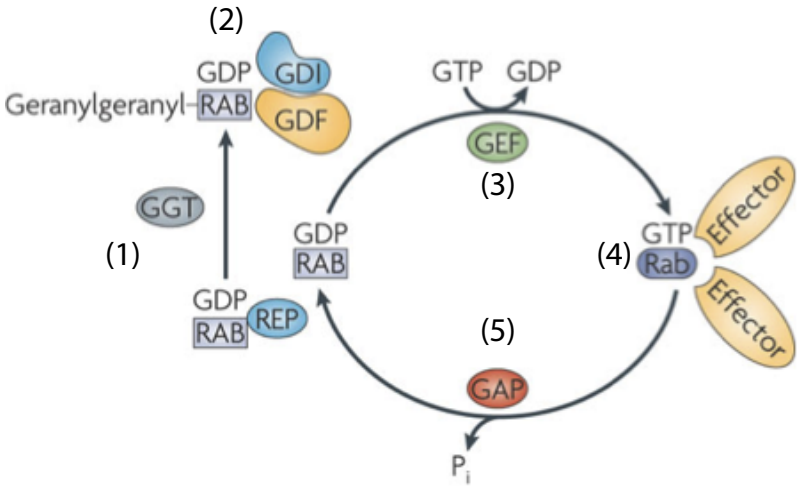

Figure 2. The RAB GTPase cycle.

(1) RAB-GDP interacts with RAB escort protein (REP) and the geranylgeranyl tranferase (GGT). **(2)** The GDI dissociation factor (GDF) promotes the dissociation of the geranylgeranyl-RAB-GDP from the GDP dissociation inhibitor (GDI)**. (3)** Conversion from the GDP to the GTP-bound active form of RAB is catalyzed by a guanine nucleotide exchange factor (GEF). **(4)** Then RAB-GTP can interact with its effector proteins. **(5)** Conversion from GTP- to GDP-bound form occurs by GTP hydrolysis, catalyzed by a GTPase activating protein (GAP). Pi, inorganic phosphate.
Adapted from (Stenmark 2009).

RAB GTPases function as specific regulators of intracellular trafficking and each transport step requires the recruitment of effector molecules that bind preferentially to the GTP-loaded active form of RABs. Indeed, like all small GTPases, the two nucleotide bound forms show evident conformational differences in the switch I and switch II regions, possessing higher affinity for effector targets in the GTP-bound conformation. Many different effectors have been identified and each pathway (vesicle formation, movement, tethering and fusion) has its unique set of effectors. Crosstalk between multiple RABs through common effectors or through the recruitment of RAB activators ensures a tightly

controlled regulation of vesicle trafficking. Spatiotemporal coordination of RABs functions is indeed ensured by diverse strategies based on positive feedback loops, effector coupling or activation coupling and RAB conversion (Stenmark 2009) (Fig.3).

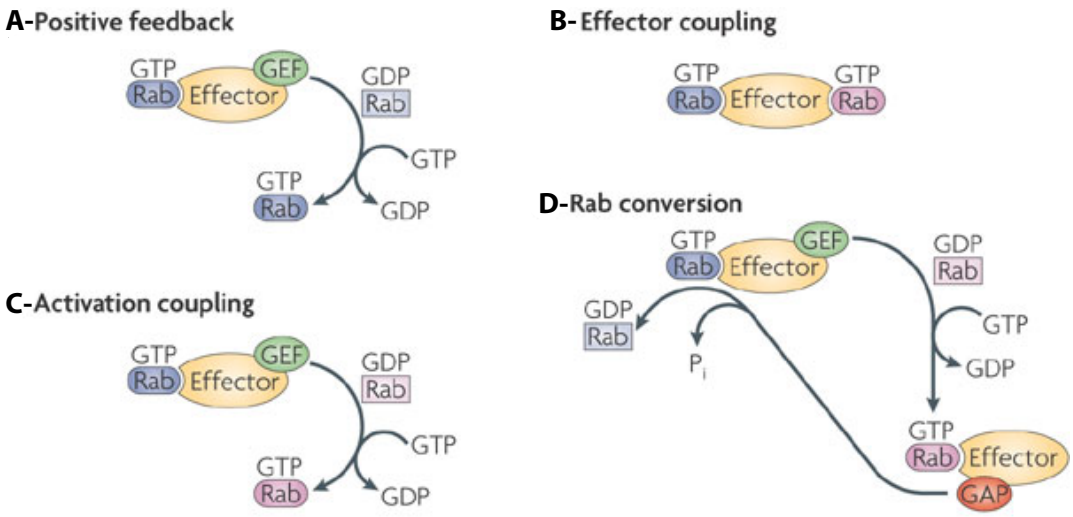

Figure 3. The coordination of RABs function.

(A) The RAB effector contains the specific GEF for the same RAB that has recruited the effector, generating a positive feedback loop. (**B)** The effector contains separate binding sites for two RABs, thus promoting the tethering between two micro-domains within the same vesicle, or membranes of two different compartments, such as Rabenosyn-5 coupling of RAB4 and RAB5. (**C)** The effector of the upstream RAB includes the GEF for the downstream one. (**D)** The effector complex activates through a GEF a second RAB which effector contains a GAP for the first RAB, generating a negative feedback loop. Pi, inorganic phosphate.
Adapted from (Stenmark 2009).

1.3 The role of RAB5 GTPases in endocytosis.

RAB5 subfamily of GTPase includes RAB5A, B and C, RAB21, RAB22A and RAB22B (also known as RAB31). Among them we focused our attention on RAB5 isoforms, a well-characterized set of master regulator of endocytosis, that show overlapping functions in the endocytic pathway.

Three RAB5 isoforms have been identified in mammals, named RAB5A, RAB5B and RAB5C, transcribed by 3 different genes and ubiquitously expressed (Bucci, Lutcke et al. 1995). More in detail, these proteins play an essential role in: i) the regulation of the initial

step of endocytosis, ii) promoting the biogenesis of early endosomes, iii) controlling homotypic fusion of these vesicles, their motility and subsequent maturation, ultimately iv) regulating the progression of intracellular trafficking. Such a variety of RAB5 functions is mediated by well defined sets of different interacting proteins and effectors (Stenmark, Vitale et al. 1995; Simonsen, Lippe et al. 1998; Christoforidis, McBride et al. 1999).

The machinery downstream of RAB5 has an extraordinary complexity and diverse studies show that RAB5 effectors function in a cooperative fashion. The first RAB5 effector identified was Rabaptin-5, a fundamental mediator of early endosome fusion which complexes with Rabex-5, a GEF of RAB5. Upon activation of RAB5, the Rabaptin-5–Rabex-5 complex induces its own membrane recruitment through Rabaptin-5, generating a positive-feedback loop that creates a membrane domain enriched in active RAB5. A second class of RAB5 effector are phosphatidylinositol-3-OH kinases (PI(3)Ks). Active RAB5 interacts with the hVPS34-p150 PI(3)K, coupling RAB5 localization to phosphatidylinositol-3-phosphate (PtdIns(3)P, PI3P) production. The concomitant presence of RAB5 and PtdIns(3)P allows the recruitment of the RAB5 effectors early endosome antigen 1 (EEA-1) and Rabenosyn-5, both involved in vesicles tethering (Zerial and McBride 2001). In particular, this latter RAB5 effector, Rabenosyn-5, shows two distinct binding sites for RAB5 and RAB4 and act as a linker between the two RABs proteins, thus promoting a physical connection of RAB5-mediated entry site and RAB4-recycling on early endosomes (Vitale, Rybin et al. 1998; Deneka and van der Sluijs 2002). Collectively, these mechanisms support the notion that RAB5 and its effectors cluster in membrane sub-compartments and their spatial segregation in well-defined membrane sub-domain favors their coordination and interaction in mediating RAB5 functions.

RAB5 shuttling between a GDP-inactive and a GTP-active form plays a fundamental role in the control of this complex network. Previous studies have identified RAB5-specific sets of GAPs and GEFs. Example of the latter are: Rabex-5, Rin1 and ALS2/Alsin, whereas the GAPs include RabGAP-5, RN-tre and p85α (the regulatory subunit of PI(3)K) (Zerial and

McBride 2001).

The essential role of RAB5 nucleotide state in membrane fusion was confirmed *in vitro* by the expression of mutants with altered GTPase activity. RAB5 Q79L, a mutant with a strong reduction in GTPase activity, enhances early endosome fusion and expands their size; conversely the GDP-locked RAB5 S34N mutant results in the accumulation of very small endocytic vesicles (Li and Stahl 1993; Stenmark, Parton et al. 1994). Furthermore, the key role of RAB5 in the assembly of the endosomal machinery has been confirmed by *in vivo* silencing of RAB5A, B and C, in mouse hepatocytes. Interestingly, no alteration in the expression of RAB5 effectors such as membrane tethering or fusion proteins was observed. Conversely, immunofluorescence and electron microscopy analysis showed a dramatic impairment in all the endo-lysosomal system, thus affecting the distribution of apical markers. Of note, alterations of all the endocytic compartments were achieved only upon loss of RAB5 below a specific threshold (Zeigerer, Gilleron et al. 2012).

1.4 The tumor suppressor function of RAB5: lessons from the fly.

Intracellular trafficking is a key process in cell proliferation control and in the establishment of epithelial cell polarity. Evidence in support of this latter contention has come from genetic studies in *Drosophila*, where only one highly conserved RAB5 GTPase gene is expressed. Indeed, early studies performed in this model system have shown that the genetic disruption of different endocytic stages perturbs both cell polarity and cell proliferation control leading to the formation of neoplastic tissues (Vaccari and Bilder 2005; Rodahl, Haglund et al. 2009). Among the identified endocytic neoplastic tumor suppressor genes (nTSG), RAB5 and some of its key effectors have been shown to play an essential role in the development of imaginal disc epithelium (Lu and Bilder 2005; Morrison, Dionne et al. 2008; Robinson and Moberg 2011). Loss-of-function mutants of

RAB5, for example, transform this epithelial tissue into a highly proliferative, invasive neoplastic mass that fails to terminally differentiate. At the molecular level, this neoplastic phenotype may be caused by alterations in a variety of different signaling pathways, affected by blockade of the endosomal function of RAB5. Among the pathways affected, loss of function of RAB5 was shown to lead to; i) disruption of polarity, as determined by alterations in the distribution of the key polarity determinant, Crumbs: ii) deregulation of cell proliferation through hyperactivation of Notch receptor (Lu and Bilder 2005); or iii) alterations of Yorkie (yes associated protein-YAP and transcriptional co-activator with PDZ-binding motif-TAZ, in vertebrates) and JNK (c-Jun NH(2)-terminal kinase) pathways, the latter already known to promote Yorkie (Yki) activity in cells with alteration in polarity (Robinson and Moberg 2011). More recent studies expanded these early findings and characterized in deeper details the mechanism leading to the RAB5-dependent neoplastic growth. It was shown that loss of RAB5 can sustain a non-cell autonomous overgrowth of the imaginal disc and surrounding tissues by accumulation of EGFR (epidermal growth factor receptor) and TNF (tumor necrosis factor) homolog Eiger, a soluble factor that activates JNK and Ras signaling pathways, which both participate inactivating the Hippo pathway and thus promoting Yorkie activity. The Hippo pathway is indeed, fundamental for the control of the co-transcription factor Yki, whose deregulation causes uncontrolled proliferation at the basis of the overgrown phenotype typically observed in the Hippo mutants. Notably, the molecular cascade at the basis of the control of Yki activity is highly conserved between *Drosophila* and mammals: and constituted by the following set of kinases: i) Warts (Lats1/2, large tumor suppressor kinase 1/2 in mammals) and the kinase Hippo (MST1/2, mammalian Ste20-like kinase 1/2 in mammals), which are brought into close spatial proximity by the scaffold protein Salvador (SAV1 in mammals) thereby promoting Hippo-kinase mediated phosphorylation of Warts. In addition, ii) Mats (MOB1A and MOB1B, Mps one binder 1a and 1b in mammals) can enhance the kinase activity of Warts that targets directly the transcriptional co-activator

Yki, preventing it from entering the nucleus. Impairment of the Hippo kinase cascade liberate Yki, which is no longer phosphorylated and free to translocate to the nucleus where it mediates the expression of a number of proliferation genes (Yu and Guan 2013). Among them, a key role was shown to be exerted by the growth factor Upd (unpaired), an homolog of IL6 (interleukin 6), which can fuel a positive feedback loop contributing to the loss of proliferation arrest of the imaginal disk tissue (Takino, Ohsawa et al. 2014).

Regardless of the mechanisms through which RAB5 interference may promote tissues overgrow, the experiments in *Drosophila* indicate that RAB5 is critical for the regulation of a diverse set of key pathways necessary for the maintenance of epithelial features and epithelial homeostasis (e.g. cell polarity, oncogene activity, YAP/TAZ-growth regulatory activity), and further point to a tumor suppressor function of RAB5

Notably, the role of RAB5 in controlling sorting and delivery of specific proteins involved in polarity establishment has also been confirmed in mouse hepatocytes *in vivo.* In this tissue, RNAi-mediated depletion of RAB5 causes not only the ablation of all the endolysosomal system, but also the alteration of the apical distribution of a subset of polarity proteins, such as the dipeptidylpeptidase 4 (DPPIV) (Zeigerer, Gilleron et al. 2012). Of note, reduction of the number of early and late endosomes, including lysosomes, was achieved only upon loss of RAB5 isoforms below a specific threshold. Furthermore, the entire endocytic pathway was completely rebuilt upon RAB5 recovery, thus confirming that the assembly of the endosomal machinery strictly requires RAB5 also *in vivo* (Zeigerer, Gilleron et al. 2012).

1.5 RAB5A promotes tumor progression in mammals.

In addition to a role in the control of early phases of tumor development, RAB5A is also emerging as a key player in tumor progression and metastatic dissemination (Lanzetti,

Palamidessi et al. 2004; Zhao, Liu et al. 2010; Torres and Stupack 2011).

A number of findings reported that the expression of RAB5A is elevated in human tumor cells and is sufficient to promote a mesenchymal mode of cell invasion in *in vitro* and *in vivo* model of cancer cell migration (Yu, Hui-chen et al. 1999; Torres, Mielgo et al. 2010; Liu, Chen et al. 2011; Torres and Stupack 2011; Onodera, Nam et al. 2012). Conversely individual ablation of the three human *RAB5* genes (*RAB5A/B/C*) has been shown to impair invasion and dissemination of different types of cancer cells (Yu, Hui-chen et al. 1999; Torres, Mielgo et al. 2010; Liu, Chen et al. 2011; Torres and Stupack 2011; Onodera, Nam et al. 2012). *In silico* meta-analysis of more than 900 breast cancer tumors revealed, for example, that among the RAB5 genes, RAB5A is overexpressed in breast cancers and its elevated expression positively correlates with poor prognosis. Moreover, the striking difference in RAB5A expression levels observed in human breast cancer was predictive of increased local and distant relapse in early stage estrogen breast cancer patients (Frittoli, Palamidessi et al. 2014). Most notably, immunohistochemical analysis of a panel of primary human breast cancers and their matched lymph node metastases showed that RAB5A expression is significantly higher in matched lymph node metastases, with respect to their primary tumors, consistent with the notion that RAB5A overexpression confers a migratory advantage to tumor cells (Frittoli, Palamidessi et al. 2014).

This latter possibility was experimentally verified combining the manipulation of RAB5 expression or function with a variety of in *vivo* and in *vitro* assays of cell invasion and metastatization on different triple negative breast cancer cell lines: MDA-MB-231 and MCF-10.DCIS.com cells, a tumorigenic derivative of normal human mammary epithelial MCF-10A cells that recapitulate features of the comedo-type ductal carcinoma *in situ* (DCIS) when injected subcutaneously into immunodeficient mice (Miller, Santner et al. 2000). Ablation of RAB5A, B and C or the expression of a RAB5A dominant negative (RAB5AS34N) impaired lymph node and lung dissemination of aggressive MDA-MB-231 cells injected into mammary fat pad without affecting the cell proliferation or survival

potential of the primary tumors. Furthermore, impairment of RAB5 function delayed the conversion of DCIS-to-IDC (invasive ductal carcinoma) of MCF10.DCIS.com xenograft model (Frittoli, Palamidessi et al. 2014), a process that requires digestion of the basement membrane and local invasion into collagenous stromal tissues (Hu, Yao et al. 2008). Conversely, the ectopic expression of RAB5A in poorly invasive HeLa cells injected heterotopically in the mammary fat pad enhanced distant lung metastatization as well as local intra-tumoral cell motility, as monitored by two-photon intravital imaging, thereby reinforcing the notion that RAB5A elevated expression may be sufficient to promote tumor dissemination.

The pro-metastatic function of RAB5A was further investigated through *in vivo* three-dimensional (3D) invasion assays. When stimulated with a potent motogenic factor, such as Hepatocyte Growth Factor (HGF), RAB5A-expressing cells extensively remodeled the collagen fibers to generate physical gaps and channels through which cells could meander in a process strictly depended on metalloprotease activity (Frittoli, Palamidessi et al. 2014). Furthermore, RAB5A elevation was shown to be sufficient to trigger the onset of invadopodia and to endow poorly degradative cells with the ability to digest ECM. On the contrary, the impairment of RAB5 expression in invasive squamous cell carcinoma that efficiently forms degradative invadopodia in the absence of motogenic factors, had negligible effects. These observations suggest that RAB5A is necessary and sufficient for the formation of these invasive structures following modulation with growth factors, which also promote a polarized migratory phenotype (Frittoli, Palamidessi et al. 2014). Under these conditions, cell signaling and trafficking pathways are activated, and membrane bound cargos undergoes polarized endo/exocytic cycles that are key to spatially restrict their activity contributing to the execution of polarized functions (Scita and Di Fiore 2010). Not surprisingly, the formation of degradative invadopodia induced either by HGF stimulation or RAB5A expression requires the expression of MT1-MMP (membrane type 1-matrix metalloproteinase), which is rapidly re-localization from early endosomes to

ventrally restricted, F-actin-rich structures in response to HGF stimulation in a RAB4 and RAB5-dependent fashion (Frittoli, Palamidessi et al. 2014).

A molecular genetic approach based on the interference with the major internalization and recycling routes unveiled the essential circuitry for MT1-MMP plasma membrane delivery. The interference with RAB4A and RAB4B, or their effector Rabenosyn-5, robustly reduced matrix degradation, indicating that the RAB5-Rabenosyn-5-RAB4A circuitry is a major route for the fast delivery of MT1-MMP to the PM in response to motogenic stimulation (Frittoli, Palamidessi et al. 2014). MT1-MMP and RAB4 were indeed co-localized on recycling endosomes that transiently and dynamically contact invadopodia along the ventral membrane. Consistent with this possibility, HGF in addition to enhance matrix degradation also promotes the acute activation of RAB5A, likely favoring the subsequent recruitment of the Rabenosyn-5-RAB4 complex onto early endosomal microdomains for recycling of MT1-MMP. Notably, the RAB5A-Rabenosyn-5-RAB4A pathway may also serve as trafficking route for cell-adhesion molecules that in addition to actin and MT1-MMP are required for the formation of fully functional invadopodia. One of the major integrins shown to be required for invadopodia formation, integrin αVβ3, primarly utilizes the RAB4 trafficking route to recycle efficiently in response to stimulation with Platelet Derived Growth Factor (PDGF) (Roberts, Barry et al. 2001; Roberts, Woods et al. 2003). Accordingly, it was found an absolute requirement for αVβ3, but not β1-containing integrins for the formation of RAB5A and HGF-induced invadopodia. Our lab further provided evidence that, as previously shown, αVβ3 utilizes RAB4 routes, like MT1-MMP, suggesting that the two proteins may be co-trafficked for efficient delivery to invadopodia.

Collectively, this set of findings and previously published data (Palamidessi, Frittoli et al. 2008) support a model in which RAB5 couples elongated protrusions with pericellular proteolysis by controlling RAB4-dependent fast recycling of MT1-MMP and β3 integrin cargos to enable efficient invasion. The relevance of this model was verified in breast

cancer lines, whose ability to invade collagen gels was impaired not only by silencing RAB5 and MT1-MMP, but also of RAB4 or β3 integrin (Frittoli, Palamidessi et al. 2014). Additionally, RAB4 interference, and likewise RAB5 silencing, delayed the conversion of MCF10DCIS.com cells from DCIS-to-IDC in *in vivo* mouse models. The observations that RAB4A is amplified in more than 14% of invasive breast cancers and upregulated in breast tumors lend further support to the notion that the RAB5/RAB4A circuitry is specifically selected in human tumors and may contribute to their invasive metalloprotease-dependent phenotype (Fig.4).

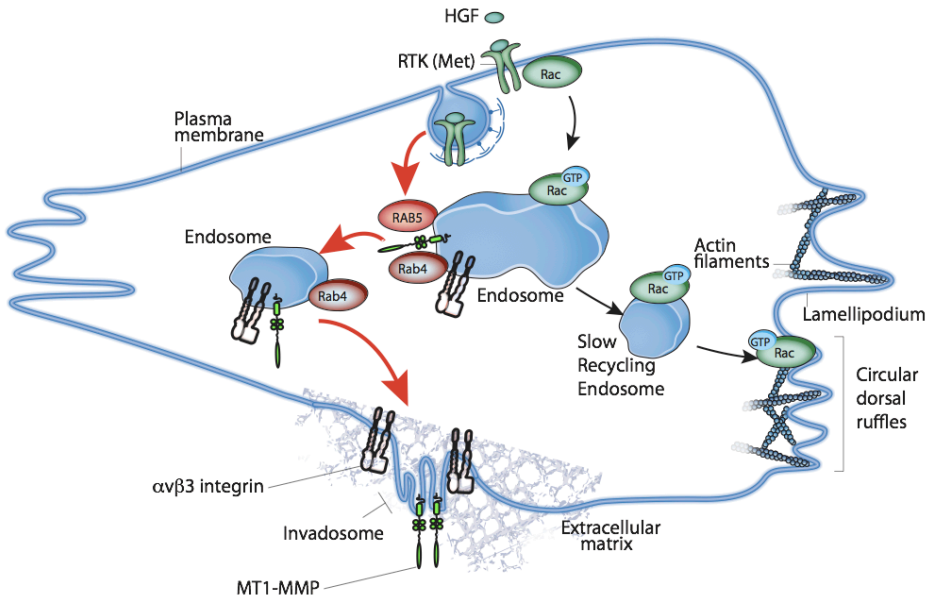

Figure 4. RAB5A promotes a proteolytic/mesenchymal invasive program.

In response to the motogenic stimuli of hepatocyte growth factor (HGF), Met receptor is internalized by clathrin- and RAB5-mediated endocytosis. RAB5A promotes the formation of endosomes containing RAC1 and its GEF, ensuring RAC1 activation and recycling to specific regions of the plasma membrane, where actin remodeling occur and migratory protrusion are then formed. The RAB5/RAB4 trafficking circuitry re-directs αvβ3 integrin and MT1-MMP to invadosomes, leading to the formation of invasive structures and matrix remodeling.
Adapted from (Frittoli, Palamidessi et al. 2014).

In keeping with a general role of RAB5 in tumor progression, RAB5A expression was also found to be elevated in ovarian cancer (Zhao, Liu et al. 2010), to be associated with the metastatic potential of human lung (Yu, Hui-chen et al. 1999) and gastric cancer (Li, Feng et al. 1999), as well as with increased migration of hepatocellular carcinomas (Fukui,

Tamura et al. 2007) and with lymph nodes metastasis in breast cancer patients (Yang, Yin et al. 2011).

Collectively, these evidences support the notion that RAB5A promotes a mesenchymal program of tumor dissemination.

2. MCF-10A cells as a model to clarify RAB5A role in tumorigenesis and tumor progression.

2.1 Modeling the development of the human mammary gland *in vitro.*

The tumor suppressor activity of RAB5 in *Drosophila* contrasts with its pro-metastatic function in advanced human cancer. One way to reconcile these apparently contradictory observations is to posit that RAB5 may exert a dual, temporally distinct function in the process of tumor development: it may act as suppressor of tumor initiation, in the early phase of tumor development, but become a promoter of metastatic phenotypes in late advance staged of tumor progression. In an attempt to rationalize these functions and dissect the underlying molecular pathways, we decided to carry out our investigation by either interfering with or overexpressing RAB5A in a normal, mammary epithelial cell line that recapitulate a number of features of mammary epithelium, including the ability to undergo a morphogenetic processes resembling gland development, *in vitro*.

MCF-10A, a normal non-transformed human mammary epithelial cell line, was derived from spontaneous immortalization of cells obtained from subcutaneous mastectomy of a 37 year old breast with benign fibrocystic disease (Soule, Maloney et al. 1990). Notably, this cell line retains the typical features of a normal breast epithelium: i) their proliferation and

survival depend on exogenously added growth factors and hormones; ii) it displays anchorage dependent growth properties; and iii) it is unable to form tumor when injected into nude mice (Soule, Maloney et al. 1990). iv) Finally, MCF-10A cells can grown in three dimensions, where they can give rise to acinar-like spheroids with an hollow lumen, apicobasal polarization and basal deposition of basement membrane components (laminin V and collagen IV), thus recapitulating the morphogenetic program of mammary gland formation (Fig. 5).

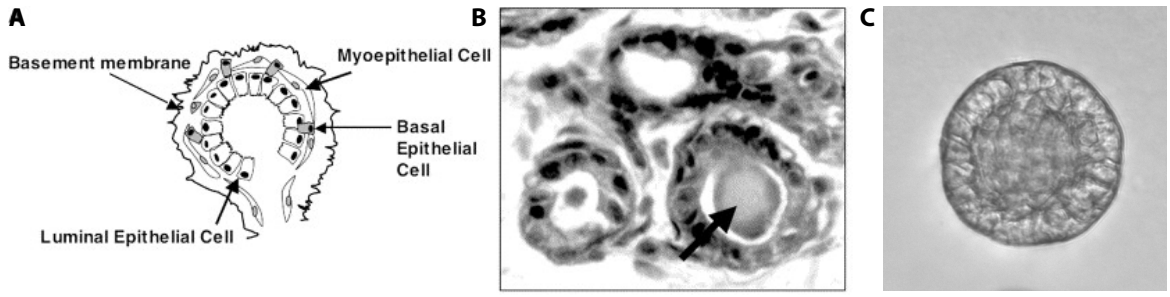

Figure 5. The morphological architecture of *in vitro* MCF-10A 3D acini resembles the structure of human mammary gland lobule *in vivo*.

(A) Schematic of the human mammary gland lobule: a hollow lumen is surrounded by an inner monolayer of polarized luminal epithelia cells and an outer monolayer composed of basal epithelial and myoepithelial cells. **(B)** Tissue section of acini *in vivo*, stained with hematoxylin and eosin. The arrow indicates accumulation of proteinaceous secretory material **(C)** Phase-contrast image of a MCF-10A acinar structure cultured on reconstituted basement membrane for 14 days, *in vitro*. The general architecture is similar to that observed *in vivo.* The hollow lumen is surrounded by polarized epithelial cells that deposit basement membrane components.
Adapted from (Debnath, Muthuswamy et al. 2003)

2.2 MCF-10A acinar morphogenesis in 3D culture.

The importance of the extracellular matrix in the regulation of growth and differentiation of normal mammary epithelial cells was first shown in rodent models and further confirmed in primary human mammary epithelial cells (Petersen, Ronnov-Jessen et

al. 1992). The maturation of *in vitro* 3D acini is characterized by the alternation of key cellular processes that are rigorously temporally regulated. MCF-10A cells cultured on reconstituted basement membrane initially proliferate creating a disorganized cluster of cells. The subsequent establishment of polarity is accompanied by the deposition of basement membrane proteins (laminin V and collagen IV) and the definition of specific subpopulation of cells. The inner population of cells loose contact with the extracellular matrix and die by anoikis, leading to the clearance of the lumen. Once a luminal hollow structure is formed, these structures stop proliferating. Around day 14, a growth-arrested and terminally differentiated acinar structure is formed, recapitulating the morphology of mammary gland lobule *in vivo* (Debnath, Mills et al. 2002; Debnath, Muthuswamy et al. 2003) (Fig. 6).

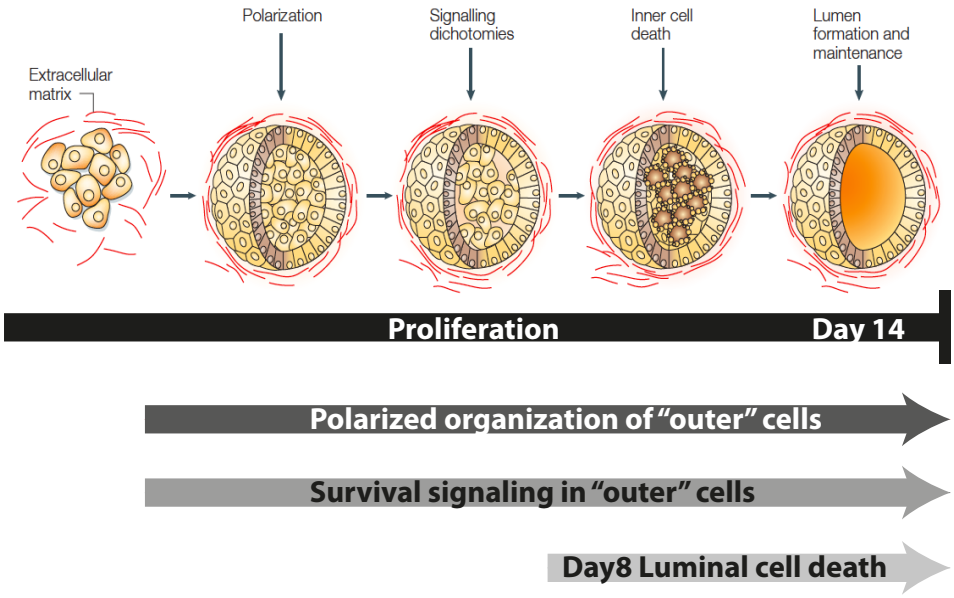

Figure 6. Schematic of biological events during MCF-10A 3D acinar morphogenesis.

MCF-10A cells follow a reproducible morphogenetic program when cultured on reconstituted basement membrane (Matrigel). During the early stages, single cells proliferate to form a cellular cluster, which starts to develop an apicobasal polarity. At day 5-8, two distinct populations of cells become evident: an outer layer in direct contact with the matrix where Akt (also known as protein kinase B or PKB) signaling pathway transduce a survival signal, and an inner subset of cells poorly polarized that loose contact with the matrix and lack Akt activation. Starting at day 8, the centrally located cells begin to die by anoikis and contributes to the formation of the hollow lumen observed in a terminally differentiated, not-proliferating acini (day 14). Adapted from (Debnath and Brugge 2005).

2.3 Three-dimensional culture of MCF-10A cells reveals oncogene-induced alteration of mammary architecture.

A caveat in monolayer cell culture is the artificial and non-physiological two-dimensional organization of cells. Moreover, traditional assays investigate cellular processes associated with tumor initiation and progression without considering critical architectural alteration of the mammary gland involved in cancer development. Conversely, differently from cells monolayers, the development of three-dimensional culture on reconstituted extracellular matrix provides the optimal system to dissect the emerging role of the matrix microenvironment in the process of morphogenesis, and tumorigenesis and to unmask neoplastic phenotypes, not distinguishable in normal culture condition (Li, Aggeler et al. 1987; Petersen, Ronnov-Jessen et al. 1992; Weaver, Howlett et al. 1995; Bissell, Rizki et al. 2003).

Three-dimensional culture of mammary epithelial cells indeed allows us to examine how the interplay between cell proliferation, cell death, and differentiation influence the structure and function of glandular epithelium, both in the normal state and during oncogene-induced early tumor formation (Spancake, Anderson et al. 1999; Herr, Wohrle et al. 2011). It has already been shown that oncogene induced transformation may affect different signaling pathways that impinge on MCF-10A acinar morphogenesis and maturation, and may cause: i) increased acinar size due to a bypass of the proliferation arrest typically observed in fully matured hollow acini; ii) block or delay of luminal clearance due to defective control over luminal localized cell death (Shaw, Wrobel et al. 2004). For example, acini expressing human papillomavirus E7 or high level of cyclin D1, both of which promote cell cycle progression by inactivation of the retinoblastoma protein (Rb), show a normal morphology but increased size caused by scheduled, excessive proliferation (Debnath, Mills et al. 2002). However, proliferating cells lacking direct contact with the matrix are nearly invariably eliminated by apoptosis and acini retain a

hollow lumen. Instead, the activation of ErbB2 oncoprotein leads to the formation of multiacinar structures with a filled lumen, a more severe phenotypic alteration characterized by the combination of hyper-proliferation, resistance to apoptosis, and a striking loss of epithelial polarity (Muthuswamy, Li et al. 2001; Debnath, Muthuswamy et al. 2003) (Fig.7).

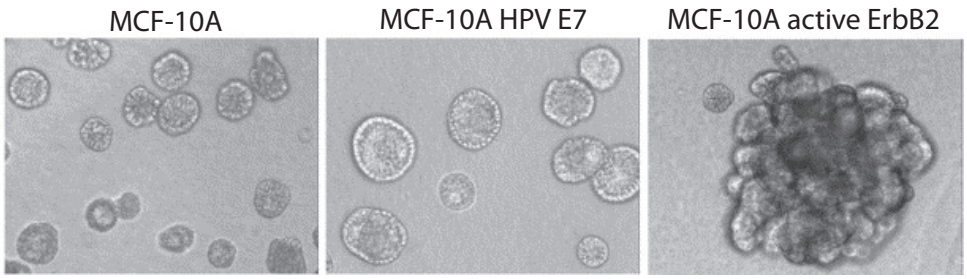

Figure 7. Oncogene expression differently affects MCF-10A acini morphogenesis and architecture.

Normal 3D architecture of acini seeded on Matrigel is shown on the left. The expression of the human papillomavirus E7 induces a hyper-proliferative phenotype and the formation of acini 30% bigger in size, without any alteration in the general architecture of acinar structures that retain hollow lumen and a correct apico-basal polarity (middle panel). Activation of ErbB2 oncoprotein during acinar morphogenesis elicits a complex multiacinar structure with filled lumen (on the right).
Adapted from (Debnath, Muthuswamy et al. 2003)

Three-dimensional culture represents, indeed, a powerful tool to investigate the effects of oncogenic stimuli that induces uncontrolled proliferation, resistance to apoptosis, loss of cell polarity and the acquisition of invasive properties, typical hallmarks of aggressive cancer phenotype.

3. Deregulation of the endocytic pathway alters different aspects of acinar morphogenesis.

3.1 Alteration of epithelial integrity and architecture synergize with oncogenes in promoting invasive phenotype.

So far, most of the studies on MCF-10A cells have investigated the effect of breast cancer-related oncogene expressed in the entire cell population, since the beginning of the morphogenetic process. Under these conditions, abnormal acinar growth and development is frequently observed reflecting only in part oncogenic alterations seen in human breast cancer. However, carcinomas typically derive from single mutated cell in a context of differentiated, normal epithelium that exerts a tumor suppressive function (Leung and Brugge 2012). This prompted us to focus the attention on the effects of oncogenes in later stages of acinar morphogenesis and homeostasis and on the importance of tissue architecture and integrity in the control of oncogene driven phenotypes.

Within this context, for example, it has been shown that concomitant perturbation of cell-matrix adhesion by MMPs and induction of c-Myc is sufficient to trigger cell translocation and luminal expansion in 3D acinar structures (Leung and Brugge 2012). A similar phenotype was observed in mature acini interfered for p120-catenin: the destabilization of cell-to-cell junctions unleashes oncogene-expressing cells from their suppressive epithelial environment and induces clonal expansion (Leung and Brugge 2012; Leung 2013). These experimental observations support the notion that epithelial organization, together with cell-to-cell and cell-matrix adhesion can modulate cellular responses to oncogenic stimuli known to drive hyper-proliferation in un-organized structures (Simpson, Yu et al. 2011).

It is relevant to point out that several lines of evidence demonstrate that in *Drosophila,* as well as in mammalian cells, the polarized organization of epithelial cells is

an overarching factor in the control not only of tissues architecture, but also of cell proliferation; indeed, disruption of proteins involved in polarity establishment causes a hyperplastic growth and cooperate with other oncogenes in driving a tumorigenic and invasive behavior (Bilder, Li et al. 2000; Wodarz 2000; Brumby and Richardson 2003) (Pagliarini and Xu 2003) (Chatterjee, Seifried et al. 2012; Xue, Krishnamurthy et al. 2013). For example, it has been shown in MCF-10A cells the correlation between disruption of cell polarity and epithelial organization with c-Myc-induced hyper-proliferation. Albeit chronic activation of c-Myc at early stages of acinar morphogenesis, when polarity in not well established, results in hyper-proliferation and transformation, acute c-Myc activation in mature and polarized structures fails to reinitiate cell cycle and transform 3D acini. Further investigation better dissected the underlying tumor promoting mechanism highlighting the notion that in order for c-Myc to release its oncogenic potential, disruption of polarity through the deregulation of Lkb1 (Par-4, a member of partitioning defective protein PAR family, known to regulate cell polarity) must occur. Although loss of the tumor suppressor gene Lkb1 alone is not sufficient to drive mammary tumorigenesis, the combination of Lkb1 deletion with c-Myc overexpression affects epithelial integrity and leads to hyper-proliferation (Partanen, Nieminen et al. 2007; Partanen, Tervonen et al. 2012).

3.2 Alteration of polarity may be induced by deregulation of endocytosis.

Even more striking and relevant to this work are the findings showing that mutation in key essential membrane trafficking factors give rise to a neoplastic over-proliferating epithelia that is often caused by altered delivery of key polarity molecules (Vaccari and Bilder 2005; Rodahl, Haglund et al. 2009). Indeed, *Drosophila* RAB5 null mutants,

similarly to syntaxin Avalanche (avl) mutants, cause multilayered, hyper-proliferative phenotypes in eye discs and follicle cells: disruption of the endocytic trafficking results in the accumulation of specific membrane proteins as Notch receptor and the apical determinant Crumbs, leading to epithelial polarity defects and a specific expansion of the apical membrane domain (Lu and Bilder 2005) (Robinson and Moberg 2011). Moreover, among the *Drosophila* homolog of RAB5 effectors, novel endocytic neoplastic tumor suppressor genes were identified: unlike Rbns-5 mutants (Rabenosyn 5 in mammalian) that disrupt the correct localization of protein controlling the planar polarity establishment (Mottola, Classen et al. 2010), mutants of Rbpn-5 (Rabaptin-5 in mammalian), the effector protein of RAB5 that promotes homotypic early endosome fusion, and Rabex 5, a RAB5 GEF, showed hyper-proliferation and a disrupted epithelium, but retaining a normal polarity (Thomas and Strutt 2014). Thus, ablation of the endocytic pathway in epithelial tissues promotes hyper-proliferation through mechanism that are not fully understood, but seems not to depend only on altered epithelial polarity.

3.3 Alteration of the endocytic machinery drives uncontrolled cell proliferation through non-cell autonomous mechanisms.

Another critical hallmark of cancer cells is the acquisition of growth factor independent proliferation, frequently achieved by the autocrine or paracrine production and secretion of soluble proliferating signals. Endocytosis, initially studied as the process responsible for nutrient internalization for cell survival, has more recently emerged as a master organizer of cell signaling. A tight control of ligand-receptor internalization, recycling and degradation allows, for example, space and time resolving of different stimuli. The integration of such different endocytic routes defines the net biological outcome (Scita and Di Fiore 2010).

Alteration in the endocytic circuitry has been shown to be associated with human cancer (Mosesson, Mills et al. 2008). Moreover, a recent genetic screen performed in *Drosophila* model suggests that dysfunction of RAB5 drives non-autonomous cell proliferation in imaginal disc epithelium, inducing the accumulation of both EGFR and Eiger (an homolog of TNF) together with a downstream activation of JNK and Ras signaling pathways. Both cascades control and inactivate the Hippo pathway, triggering Upd (an IL6 homolog) expression and secretion, thus promoting cell proliferation (Takino, Ohsawa et al. 2014). Similar mechanisms has been observed in mammalian: in breast cancer, EGF independent growth was shown to be sustained by the increase in the secreted factor Amphiregulin (AREG), an EGFR ligand initially identified in the human breast carcinoma cell line MCF-7 after treatment with PMA (phorbol 12-myristate 13-acetate)(Shoyab, McDonald et al. 1988). Importantly, evidences collected in MCF-10A, a human normal mammary epithelial cell line strongly dependent on EGF to proliferate, support that an Hippo-dependent, non-cell autonomous mechanism observed in *Drosophila* might also be operative in mammalian system. Of note, the ectopic expression of YAP or TAZ, downstream effectors of the Hippo pathway, is sufficient to sustain EGF-independent growth through the secretion of a diffusible factor, AREG. Hence, YAP- or TAZ-dependent secretion of AREG identifies this EGFR ligand as a direct effector of the Hippo pathway with implications on the regulation of both physiological and malignant cell behavior (Zhang, Ji et al. 2009; Yang, Morrison et al. 2012).

4. The EGF-like growth factor Amphiregulin and its role in physiological and pathological conditions.

4.1 The ErbB/HER family of protein-tyrosine kinases.

Mammary epithelial tissues, as well as the *in vitro* model MCF-10A cells, strongly depend on EGF for their growth and proliferation. The specific binding of EGF with its receptor EGFR, activates a signal transduction cascade that modulates cell proliferation, survival, migration and differentiation.

EGFR is a member of the ErbB/HER (human epidermal growth factor receptor) family of receptors, originally named ERBB because of their homology with *v-erbB,* the erythroblastoma viral gene. This family comprises four receptor tyrosine kinases: EGFR (ErbB-1/HER1), HER2 (ErbB-2), HER3 (ErbB-3), and HER4 (ErbB-4) which are activated by ligand-induced dimerization. In human, the receptor homo- or heterodimerization together with the identification of more than 30 different ligands, generate a complex network of cellular responses (Yarden 2001). Interestingly, ErbB-2 has no ligands and ErbB-3 is devoid of kinase activity. Despite the described deficiencies, both of these receptors generate cellular signals by heterodimerization with other ligand-occupied ErbBs. ErbB-2, especially, is the preferred partner in heterodimeric complexes with the other family members, and ErbB-3 heterodimers are potent inducers of intracellular signals (Yarden and Sliwkowski 2001) (Fig.8).

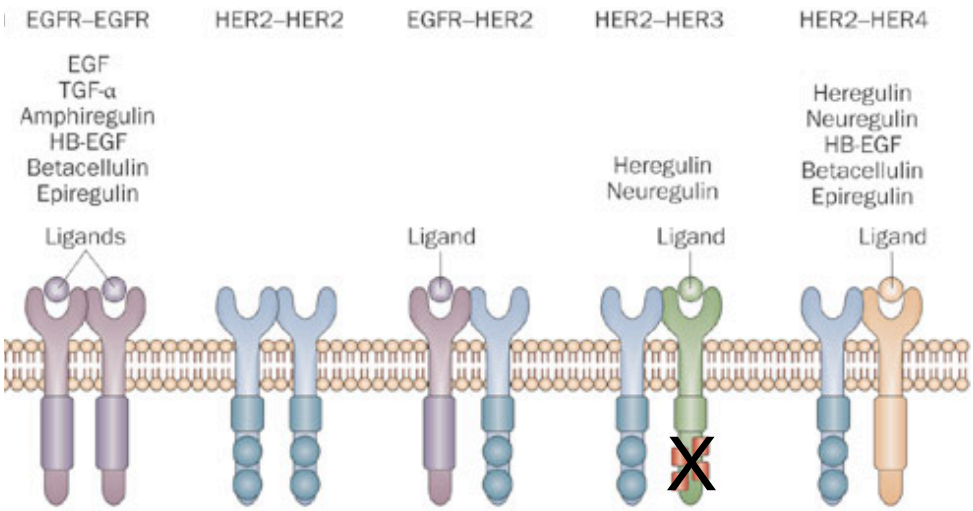

Figure 8. Dimerization and ligand specificity of ErbB/EGFR family members.

Each receptor is characterized by an extracellular ligand-binding domain, a transmembrane lipophilic domain and an intracellular tyrosine kinase domain. Trans-phosphorylation of tyrosine residues relies upon receptor dimerization and is induced by ligand binding. Receptor phosphorylation causes activation of downstream signaling pathways. Known receptor dimerization and corresponding ligands are shown. No ligand for HER2 has been identified. The kinase domain of HER3, which is marked with a cross, is kinase-impaired.
Adapted from (Linardou, Dahabreh et al. 2009)

After ligand binding, ErbB/HER family receptors activate a set of canonical biochemical cascaded including: the mitogen-activated protein kinase (MAPK), the phosphatidylinositol 3-kinase (PI3K)/Akt and the phospholipase Cγ (PLCγ) pathways. These signaling pathways invariably lead to the activation of several transcriptional regulators that modulate proliferation, apoptosis, migration and adhesion (Scaltriti and Baselga 2006).

The duration, intensity and localization of the activity of these signaling cascades are tightly regulated. Endocytosis is one mechanism through which signal attenuation is achieved. Indeed, it has been shown, for example, that EGFR in physiological conditions (low doses of EGF) is mostly internalized via clathrin-dependent endocytosis and recycled back to the plasma membrane, whereas at higher doses of EGF, clathrin-indipendent endocytosis targets primarily the receptor to degradation *via* the lysosomal pathway (Sigismund, Woelk et al. 2005) (Sorkin and von Zastrow 2009).

ErbB/HER receptors family has been also implicated in the acquisition of malignant

phenotypes like uncontrolled proliferation, resistance to apoptosis, angiogenesis and metastasis. Consistently, they have been one of the most extensively studied protein families with respect to their bio-physiological properties and use as prognostic and predictive markers in various tumor types (Zaczek, Brandt et al. 2005). A case in point is represented by ErbB-2. ErbB-2 amplification is a frequent occurrence in breast and ovarian cancer malignancies, and it is associated to aggressive diseases, predicting overall survival and time to relapse (Slamon, Clark et al. 1987) (Slamon, Godolphin et al. 1989). Similarly, in many different cancer types ErbB-1 is constitutively activated as a result of specific mutation in the autocrine kinase loop or through events that lead to its upregulation and elevated expression (Klijn, Berns et al. 1992; Holbro and Hynes 2004).

4.2 The EGF-like growth factor Amphiregulin.

Mammary gland development is probably the best-studied epithelial organ morphogenesis regulated by ErbB signaling. Among the identified ligands involved in this process, a fundamental role is played by Amphiregulin (AREG), a well-characterized ligand of EGFR (HER1/ErbB-1). AREG protein is firstly synthetized as a transmembrane polarized glycoprotein precursor (Pro-AREG), with the mature soluble AREG processed by proteolytic cleavage mediated by TACE (TNFα converting enzime or ADAM17). Its N-terminus contains six spatially conserved cysteine residues, flanked by a set of semi-conserved amino acids, the so-called EGF domain, and two potential nuclear targeting sequences. Both Pro-AREG and AREG are involved in the activation of specific cell response throught a juxtacrine (Pro-AREG) and autocrine/paracrine (AREG) signaling. Upon EGFR binding, AREG induces its activation by homo- or heterodimerization and engages different signaling pathways, including Ras/MAPK, PI3K/Akt, mTOR

(mammalian target of rapamycin), STAT (Signal Transducer and Activator of Transcription) and PLCγ (Fig.9).

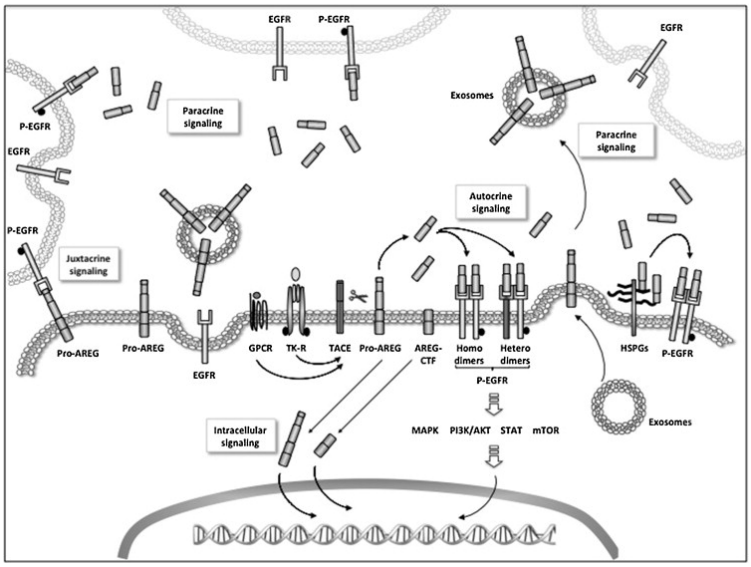

Figure 9. Schematic of AREG cell signaling strategies.

Membrane bound Pro-AREG elicits a juxtacrine signaling with neighboring cells or a paracrine signaling when included in exosomes. Alternatively, the cleavage of Pro-AREG by TACE can be stimulated by GPCRs (G-protein coupled receptor) and RTKs (receptor tyrosine kinases) ligands: soluble AREG can trigger autocrine or paracrine signaling. The interaction of AREG with EGFR induces homo- or heterodimerization of the receptor and its activation by cross-phosphorylation. pEGFR triggers the activation of downstream intracellular signaling pathways.
Adapted from (Berasain and Avila 2014).

Considering the multiple cellular responses modulated by AREG, it is not surprising that it is involved in cell proliferation, apoptosis and migration of different cell types, both in physiological and pathological processes (Busser, Sancey et al. 2011; Berasain and Avila 2014).

4.3 Amphiregulin role in physiological mammary gland development.

Within the physiological context of mammary gland development, AREG has been shown to mediate specifically pubertal mammary ductal development, induced both by Estrogen (ER) and Progesteron Receptors (PR) activation (McBryan, Howlin et al. 2008).

In the former case, it has been shown first *in vitro* and confirmed *in vivo*, that AREG expression is controlled by estrogen secretion. These findings highlight the notion that AREG is a key paracrine mediator of ERα signaling fundamental for epithelial cell proliferation during the pubertal ductal elongation, but not for earlier or later stages of mammary gland development (Ciarloni, Mallepell et al. 2007). ERα, AREG and EGFR knockout mice phenocopy each other, showing a clear deficiency in the morphogenesis of mammary gland ducts, supporting the hypothesis that this signaling cascade initiated by estrogens is mediated by AREG interaction with EGFR.

In the latter case, both prior and at puberty, progesterone acting through its specific receptor PR, causes the formation and proliferation of the mammary gland end buds, which was dependent on a significant increased AREG expression (Aupperlee, Leipprandt et al. 2013). Furthermore, branching morphogenesis requires a constant crosstalk between the developing epithelia and the surrounding stroma. In this process, TACE mediates the release of epithelial AREG that binds and actives stromal EGFR, thus orchestrating mammary duct morphogenesis (Sternlicht, Sunnarborg et al. 2005). Taken together, these evidences support the notion that AREG is required for normal ductal morphogenesis.

4.4 Amphiregulin in breast cancer.

In pathological conditions, AREG expression is correlated with inflammation and it is up-regulated in a wide variety of human cancer. In keeping with these observations, AREG overexpression can sustain growth factor independent proliferation of transformed cells. In particular, many studies performed both *in vitro* and *in vivo* on breast cancer tissues suggest that AREG play a key role in driving the initiation and progression of human breast cancer (Busser, Sancey et al. 2011). Accordingly, AREG overexpression in

different breast cell lines was shown to confer EGF-independent proliferation ability and to promote motility and invasion, typical hallmarks of cancer progression (Willmarth and Ethier 2006).

Converseley, the inhibition of AREG expression by RNA interference has been shown to revert the malignant phenotype and suppress the tumorigenicity of human breast epithelial cell lines (Ma, Gauville et al. 1999). Additionally, AREG expression in mammary epithelial cell lines increases the expression of TGFβ1 (transforming growth factor beta 1), which synergizes with AREG in stimulating the production of uPA (urokinase-type plasminogen activator), promoting protease production, and consequently breast cancer progression (Giusti, Desruisseau et al. 2003).

4.5 Amphiregulin transcriptional control.

A variety of regulatory pathways control the production and secretion of this growth factor. Studies performed on AREG promoter identified diverse functional elements that may explain its modulation by multiple inputs. Among these regulatory sequences, an estrogen responsive element (ERE) was identified by ChiP (chromatin immunoprecipitation) analysis, thus pointing to a direct ER driven transcriptional regulation of AREG expression by binding of ER to AREG gene regulatory sequence (Martinez-Lacaci, Saceda et al. 1995; Britton, Hutcheson et al. 2006) (Ciarloni, Mallepell et al. 2007). Additionally, in breast cancer under hypoxic conditions, the overexpression of HIF-2α (Hypoxia Inducible Factor 2 α, a well known mediator of cell response to local tissue hypoxia) promotes the autotrophic AREG/EGFR/ErbB4 pathway that is capable of sustaining a cell autonomous growth, thereby overcoming unfavorable microenvironment and hostile growth conditions. Although ChiP data showed a physical interaction of HIF-

2α with AREG promoter region, this gene regulation has been shown to be HRE (hypoxia responsive element)-independent, likely suggesting additional so far unrecognized regulatory elements that cooperates with HIF-2α to control AREG transcription (Bordoli, Stiehl et al. 2011; Stiehl, Bordoli et al. 2012). Finally, YAP and TAZ, emerging co-transcriptional regulators that are often amplified in tumors and associated with malignant transformation, have also been shown to mediate AREG transcription (Zhang, Ji et al. 2009; Yang, Morrison et al. 2012). Studies performed on MCF-10A cells demonstrated that the expression of YAP or TAZ was sufficient to enhance cell proliferation of non-expressing cells through a non-cell-autonomous mechanism. The EGFR ligand AREG was identified as the downstream effector of the Hippo pathway responsible for EGF-independent growth both in 2D and 3D. The strong correlation between these two signaling cascades was confirmed by interfering at different levels of the Hippo pathway: abrogation of YAP/TAZ negative regulators LATS1 and 2 induces AREG up-regulation; conversely TEAD transcription factor ablation completely abolishes AREG overexpression. These evidences, together with ChiP-based assays, identify another regulatory pathways controlling the production and secretion of AREG, specifically mediated by TEAD in TAZ expressing cells (Zhang, Ji et al. 2009; Yang, Morrison et al. 2012).

4.6 Hypoxia regulation of endocytosis.

One of the typical hallmark of cancer progression is a state of self-sufficiency that supports cell autonomy (Hanahan and Weinberg 2000). Cancer cells indeed may acquire the capability to express and secrete growth factor in order to sustain their own proliferation *via* either an autocrine or paracrine mechanism.

Oxygen deprivation or oncogenic activation of HIF has been correlated with cancer progression and poor prognosis. In hypoxic conditions, proliferation and cell survival may be supported by a deregulation of RTKs-mediated signaling pathways; or by the expression and secretion of specific growth factors. In the former case, increased EGFR half-life can result in a prolonged and accentuated EGFR signaling (Wang, Roche et al. 2009). In this conditions, endocytosis-mediated de-activation of EGFR has been indeed shown to be altered through the attenuation of RAB5-mediated early endosome fusion and a significantly reduced expression of Rabaptin-5, a key RAB5 effector, was documented to occur in hypoxic primary breast and kidney tumors (Wang, Roche et al. 2009). In the latter case, hypoxia is one of the pathways that control the expression of the EGFR ligand AREG and the up-regulation of this secreted factor has been shown to allow growth factor independent proliferation of transformed cells (Bordoli, Stiehl et al. 2011; Stiehl, Bordoli et al. 2012).

Given these evidences, further investigations will elucidate if, in hypoxic conditions, the alteration of vesicles trafficking and endocytic regulators, RAB5A in particular, may represent the common hub triggering both a prolonged half-life of EGFR and the up-regulation and secretion of the EGFR ligand AREG, thus sustaining a state of self-sufficiency.

5. Cell migration.

5.1 The diverse strategy of cell motility.

Cell migration is a complex process involved both in physiological and pathological conditions. Indeed, proper embryogenesis, immune surveillance and tissue homeostasis all relies on the tight regulation of cell locomotion, which is often hijacked during pathologies such as chronic inflammation or cancer progression.

The balance of different extracellular and intracellular structural and molecular determinants defines the multiple and diverse motility strategies that a cell can adopt in order to cope with micro-environmental cues (Friedl and Wolf 2010) (Fig.10).

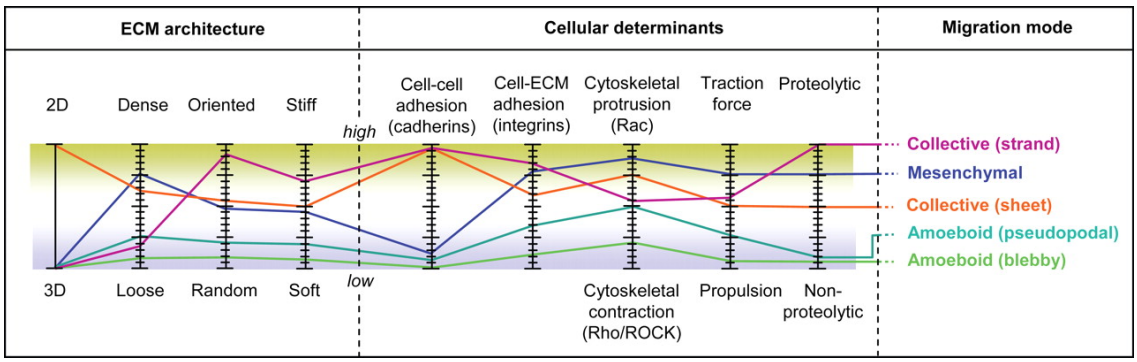

Figure 10. The migratory mode is influenced by micro-environmental and cellular parameters.

The combination of ECM architecture properties together with cellular determinants defines the migratory strategy adopted by motile cells. Each colored line represent the diverse strategies adopted depending on the intensity (dashed vertical lines) of each parameter.
Adapted from (Friedl and Wolf 2010)

Each of these modes is driven and regulated by distinct molecular pathways. To exemplify this notion, it is evident that cell can move either collectively or as single cells (amoeboid and mesenchymal modes). Within single cell locomotion, ameoboid migration is thought to resemble motility strategy and morphology typically ascribed to the amoeba *Dictyostelium discoideum.* Amoeboid *Dictyostelium* motility involves Rho-Rock (*Rho-*

associated protein kinase)-dependent actomyosin contractility, that drives blebbing-like movements of rounded and loosely adherent cells. Cells displace matrix fibrils and squeeze across the narrow spaces without requiring extensive remodeling of the extracellular matrix (ECM) or its degradation mediated by protease activity (Friedl 2004; Lammermann and Sixt 2009; Madsen and Sahai 2010). Conversely, in the mesenchymal motility mode cells adopt an elongated, fibroblast-like morphology, more akin to the prototypical 2D motility classically described by Abercrombie back in the sixty (Abercrombie 1961). Locomotion relies on a dynamic integrin-mediated attachment to the extracellular matrix and on the formation of RAC-dependent, F-actin rich protrusions that drive directional motility coupled with pericellular proteolysis and high MMP activity (Wolf, Mazo et al. 2003; Palamidessi, Frittoli et al. 2008; Sanz-Moreno, Gadea et al. 2008; Egeblad, Nakasone et al. 2010; Kessenbrock, Plaks et al. 2010). Likewise, the described single cell migratory mode sustains the normal morphogenetic process but also cancer dissemination, where single cells detach from the mass and migrate in a secondary tissue to initiate metastatic growth (Fig. 11, top panels).

Otherwise, the maintenance of stable cell-to-cell adhesions among migrating cells allows cells to move as clusters (typical of primary cancer lesions) or as a multicellular connected sheet (frequently observed in epithelia) in the so-called collective locomotion. Among cell-cell contacts, adherens junctions (AJs) are common structures observed in epithelial collective migration and are mainly composed of cadherins, in particular E-cadherin in epithelial cells (Friedl and Gilmour 2009). Also collective locomotion relies on adhesion to the substrate and protease activity in order to allow migration across the extracellular matrix, but with additional cell-to-cell adhesions. Finally, other locomotory strategy has been identified, including: i) mesenchymal chains, when elongated cells move in a loose chain-like fashion; ii) collective branching, typical of mammary gland morphogenesis; and iii) collective vascular sprouts of endothelial cells from new blood vessel that mature into a growing strand containing a lumen (Fig.11, bottom panels) (Friedl 2004).

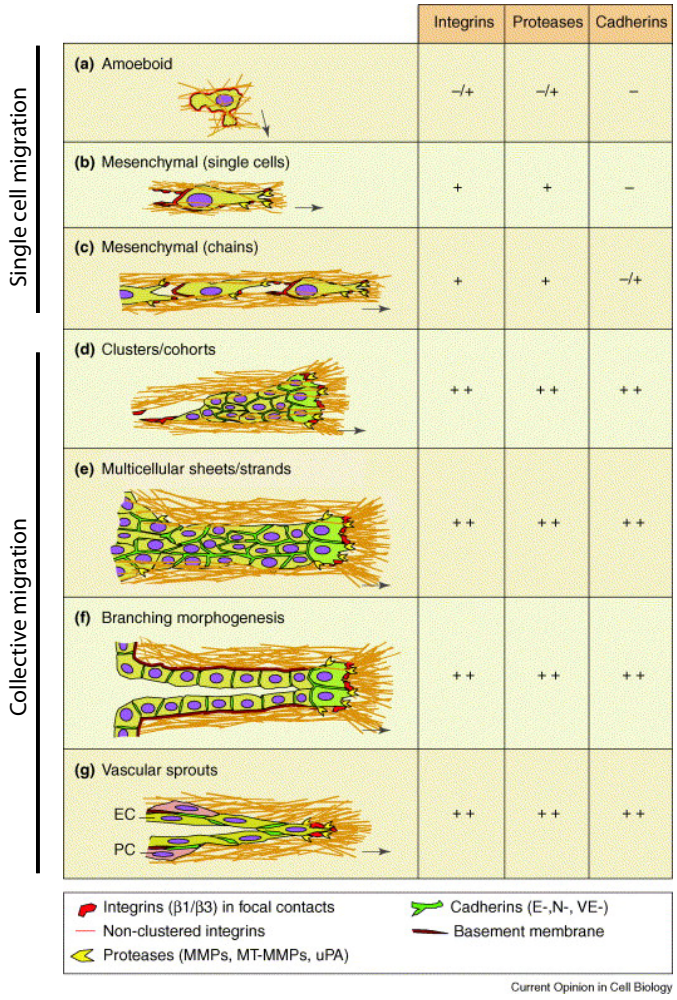

Figure 11. Cell migration strategies differently rely on adhesion, proteolytic activity and cell-to-cell adhesions.

Different migratory modes are shown, divided in the two main categories: single *vs* collective cell locomotion. Integrins, proteases and cadherins dependency is shown. For details refer to the text.
Adapted from (Friedl 2004)

As already anticipated, collective locomotion of cohesive group of cells is a typical physiological mechanism involved in embryogenesis and tissues or organs formation. Remarkably, however, a similar collective behavior is also displayed by cancer cells during tumor progression and invasion, particularly in those of epithelial origin.

5.2 The plasticity of cell motility.

In tumor progression, neoplastic cells invade through the basement membrane and diverse types of stromal ECM that provide on one hand a substrate for adhesion and traction, but on the other hand impose biomechanical resistance (Friedl and Alexander 2011). Tumor cells flexibly employ the described diverse modes of migration and switch between them depending on both intrinsic as well as microenvironmental factors (Wolf and Friedl 2006). This adaptive capability is termed plasticity. Within this context, the transition from cells migrating as a group to single motile cells is called epithelial to mesenchymal transion (EMT) and it usually occurs when cell-to-cell adhesions are lost and epithelial cancer undergo to progressive de-differentiation (Thiery, Acloque et al. 2009) (Giampieri, Manning et al. 2009). Conversely, when cell-to-cell or cell-ECM adhesions and pericellular proteolysis are weakened, single cells detach from the tumor mass and adopt an amoeboid motility mode, in a collective to amoeboid transition (CAT) (Hegerfeldt, Tusch et al. 2002). Interestingly, it has been shown that a reverse transition from amoeboid to mesenchymal locomotion (AMT) can also take place, at least *in vitro*. For instance, treatments with ROCK inhibitors or RAC hyper-activation induce AMT; conversely, protease inhibitors or integrin antagonists can cause mesenchymal to amoeboid transition (MAT) (Sahai and Marshall 2003; Wolf, Mazo et al. 2003) (Fig.12).

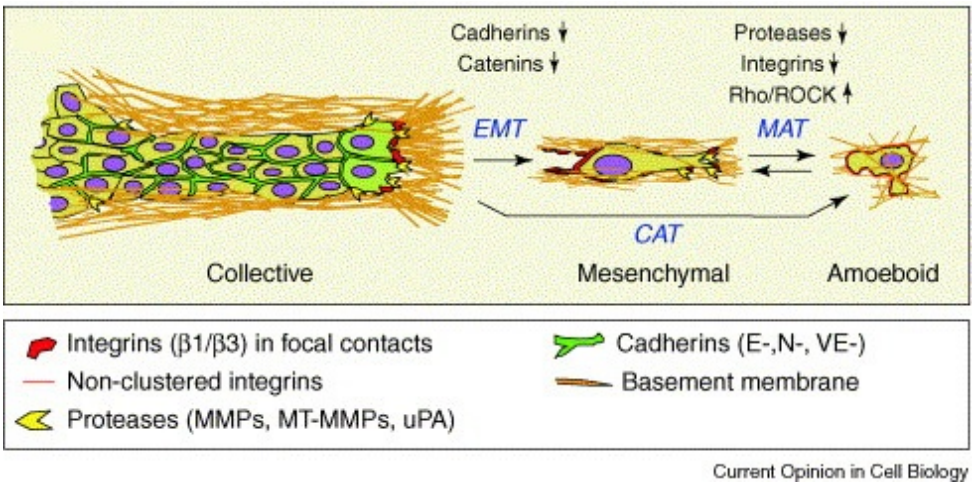

Figure 12. Neoplastic cells can adapt to different microenvironment by switching motility strategy.

Loss of cell-to-cell interactions induces single cell detachment from the primary tumor mass and migration in a protease and integrin dependent (EMT) or independent (CAT) motility mode. In individual cells, the weakening of cell to ECM interaction and the inhibition of proteolysis results in MAT.
Adapted from (Friedl 2004)

While these two single motility modes are often defined as distinct behavior, it is more accurate to define them as a continuous spectrum with intermediate phenotype. Cancer cells can, indeed, exploit a wide spectrum of migratory modes, ranging from single to collective, from proteolytic to protease independent and from adhesive to non-adhesive strategies, easily adapting to the surrounding microenvironment. This plasticity represents also a mechanism that provides migratory-based escape strategies after specific pharmacotherapeutic treatment, thus prompting an alternative method of cancer dissemination and resistance to single metastatic inhibitory agents.

5.3 Epithelial collective locomotion.

Collective locomotion of cohesive groups of cells is a typical hallmark of remodeling events involved in processes of embryogenesis, tissue repair and cancer invasion.

Some specific features define collective migration and ensure cells to move as a unique unit: i) cell-to-cell junctions are conserved during cell movement and cells within the group remain physically but also functionally connected; ii) actin cytoskeleton organization generates traction and lamellipodia protrusion forces, transmitting migratory cues along the moving cell group; iii) a tightly regulated focal adhesions turnover ensures coordinated monolayer to move across a two-dimensional extracellular matrix substrate (Theveneau and Mayor 2013).

Epithelial locomotion is a widely investigated kind of collective migration, sustained by different mechanism that involves cell-cell cohesion, cell-ECM adhesion, migratory protrusions and actomyosin contractily.

A typical approach for *in vitro* studies of epithelial collective locomotion is the wound healing assay: when epithelial cells are presented with a cell free area created by a scratch in the monolayer, they move collectively toward the artificial gap to heal the wound, until the monolayer is established again. Cells within the sheet maintain cell-to-cell junctions and show typical mechanism occurring *in vivo* (Liang, Park et al. 2007).

Intriguingly, as well as in wound healing, it has been shown that collectively migrating cells form specific patterns, similar to ordered motions seen in natural systems such as fish schools, bird flocks and fluids (Li and Sun 2014). This similarity led to a new approach in the quantification of wound healing and cell streaming processes, applying typical software and methods firstly designed to model natural systems. Cell Image Velocimetry (CIV) represents an example of this kind of approach (Milde, Franco et al. 2012).

5.4 RAB5A modulation of RAC1 driven migratory protrusions.

The cell free space of a wounded monolayer is a potent motility signal that stimulates cells in the first rows to migrate to heal the wound. Cells at the leading front sense a directional cue and extend persistent, and dynamics lamellipodia that drive the full sheet forward. Lamellipodia are flat, plasma membrane protrusions, anchored to the underlying surfaces during forward protrusion of motile cells (Small, Stradal et al. 2002).

A specific role of RAC1, a member of the Rho-GTPases family, has been well characterized in promoting lamellipodia formation. RAC1 activation, mediated by its GEFs, induces a dramatic increase in actin polymerization and the formation of a branched network of actin filaments that pushes the plasma membrane and sustains the formation of broad migratory protrusions (Nobes and Hall 1995; Nobes and Hall 1999). Lamellipodia are than stabilized by adhesion with the ECM, thus allowing the conversion of propelling actin-based forces into traction forces that sustain cell locomotion; conversely its depletion has been shown to impair lamellipodia formation and cell migration (Ridley, Paterson et al. 1992; Ridley, Schwartz et al. 2003).

Activated RAC1, the key coordinator of actin dynamic, mediates the formation of migratory protrusion in response to the internalization of activated growth factor receptor tyrosine kinases, thus representing a downstream target of RTKs. Re-localization of activated RAC1 to specific area of the plasma membrane, where actin remodeling induces the formation of migratory protrusions has been proposed to be mediated by polarized vesicular transport. Within this context, the endosomal-recycling pathway, dependent on the small GTPase RAB5A, has been shown to play an essential role in spatial restriction of RAC1 activation and hence directional cell locomotion. Concordantly, different studies support the fundamental role of RAB5A in promoting mesenchymal locomotion. It has been shown, for example, that the expression of RAB5A in poorly motile, amoeboid HeLa cells is necessary and sufficient to induce the formation of elongated, polarized cell

protrusions, promoting cell locomotion. In particular, the formation of migratory protrusion, such as lamellipodia and dorsal ruffles, is mediated by RAB5A regulation of endocytosis and spatially restriction of RAC1-mediated actin dynamics to specific region of the plasma membrane (Lanzetti, Palamidessi et al. 2004; Palamidessi, Frittoli et al. 2008) (Fig. 13).

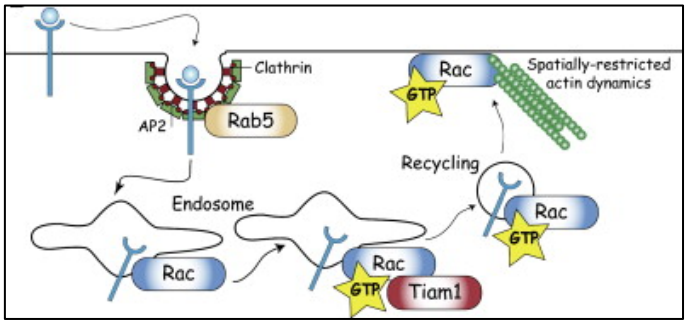

Figure 13. Schematic of the RAB5-dependent control of RAC1 activation relocalization to the plasma membrane.

Clathrin- and RAB5-mediated endocytosis control RAC activation induced by motogenic stimuli: RAC and its GEF Tiam1 are simultaneously recruited onto endosomal membranes and activated RAC is recycled to specific regions of the plasma membrane to promote actin remodeling and migratory protrusion formation. Adapted from (Palamidessi, Frittoli et al. 2008)

5.5 RAB5A is involved in the dynamic turnover of focal adhesions.

As already mentioned in sections before, the interaction of the cell with the extracellular matrix is essential to sustain migration. Cell-matrix adhesions represent sites where actin cytoskeleton converges with fibers of the ECM, creating a mechanical link between the cell and the substrate (Nobes and Hall 1995). Among the diverse kind of adhesion, focal adhesions (FAs) are highly dynamic structures usually linked to actomyosin stress fibers that undergo to a spatiotemporally regulated turnover, particularly during cell migration (Ridley, Schwartz et al. 2003). In motile cells, FAs form at the

leading edge and establish transient attachment of the cell to the substrate. Subsequently, these dynamic structures must be disassembled to allow the detachment of cell rear and cell to move. In agreement with this observation, the impairment of FAs disassembly inversely correlates with cell motility.

Together with activation and spatial restriction of RAC1 in protrusion formation, RAB5 has also emerged as an important regulator of FAs turnover, directly influencing several aspects of cell migration. The depletion of RN-tre, a GAP of RAB5, was indeed increasing FAs turnover and cell migration, by enhancing the endocytosis of β1 integrin, one of the components of FAs, already shown to be required in traction forces generation at the leading front and in maintaining migration speed (Hegerfeldt, Tusch et al. 2002; Palamidessi, Frittoli et al. 2013) (Maruthamuthu, Aratyn-Schaus et al. 2010). The localization of RN-tre both at the level of FAs and in RAB5-positive vesicles close to the ventral plasma membrane further confirmed the involvement of RAB5 in FAs assembly and disassembly circuitry. More in detail, turning off RAB5, RN-tre acts as a ‘‘brake’’ in cell motility and stabilizes FAs by the inhibition of RAB5-mediated β1 integrin endocytosis. This FAs stabilization strongly impairs cell motility (Palamidessi, Frittoli et al. 2013).

Additional confirmation of the role of RAB5 in FAs dynamics comes from recent data showing the interaction of RAB5 with FAs components and its involvement in the control of Focal Adhesion Kinase (FAK) phosphorylation/dephosphorylation rate, thus controlling FAs disassembly (Mendoza, Ortiz et al. 2013).

5.6 Cell-to-cell adhesions mediate cell cohesion and coupling within the migrating epithelial sheet.

A typical hallmark of collective migration is the maintenance of stable cell-to-cell adhesions, a class of cell-cell contact including adherens junctions (AJs), tight junctions (TJs) and desmosomes (Niessen 2007). The common structures observed in epithelial collective migration are AJs, which are mainly composed of cadherins, in particular E-cadherin in epithelial cells (Friedl and Gilmour 2009). As opposed to individual cell, in collective epithelial cell locomotion cells at the leading front retain intact cell-to-cell adhesions with cells in the rows behind, thus mechanically holding the epithelial sheet together and promoting multicellular coordination. Moreover, strength and stability of cell-cell junctions affect collective migration output and efficiency. Indeed, intermittent and transient cell-to-cell adhesions result in a coordinated but individual cell motility with short-lived contacts between cells within the monolayer, as it has been shown in cranial neural crest cells (Teddy and Kulesa 2004). Whereas, total depletion of cell-to-cell contacts lead to disaggregation of the migrating sheet and single cell independent migration both in speed and direction (Simpson, Selfors et al. 2008).

Cadherin-based junctions interact with different cytoplasmic proteins that link them to actin cytoskeleton, thus transmitting forces generated by actomyosin contractility from one cell to the neighboring ones (Maruthamuthu, Aratyn-Schaus et al. 2010). Thus, in homophilic adherens junctions, the cytoplasmic tail of E-cadherin binds to p120 catenin and β−catenin. β−catenin in turn binds α−catenin, which interact with actin and modulate actin filaments organization. Additionally, the transcriptional co-activator β−catenin transduced mechanical signals from the adherens junction to the nucleus, thus identifying AJs as mechanosensory structure that can detect not only changes in cell-to-cell contacts but also mechanical stress (Yonemura 2011) (Baum and Georgiou 2011).

6. Cell invasion

6.1 MCF10.DCIS.com cells as a model of the transition from *in situ* to invasive breast carcinoma.

MCF-10.DCIS.com cell line represents a nearly ideal system to study cancer progression due to fact that once injected into recipient mice, these cells faithfully recapitulate all the prototypical features of human DCIS (Ductal carcinoma *in situ*) *comedo*-like lesion (a more aggressive type of DCIS with central necrosis), including their spontaneously propensity to progress toward an invasive breast cancer phenotype (Hu, Yao et al. 2008; Behbod, Kittrell et al. 2009). To generate this cell line, MCF-10A cells were stably transfected with the mutated human T-24 oncogene H-Ras and MCF-10.DCIS.com cell line was derived from xenograft lesions obtained after sequential trocar passages of a lesion generated from H-Ras-mutated MCF-10A cell line (Basolo, Elliott et al. 1991; Russo, Tait et al. 1991; Miller, Soule et al. 1993; Miller, Santner et al. 2000).

Studies performed on a cohort of invasive ductal carcinoma (IDC), the invasive evolution of DCIS lesion, reported a specific hepatocyte growth factor (HGF)/c-Met (also called HGFR, hepatocyte growth factor receptor) pattern of expression: although HGF was homogenously expressed in cancer cells, c-Met staining was accentuated at the cancer front. Additionally, this specific co-expression pattern was associated to a paracrine pathway and correlated with histologic grade, lymph node involvement and decreased disease-free survival (Edakuni, Sasatomi et al. 2001). The paracrine role of HGF/c-Met signaling in the regulation of tumor cell migration and invasion has also been confirmed in MCF-10.DCIS.com cells. Indeed, the stimulation with HGF of MCF-10.DCIS.com acini grown into matrigel/collagen 3D matrices was sufficient to convert them into aberrantly,

multiprotrusive and invasive structures resembling the DCIS to IC transformation (Jedeszko, Victor et al. 2009) (Fig.14). Importantly, this model represents a useful strategy to investigate invasive progression in a controlled, and genetically tractable manner in *in vitro* culture.

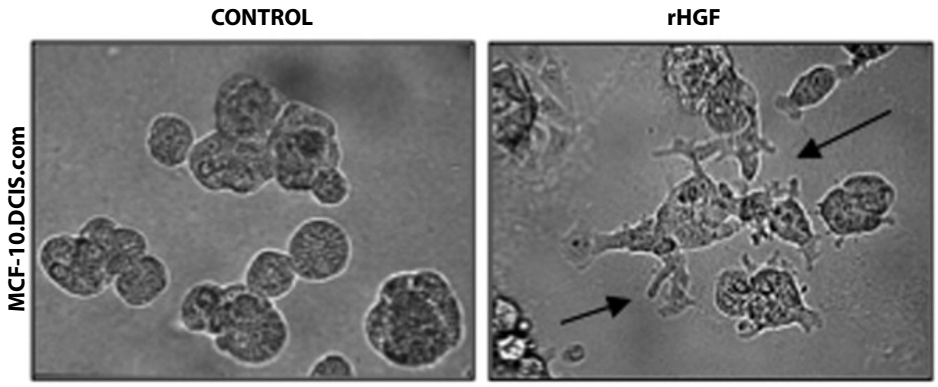

Figure 14. Recombinant HGF stimulates invasive outgrowths in MCF-10.DCIS.com cells.

MCF10.DCIS cells were grown in three-dimensional reconstituted basement membrane in absence (CONTROL) or presence of 100 ng/ml HGF (rHGF). Arrows indicate invasive outhgrowths.
Adapted from (Jedeszko, Victor et al. 2009).

Aim of the project

Based on the outlined background the aim of the present PhD project was two fold:

1) To dissect the role of RAB5A in the morphogenetic process of mammary epithelial development. To this end, we combined inducible expression systems, in which oncogene expression can be switched on and off at will, with 3D culture on reconstituted basement membrane to mimic normal or oncogene-altered mammary gland development at different stages. RAB5A WT or its dominant negative form RAB5AS34N (an inactive GDP-locked form of RAB5A) were expressed in MCF-10A cells exploiting a doxycycline inducible system that allows the controlled and conditional expression of the gene of interest. This strategy provided us a flexible tool to modulate RAB5A mediated endocytosis and to investigate the effects of deregulation of this key endocytic protein on MCF-10A acinar morphogenesis, integrity and growth factor dependent proliferation.

2) To delineate the mechanisms through which RAB5A altered function or expression impact not only on mammary gland morphology, but also on the mode of migration that may be harnessed during cancer progression. To this end, we focused specifically on the role of RAB5A in collective cell locomotion, a typical motility mode frequently seen in invasive solid tumors of epithelial origins, such as breast carcinoma. We initially utilized normal mammary epithelial cells as a model system in order to reveal fundamental processes that may be affected by deregulation of RAB5A, an event that is frequently observed in breast cancer and may therefore be relevant for breast cancer pathogenesis.

MATERIALS AND METHODS

Plasmids, antibodies and reagents

Doxycycline-inducible pSLIK-neomycin (neo) lentiviral vectors carrying RAB5A WT or RAB5AS34N sequences were obtained by Gataway Technology (Invitrogen), following the manufacturer's protocol. The plasmid pBABE-puromycin (puro)-GFP was purchased from Addgene.

Total ERK1-2 (p44/42 MAPK), phospho-ERK1/2 (Tyr202-Tyr204), phospho-EGFR (Tyr1068), total AKT, phospho-AKT (Ser473) and cleaved caspase 3 antibodies were purchased from Cell Signaling; mouse monoclonal antibodies raised against actin, α–tubulin and vinculin were from Sigma-Aldrich; RAB5A (S-19) and EEA-1 (N-19) antibodies from Santa Cruz Biotechnology; anti-paxillin was from Zymed; anti-Ki67 from Dako; anti-Laminin V from Millipore and anti-Giantin from Covenance; total EGFR antibody was raised against amino acids 1172-1186. Anti-E-cadherin was from BD transduction Laboratories. hAREG (1 μg/ml) neutralizing antibody was from R&D Systems and control IgG (1 μg/ml) from Jackson ImmunoResearch. AlexaFluor 488 transferrin was purchased from Abcam. Secondary antibodies conjugated to horseradish peroxidase were from Bio-Rad; FITC- and Cy3-secondary antibodies from Jackson ImmunoResearch, AlexaFluor 488 was from Molecular Probes. TRITC- and FITC-conjugated phalloidin were from Sigma Aldrich.

Recombinant human Amphiregulin was purchased from R&D Systems. MEK1 inhibitor PD325901 was purchased from Millipore, Mitomycin C from Sigma Aldrich and EGFR

inhibitor Cetuximab was kindly provided by Dr. Maria Rescigno (IEO-Milan). Growth Factor Reduced BD Matrigel^{TM} Matrix Basement Membrane was from BD Biosciences, purified bovine atelo-collagen (PureCol) was from Advanced Biomatrix. Recombinant Human HGF was from R&D Systems.

Cell cultures and transfection

MCF-10A cells were maintained in DMEM/F12 medium (Invitrogen) supplemented with 5% horse serum, 0.5 mg/ml hydrocortisone, 100 ng/ml cholera toxin, 10 μg/ml insulin and 20 ng/ml EGF (Soule, Maloney et al. 1990). MCF-10.DCIS.com cells were kindly provided by Dr. John F. Marshall (Barts Cancer Institute, Queen Mary University of London) and maintained in the same media of MCF-10A without cholera toxin. Cells were grown at 37 °C in humidified atmosphere with 5% CO2.

MCF-10A and MCF-10.DCIS.com cells were infected with pSLIK-neo-EV (empty vector control), pSLIK-neo-RAB5A WT and pSLIK-neo-RAB5AS34N lentiviruses and selected with the appropriate antibiotic to obtain stable inducible cell lines. Constitutive expression of GFP was achieved by retroviral infection of MCF-10A EV cells with pBABE-puro-GFP vector.

Generation of lentiviruses and retroviruses particles

Packaging of lentiviruses or retroviruses was performed following standard protocols. Four batches of viral supernatant were collected and filtered through 0.45 μm filters. Cells were subjected to four cycles of infection and selected using the appropriate antibiotic: neomycin for pSLIK vector (150 μg/ml) or puromycin for pBABE vector (2 μg/ml). After several passages, stable bulk populations were selected and tested for i) the homogeneity of the cell pool by immunofluorescence staining, and ii) induction efficiency by Western Blotting and quantitative RT-PCR (qRT-PCR).

RNA interference

MCF-10A EV cells were seeded the day before to be 60-80% confluent at the time of transfection. siRNAs (small interfering RNAs) delivery was achieved by mixing 1 nM of specific siRNAs with Optimem and Lipofectamine RNAiMAX Transfection Reagent (Life Technologies). The sets of oligos used for knocking down specific genes are listed in the table below. All siRNAs were purchased from Life Technologies. For each RNA interference experiment, negative control was performed with the same amount of scrambled siRNAs. Knocking down efficiency was controlled by qRT-PCR.

Gene target	Sequence 5' to 3'
RAB5A oligo 1	CAAGCCTAGTGCTTCGTTT
RAB5A oligo 2	GCCAGAGGAAGAGGAGTAGACCTTA
RAB5B oligo 1	CGACATTACTAATCAGGAA
RAB5B oligo 2	GCAGATGACAACAGCTTATTGTTCA
RAB5C oligo 1	GGACAGGAGCGGTATCACA
RAB5C oligo 2	TCCGCTTTGTCAAGGGACAGTTTCA
RAB21	GGGTCCAATTTACTACAGA
RAB22A	TGAGCTACATAAATTCCTA
RAB31	GGAATACGCTGAATCCATA

Table 1. List of oligos and corresponding 5' to 3' sequences, utilized in the RNA interference experiments.

Total RNA extraction and reverse transcription

2D monolayers and 3D acini were lysed by Trizol Reagent (Invitrogen). Total RNA was extracted using RNeasy Mini kit (Qiagen) and quantified by NanoDrop to assess both concentration and quality of the samples. Reverse transcription was performed using SuperScript VILO cDNA Synthesis kit from Invitrogen.

Affymetrix analysis

MCF-10A cells were seeded in complete media and doxycycline-induced for 72 hours. Total RNA extraction and reverse transcription were performed as described in the section before. The experiment has been performed three times with two technical replicates. Gene lists were ranked according to the log2 ratio and a p value ≤ 0.05.

Quantitative RT-PCR detection of mRNAs

Gene expression was analysed using TaqMan Gene expression Assay (Applied Biosystems). More in details, 0.1 ng cDNA was amplified, in triplicate, in a reaction volume of 25 µl with 10 pMol of each gene-specific primer and the SYBR-green PCR MasterMix (Applied Biosystems). Real-time PCR was performed on the 14 ABI/Prism 7700 Sequence Detector System (PerkinElmer/Applied Biosystems), using a pre-PCR step of 10 min at 95°C, followed by 40 cycles of 15 s at 95°C and 60 s at 60°C. Specificity of the amplified products was confirmed by melting curve analysis (Dissociation Curve TM; PerkinElmer/Applied Biosystems) and by 6% PAGE. Samples were amplified with primers for each gene (listed in the table below) The Ct values were normalized to the GAPDH curve. Results were quantified using the $2^{-\Delta\Delta CT}$ method. PCR experiments were performed in triplicate.

Gene name	Primer assay ID
GAPDH	Hs99999905_m1
RAB5A	Hs00702360_s1
RAB5B	Hs00161184_m1
RAB5C	Hs00428044_m1
AREG	Hs00950669_m1
RAB21	Hs00209226_m1
RAB22A	Hs00221082_m1
RAB31	Hs00199313_m1
CTGF	Hs00170014_m1
Progesteron Receptor (PGR)	Hs00172183_m1
Estrogen Receptor (ESR1)	Hs00174860_m1
HIF2a (EPAS1)	Hs01026149_m1

Table 2. List of primer assay IDs and corresponding target genes, utilized for qRT-PCR analysis.

MTT proliferation assay

Cell proliferation was assessed by MTT ([3-(4,5-dimethylthiazol-2-yl)-2,5-diphenyltetrazolium bromide) assay following the standard protocol. Briefly, cells were seeded at $2*10^3$ cells/well in 96-well plates and maintained in complete medium. Cell proliferation was assessed at different timepoints, with a 24 hours interval. 500 μg/ml MTT (Sigma-Adrich) was added to each well. After 2 hours of incubation at 37°C, the MTT solution was carefully removed and 100 μl of DMSO was added to each well. Plates were incubated 15 minutes at room temperature in agitation. Absorbance was measured at 570 nm using a VICTOR3 V Multilabel Counter (PerkinElmer model 1420). Each condition was performed with quadruple technical replicates.

Quantification of cell proliferation rates

For conditioned media experiments, doxycycline-induced MCF-10A EV and RAB5AS34N cells were plated in fresh media without EGF. Conditioned media from similar number of cells were collected after 4 days and filtered through 0.45 μm filters to eliminate any debrides or floating cell. Cleared conditioned media were applied onto parental MCF-10A cells seeded in 96-well plate ($2*10^3$ cells/well) and cell proliferation was monitored taking images every 2-3 days by differential interference contrast (DIC) imaging, using a 10x objective. The number of cells/field was manually counted at each time-point by Cell Counter ImageJ software plugin.

In neutralizing antibody experiment, rAREG (20 ng/ml), normal goat IgG (1 μg/ml, negative control) and anti-hAREG antibody (1 μg/ml) were added to the media at the moment of seeding of induced-cells.

The same procedure was applied for Cetuximab treatment (10 μg/ml or 20 μg/ml) in EGFR inhibition experiment.

Analysis of apoptosis rate by FITC-Annexin V/PI staining

FITC-Annexin V/propidium iodide (PI) staining was performed using flow cytometry. Doxycycline-induced MCF-10A cells were seeded in complete media 72 hours in sub-confluency conditions. $5*10^5$ cells were collected together with the supernatant and precipitated by centrifugation at 2,000 rpm 7 minutes. Cells pellets were washed one time in annexin buffer (1 M HEPES, 5 M NaCl, 1 M $MgCl_2$, 1 M $CaCl_2$, 50 mM KCl and H_2O). Samples were resuspended in 50 μl of 1.5 μg/ml annexin V-fluorescein isothiocynate diluted in annexin buffer and incubated 1 hour at room temperature, protected from light. Cells were washed again in annexin buffer and resuspended in 500 μl of 10 μg/ml propidium iodide diluted in PBS. Flow cytometric analysis was immediately performed using a FACS CantoII Instrument (Becton Dickinson). 30,000 events were acquired for

each cell line. Data analysis was performed by FACS Diva 6.1.1 software. An example of a scatter plot obtained after FITC-Annexin V/PI staining and relative identified subpopulations of cells are shown in figure 15.

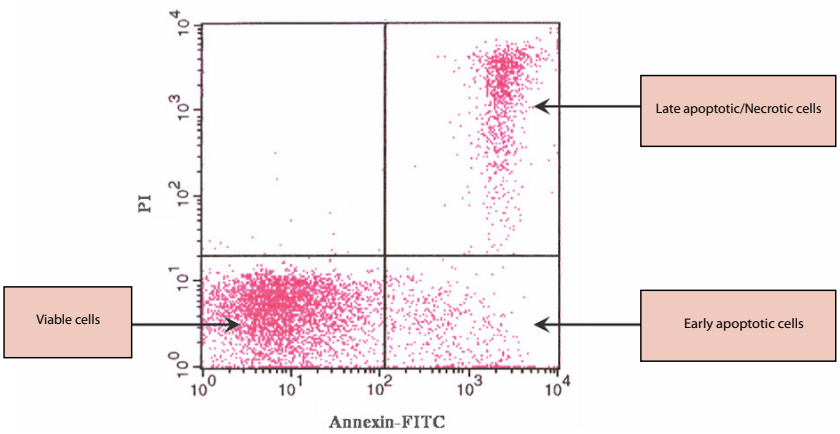

Figure 15. Scatter plot obtained through Annexin V-FITC/PI staining.
One of the earliest features of apoptosis is the loss of plasma membrane asymmetry. In apoptotic cells, the membrane phospholipid phosphatidylserine (PS) is translocated from the inner to the outer leaflet of the plasma membrane, becoming available for binding of Annexin V-FITC, a Ca2+-dependent phospholipid-binding protein showing high affinity for PS. Viable cells with intact membranes exclude PI, whereas the membranes of dead and damaged cells are permeable to PI. Cells that are viable are both Annexin V-FITC and PI negative. While cells that are in early apoptosis are Annexin V-FITC positive and PI negative and cells that are in late apoptosis or necrotic are both Annexin V-FITC and PI positive.

Cell cycle profiling

Cell cycle profiling was performed exploiting two different strategies to synchronize cells. Doxycycline-induced MCF-10A cells were plated 48 hours in complete medium without EGF, to arrest cell growth and synchronize them in G0 phase. Cell cycle was released by replacing the starvation medium with fresh complete medium supplemented with EGF. All experimental steps were performed in doxycycline-induced conditions.

Alternatively, cell cycle progression was investigated by Double Thymidine Block assay. Briefly, MCF-10A cells were seeded at 30% confluency in complete medium in the presence of EGF and doxycycline. Then, cells were treated with 2 mM thymidine blocking solution and after 15 hours, thymidine was removed by washing with 1X PBS. Cells were released adding fresh complete medium (+EGF and doxycycline) for 9 hours. A second 2

mM thymidine pulse was performed and to better synchronize the cell cycle, EGF was not added in this latter thymidine pulse. After 15 hours, cells were washed with 1X PBS and fresh complete medium, supplemented with EGF and doxycycline, was added to cells to induce cell cycle re-initiation.

For both the described strategies, samples were collected at different timepoints to monitor cell cycle progression. $1*10^6$ cells were collected together with the supernatant, washed two times with 1X PBS and centrifuged at 3,000 rpm 5 minutes. Pellets were re-suspended in 250 μl of 1X PBS and fixed by adding drop-wise 750 μl of pure ethanol while vortexing. After 1 hour incubation on ice, samples were washed in 1 ml of PBS+1% BSA (bovine serum albumin) and re-suspended in 1 ml of assay buffer containing 50 μg/ml PI and 250 μg/ml of RNase A. PI staining was carried out overnight at 4°C. Flow cytometric analysis was performed using a FACS CantoII Instrument (Becton Dickinson). 20,000 events were acquired for each condition and data were analysed by ModFit LT3.0 software. A typical cell cycle profiling is shown in figure 16.

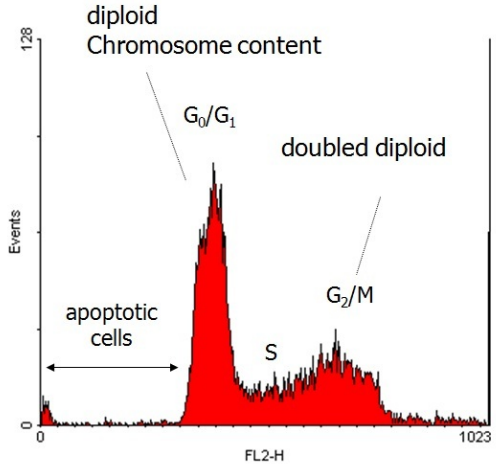

Figure 16. Flow cytometric analysis of cellular DNA content.
The propidium iodide fluorescence detected by FACS is proportional to the amount of DNA present in cells and it allows the identification of the proportion of cells that are in the different cell cycle phases.

Immunoblotting

For protein extraction, cells were lysed in JS buffer containing proteases inhibitors and cell lysates were cleared by centrifugation at 13,000 rpm for 30 min at 4°C. Protein concentration was quantified by Bradford colorimetric protein assay. The same amount of protein lysates was loaded onto polyacrylamide gel in 5X SDS sample buffer. Proteins were transferred onto Protran Nitrocellulose Transfer membrane (Whatman), probed with the appropriate antibodies and visualized with ECL Plus western blotting detection reagents (GE Healthcare). Membrane blocking and incubation in primary or secondary antibodies were performed for 1h in TBS/0.1% Tween/5% BSA for antibodies recognizing phosphorylated proteins or in TBS/0.1% Tween/5% milk for antibodies recognizing the total proteins. Primary antibodies were diluted 1:1,000 and secondary antibodies 1:10,000 as suggested by the manufacturer. Where specified, cells were EGF-starved for 9 hours and treated with 100 ng/ml EGF for different time-points.

Microscopes equipment

Wide-field fluorescence images were taken by an AX70 (Olympus) microscope equipped with a 12 bit b/w camera (FviewII, Olympus). Confocal images were taken with a Leica TSC SP2 AOBS confocal microscope controlled by Leica Confocal Software and equipped with violet (405 nm laser diode), blue (argon, 488 nm), yellow (561 nm Solid State Laser), and red (633 nm HeNe Laser) excitation laser lines. A 63x oil-immersion objective lens (HCX Plan-Apochromat 63x NA 1.4 Lbd Bl; Leica) was used for image acquisition. Time-lapses were performed by motorized Olympus IX81 Inverted microscope, driven by an "Olympus Scan^R" software and equipped with a "Hamamatsu Orca-AG" CCD camera 12 bit (pixel size = 6.45 μm), and 10x or 20x (and an additional 1.6x magnification lens where indicated) objectives. Wound healing, cell protrusions and cell streaming assays were performed using an environmental microscope incubator set to 37°C and 5% CO_2 perfusion.

Immunofluorescence

Cells ($1*10^5$) were seeded in a 6-well plate containing glass coverslips and treated as indicated in the text and in figure legends. Coverslips were fixed in 4% paraformaldehyde (PFA) and permeabilized with 0.1% Triton X-100 and 1% BSA 10 minutes. After 1X PBS washes, primary antibodies were added for 1 hour at room temperature. Coverslips were washed in 1X PBS before secondary antibody incubation 1 hour at room temperature, protected from light. FITC- or TRITC-phalloidin was added in the secondary antibody step, where applicable. After removal of not specifically bound antibodies by 1X PBS washing, nuclei were stained with 0.5 ng/ml DAPI. Coverslips were post-fixed and mounted on glass slides in anti-fade mounting medium (Mowiol). Antibodies were diluted in 1X PBS and 1% BSA. Images were acquired by wide-field fluorescence microscope or confocal microscope, as indicated in figure legends.

E-cadherin staining was analyzed by confocal microscopy and images were processed to obtain the straightness index of the junction. "Junction length" was measured by tracking a straight line and "junction tracking" was obtained tracking manually the same junction following its profile. The straightness index of the junction has been quantified as the ratio of the junction length and the junction tracking of the junction. Value close to one indicates straight junction (Fig. 17).

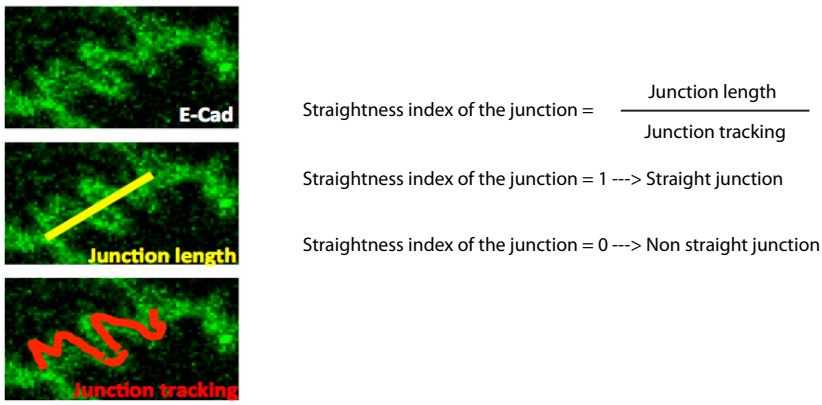

Figure 17. Quantification of the straightness index of the junction.
For more details refer to the text.

Transferrin internalization assay

Cells were grown on glass coverslips 48 hours in the presence or absence of doxycycline. Cells were starved in DMEM supplemented with 2 mM L-glutammine, 20 mM HEPES and 0.2% BSA for 4 hours before experiments. Media was replaced by fresh L15 media (Gibco) containing 5 µg/ml AlexaFluor 488 transferrin (Abcam) and incubated 30 minutes at 4°C. To induce transferrin internalization, samples were transferred to 37°C for 15 minutes. The residual surface-bound transferrin was removed by cold mild acid washing (150 mM NaCl, 1 mM CaCl2, 20 mM CH_3COONa). Cells were washed with cold 1X PBS before fixation with 4% paraformaldehyde. Indirect immunofluorescence staining was performed on permeabilized cells by incubation with RAB5A antibody and Cy3-conjugated secondary antibody. Images were acquired by wide-field fluorescence microscope.

Overlay three-dimensional culture of MCF-10A cells on reconstituted basement membrane

Three-dimensional cultures were performed as described previously, adding some modification to the original protocol. Of note, the already described overlay method has been exploited for some beneficial features: i) compared with the total embedding procedure, overlayed acini are larger, making easier the identification of the hollow lumen and anoikis occurring in lumen formation stage; ii) proteins are easier to be extracted for immunoblotting analysis; iii) acini staining *in situ* allows confocal analysis of the localization of typical subcellular markers. Schematic of the experimental procedure is shown below, in figure 18.

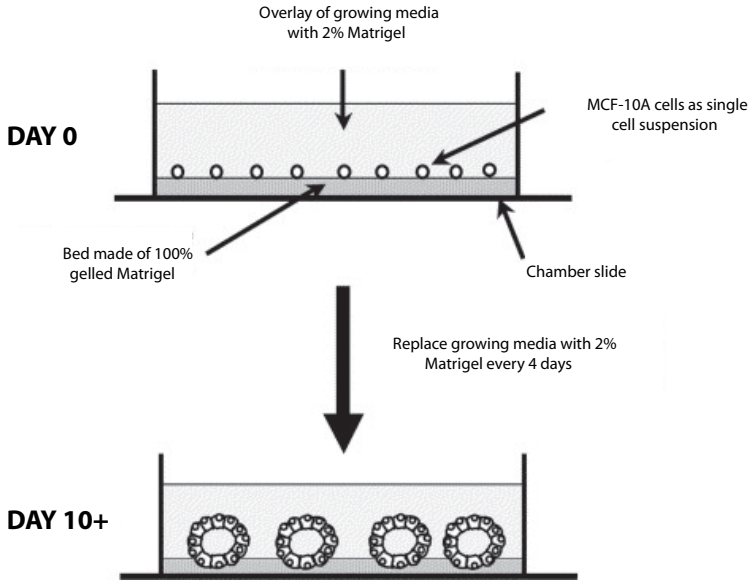

Figure 18. Schematic of the overlay method for culturing MCF-10A in 3D.
For more details, refer to the text.
Adapted from (Debnath, Muthuswamy et al. 2003).

Nunc Lab-Tek II 8-wells Chamber Slide (Thermo Scientific) was coated with 40 μl of 12 mg/ml Growth Factor Reduced BD Matrigel™ Matrix Basement Membrane (BD Biosciences) and allowed to solidify 30 minutes at 37°C. To avoid cell clumps and make sure each acinar spheroid was deriving from one single cell, doxycycline-induced cells were carefully re-suspended and seeded as a single cell suspension at $2.5*10^3$ cells/well in growing media containing 2% matrigel and 5 ng/ml EGF (were specified). Each condition was performed with technical duplicate. Cells were grown at 37°C with 5% CO_2 and growing media was replaced every 4 days. Acini morphogenesis was monitored from seeding (day 0) to longer timepoints (day 28), taking images every 3 days by differential interference contrast (DIC) imaging using a 10x objective.

In growth arrested acini experiments, MEK1 inhibitor PD325901 was added together with doxycycline.

In the mixed culture experiment, not-labeled MCF-10A RAB5AS34N cells were co-cultured with GFP-labeled control MCF-10A EV at a ratio of 1:1. Growing media

containing 2% Matrigel was supplemented with EGF and doxycycline where indicated. Both DIC and fluorescence images were acquired.

Analysis of morphogenetic parameters within 3D cultures

Acini staining was performed optimizing the protocol previously described (Debnath, Muthuswamy et al. 2003). Acini were fixed in 2% paraformaldehyde 5 minutes in agitation. To remove PFA, samples were washed three times with 1% glycine diluted in 1X PBS, 5 minute/wash with gentle agitation. After permeabilization in 1X PBS containing 0.5 % Triton X-100 for 10 minutes at 4°C, acini were washed again three times with 1% glycine diluted in 1X PBS, 5 minute/wash with gentle shaking. Primary antibodies were diluted in IF Buffer (130 mM NaCl, 7 mM Na_2HPO_4, 3.5 mM NaH_2PO_4, 7.7 mM NaN_3, 0.1% bovine serum albumin, 0.2% Triton X-100, 0.05% Tween-20) and incubated overnight at 4°C, with gentle agitation. Samples were rinsed three times (5 minutes each) with 1X PBS and incubated 1 hour with AlexaFluor-secondary antibodies diluted in IF Buffer at room temperature. Un-bound antibodies were removed by three washes in 1X PBS, 5 minute/wash with gentle shaking. Lastly, nuclei were stainined with 0.5 ng/ml DAPI. Acini were washed in 1X PBS and post-fixed in 2% PFA before mounting with fresh antifade mounting medium. Different combinations of antibodies were used: acini were stained with Ki-67 and cleaved caspase 3 antibodies to assess proliferation and apoptosis rates; DAPI, Laminin V and Giantin antibodies were used to study acinar architecture and development. Images were acquired with a Leica TSC SP2 AOBS confocal microscope and a 63x oil-immersion objective lens. ImageJ software was used for image analysis.

Secreted Amphiregulin detection

Doxycycline-induced MCF-10A cells were grown in 2D 4 days in the absence of EGF. Conditioned media, deriving from a similar number or cells, were collected and filtered to eliminate any debrides. Cleared media were applied onto RayBio Human Amphiregulin ELISA kit (RayBiotech) and assayed following the manufacturer's protocol. Briefly, Amphiregulin standard was serially diluted in Assay Diluent B, in a range from zero to 4,000 pg/ml. Samples were tested either pure or diluted 5 times in Assay Diluent B. 100 µl of standard or samples were added to each well and incubated 2.5 hours at room temperature with gentle shaking. The plate was washed 4 times with wash solution using a muti-channel pipette and carefully removing the liquid at each step. After the last wash, 100 µl of biotin antibody was added to each well and incubated 1 hour. The plate was washed as described before and incubated 45 minutes with 100 µl of Streptavidin Solution. The solution was discarded and after washing steps, 100 µl of TMB One-Step Substrate Reagent was added to each well and incubated 30 minutes in the dark. The colorimetric reaction was stopped adding 50 µl of Stop Solution/well and the plate was read immediately at 450 nm by VICTOR3 V Multilabel Counter (PerkinElmer model 1420). All incubation steps were performed at room temperature with gentle shaking. Amphiregulin concentration was calculated plotting the standard curve on a log-log plot with standard concentration on the x-axis and absorbance on the y-axis and drawing the best-fit straight line (as indicated in the manufacturer's protocol). Samples concentrations were calculated considering dilution factors.

Wound healing assay

Cells were seeded in 6-well plate ($1.5*10^6$ cells/well) in complete medium and cultured until a uniform monolayer had formed. RAB5A expression was induced, were indicated, 16 hours before performing the experiment by adding fresh complete media supplemented

with 2.5 μg/ml doxycycline to cells. Cells monolayer was scratched with a pipette tip and carefully washed with 1X PBS to remove floating cells and create a cell-free wound area. The closure of the wound was monitored by time-lapse recording picture of 10 positions/condition. Olympus ScanR inverted microscope with 10x objective was used to take pictures every 5 minutes over a 24 hours period. The assay was performed using an environmental microscope incubator set to 37°C and 5% CO_2 perfusion. After cell induction, doxycycline was maintained in the media for the total duration of the time-lapse experiment. The percentage of area covered by cells (area coverage %) overtime and wound front speed were calculated by MatLab software. In Mitomycin C experiment, 1 μg/ml inhibitor was added together with doxycycline in fresh media 16 hours before scratching the monolayer.

For wound healing assay performed on interfered cells, $2.5*10^5$ cells/well were plated in a 6 well plate and interfered the day after with 1 nM of siRNAs, following the same conditions already described in "RNA interference" section. Confluent and stable monolayers were scratched and cell migration was recorded by time-lapse microscopy.

Kymograph analysis of cell protrusions

Wound healing assay was performed by Ibidi Culture Inserts (Ibidi) to avoid debrides affecting the quality of the kymograph analysis. Inserts were placed in a 12-well plates and MCF-10A cells were plated in each chamber, $5*10^4$ cells/chamber. 16 hours before starting the experiment, growing media was replaced with fresh complete media containing 2.5 μg/ml of doxycycline to induce RAB5A expression. Cell-free, wound area was created by removal of the insert. Cell migration was monitored by Olympus Scan^R inverted microscope with 20x objective (with an addictional 1.6x magnification lens). Pictures were taken with shorter time frame to better evaluate protrusion dynamics. Images from 10 positions/condition were recorded every 30 seconds over 1 hour period. To measure the

dynamic of protrusive structures Kymograph plugin of ImageJ software was used. More in detail, a linear ROI (region of interest) was drawn on the protrusion of the migrating cell (Fig.19A). The software recorded changes of certain intensity and contrast in grey value of the moving structure. A new image (the kymograph) was assembled: the y axis representing a time axis (t) and the unit was the time interval set up in the time-lapse experiment (seconds); and the x axis representing the distance (s) and the unit was the pixel size of the camera.

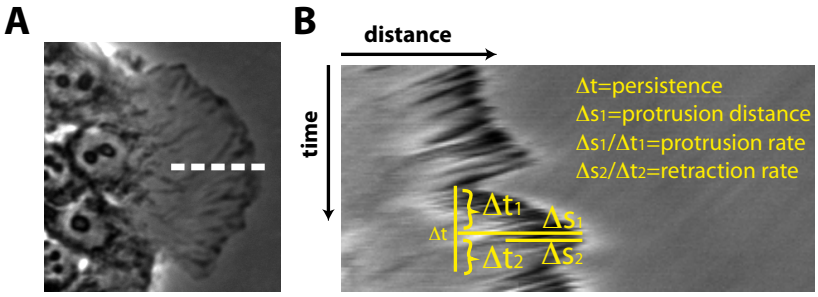

Figure 19. ROI tracking on the migratory protrusion and schematic of a typical kymograph analysis.
(A) Example of ROI tracking on the protrusion of cells at the leading front of the migrating sheet. **(B)** Example of kymograph and relative formulas to calculate protrusion dynamic parameters.

Dynamic parameters were measured on kymograph images: persistence (Δt), protrusion rate ($\Delta s_1/\Delta t_1$) and retraction rate ($\Delta s_2/\Delta t_2$) (Fig.19B). The same time interval and ROI length were set in the analysis of each condition.

Quantification of focal adhesions

Focal adhesions were analyzed in wound healing conditions, focusing on cells at the leading front. MCF-10A cells were seeded $7*10^5$ cells in ibiTreat μ-Dish $^{35\ mm,\ high}$ (Ibidi) and maintained in complete growing medium supplemented with EGF till reaching the complete confluency. The monolayer was induced by doxycycline and 16 hours later, the wound was made by scratching it through a pipette tip. Floating cells were removed by sequential washing and fresh media with EGF and doxycycline was replaced. Migrating epithelial sheets were fixed in 4% paraformaldehyde, before the complete closure of the

wound. Samples were permeabilized with 0.1% Triton X-100 and 2% BSA 10 minutes and blocked 1 hour in 1X PBS containing 2% BSA. Anti-Paxillin or anti-Vinculin primary antibodies were incubated overnight at 4°C, with gentle shaking. Culture dishes were washed in 1X PBS and secondary AlexaFluor-antibodies were incubated 1 hour at room temperature, protected from light. FITC- or TRITC-phalloidin was added in the secondary antibody step, where applicable. Cells were washed and nuclei were stained with 0.5 ng/ml DAPI. Last, samples were post-fixed and stored in 1X PBS at 4°C. Images were taken with a Leica TSC SP2 AOBS confocal microscope and analyzed by ImageJ software: pictures were transformed in binary images using the automatic threshold function and analyzed with Analyze Particle plugin of ImageJ software. Focal adhesions quantification is shown as relative focal adhesion size referred to control cells.

Cell Image Velocimetry

Quantitative analysis of movies obtained from wound healing assay was performed using the Cell Image Velocimetry (CIV) MatLab toolbox. This approach is based on the combination of cell layer segmentation together with image velocimetry algorithm. Among the important features related to this strategy, CIV analysis allows to automatically quantify the advancing front as well as the velocity and directionality of cells inside the migrating monolayer.

First, images are processed enhancing intensity and contrast to clearly discern between cell layers and the background. Based on this, a cell layer segmentation algorithm detects the progression of migrating fronts in consecutive frames and designs a mask for each layer at each frame. Second, a Particle Image Velocimetry (PIV) based algorithm detects the movement of cells within the layers. Last, a quantification step combines mask and PIV data to calculate wound orientation, front speed and mean angular correlation, assigning a specific color code depending on the direction of migration. Coordinated cell migration is

quantified considering mean angular correlation values (with correlation bin size of 100 μm or 80 μm, corresponding to about 4-6 or 2-4 cell rows respectively, depending on the dimension of the wound and cells rows/migrating front in the field available for the analysis) (Milde, Franco et al. 2012).

Cell streaming assay

MCF-10A cells were seeded in 6-well plate ($1.5*10^6$ cells/well) and maintained in complete medium until a uniform and stable monolayer had formed. RAB5A expression was induced 16 hours before performing the experiment. Comparable cell confluence were tested by taking pictures by differential interference contrast (DIC) imaging using a 10x objective and counting the number of nuclei/field. Cell streaming was monitored by time-lapse Olympus Scan^R inverted microscope with 10x objective, taking images every 5 minutes over a 12 hours period. Single cells within the monolayer were manually tracked for 12 hours by "Manual Tracking" plugin of ImageJ software. Migration parameters were obtained by Chemotaxis and Migration Tool ImageJ software plugin.

Single cell random motility assay

Single cells migration was monitored in normal growing conditions. Briefly, cells were seeded sparsely in a 6-well plate ($2*10^4$ cells/well) in complete media supplemented with 20 ng/ml EGF. Doxycycline (2.5 μg/ml) was added to the media 16 hours before starting the experiment. Random cell motility was monitored over a 24 hours period. Pictures were taken every 5 minutes from 10 positions/condition, using a motorized Olympus Scan^R inverted microscope with 10x objective. All the experiments were performed using an environmental microscope incubator set to 37°C and 5% CO_2 perfusion. Single cells were manually tracked using Manual Tracking Tool ImageJ software plugin. Migration plot and

relative parameters were obtained by Chemotaxis and Migration Tool ImageJ software plugin.

In random migration assay performed on RNA interfered cells, MCF-10A cells were seeded the day before ($2.5*10^5$) and interfered with 1 nM of oligos with the same procedure already described in "RNA interference" section. One day after transfection cells were detached and plated to perform the random migration assay. Cells were doxycycline-induced 16 hours before starting the experiment.

MCF-10.DCIS.com cells 3D invasion assay

Invasion phenotype of MCF-10.DCIS.com cells grown in 3D was performed as previously described (Xiang and Muthuswamy 2006). All the coating steps to prepare the chumber slide were performed on ice to avoid a fast and not regular polymerization of the basement membrane substrate. First, 500 μl of atelo-collagen type I (Purecoll, 3.2 mg/ml) was mixed with 62.5 μl of sterile 1X PBS 10x, 62.5 μl of sterile 0.1 M NaOH and 10 μl of 0.1 N HCl to bring the final pH close to 7.5. On ice, we mixed collagen and Matrigel in equal amount such that the final concentration of collagen was 1.6 mg/ml. Nunc Lab-Tek II 8-wells Chamber Slide were coated with 40 μl of mix collagen/Matrigel and allowed to solidify for 1 hour at 37°C. Meanwhile, cells were collected, counted and seeded as single cell suspension at $2.5*10^3$ cells/well in growing media containing 2% Matrigel and 5 ng/ml EGF. RAB5A expression was induced 4 days after seeding and invasive outgrowth was stimulated by 100 ng/ml HGF treatment. Images were taken every 3 days by differential interference contrast (DIC) imaging. Invasive outgrowths were defined as consisting of two or more cells migrating away from their structure of origin. A minimum of 20 images was analyzed for each experimental condition.

Statistical analysis

Student's unpaired t test was used for determining the statistical significance. Significance was defined as $^{*}p < 0.05$; $^{**}p < 0.01$; $^{***}p < 0.001$ and $^{****}p < 0.0001$. Statistic calculations were performed with GraphPad Prism Software. Data are expressed as mean±SEM.

RESULTS

Generation and characterization of stable inducible MCF-10A cell lines expressing RAB5A WT or RAB5AS34N.

To investigate the impact of deregulation of RAB5A expression or function in normal epithelial mammary cells, we chose a human non-transformed mammary epithelial cell line, MCF-10A. MCF-10A cells were infected with a doxycycline inducible lentiviral pSLIK vector carrying RAB5A WT or RAB5AS34N, a useful strategy to time-control the expression of our gene of interest.

After neomycin selection, stable inducible bulk populations were analyzed for the level of expression of RAB5A both by Western Blotting (Fig. 20A) and Immunofluorescence (Fig. 20B). Once confirmed the efficiency of the inducible system and the homogeneity of the bulk population, we proceeded with the functional characterization of the cell lines.

To determine whether genetic manipulation of RAB5A directly impact on its function in endosomal biogenesis and receptor internalization, we stained cells to detect endosomal compartment and performed internalization assays. Doxycycline-induced cells were seeded on coverslip and immunostained for EEA-1 (the early endosomal antigen 1), whose association with endosomal membranes has been demonstrated to be dependent on the activation state of RAB5A (Simonsen, Lippe et al. 1998; Christoforidis, McBride et al. 1999). As expected, the expression of RAB5A WT induced the formation of enlarged, EEA1-positive endosomes. Conversely, in MCF-10A cells expressing RAB5AS34N, a

dominant negative RAB5A mutant (Stenmark, Parton et al. 1994), EEA-1 staining was lost from the endosome and homogeneously distributed into the cytoplasm, demonstrating that RAB5A activation is essential for EEA-1 association with endosomal membranes (Fig. 20B).

A well-accepted assay to monitor the efficiency of endocytosis is transferrin internalization. This ligand by binding to its cognate receptor is constitutively internalized through clathrin-dependent endocytosis. Transferrin internalization was assessed on un-induced control and doxycycline-induced MCF-10A RAB5AS34N cells. In this assay, cells were incubated with AlexaFluor488-conjugated transferrin, and then washed with a mild acid solution to remove all the transferrin that had not been internalized. Compared with control cells, RAB5AS34N-expressing cells showed a reduced number of vesicles containing the fluorescently labeled transferrin (Fig. 20C, D).

As expected, genetic manipulation of RAB5A by the expression of its dominant negative form RAB5AS34N, alters its function both in endosomal biogenesis (Fig. 20B) and receptor internalization (Fig. 20C,D).

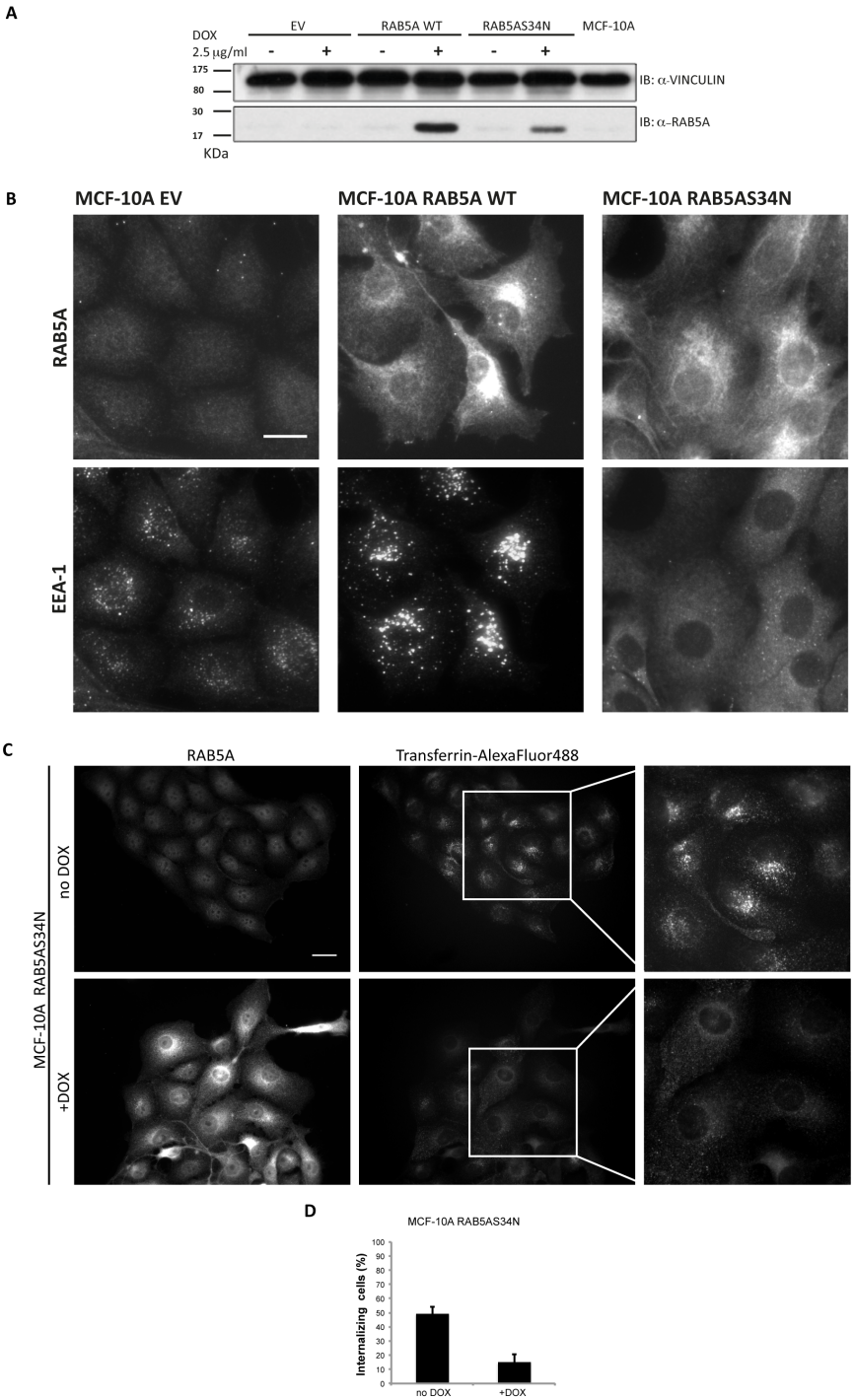

Figure 20. The expression of RAB5A WT or RAB5AS34N alters the endosomal compartment.

(**A**) 30 µg of lysates of the indicated cell lines were loaded on a 15% polyacrylamide gel. Nitrocellulose membrane was blot by mouse monoclonal anti-human vinculin antibody or rabbit polyclonal anti-human RAB5A antibody. Vinculin was used as loading control. (**B**) Cells were seeded on coverslips and induced 72 hours by 2.5 µg/ml doxycycline, fixed in 4% paraformaldehyde and stained with anti-human RAB5A or anti-human EEA-1 antibody, to be analyzed by wide field microscopy. Representative images are shown (Scale bar, 20 µm). (**C**) Cells in un-induced or doxycycline-induced conditions were treated 15 minutes with fluorescent transferrin. Not-internalized transferrin was removed by mild acid wash. Coverslips were fixed and stained to detect RAB5AS34N expression and internalized fluorescent transferrin. Representative fluorescence images and relative insets are shown (Scale bar, 40 µm). (**D**) Quantification of the percentage of cells showing internalized transferrin is shown, counting 100 cells/condition. Error bars represent the standard deviation.

RAB5A expression alters MCF-10A cells proliferation rate and EGF-dependency, without affecting apoptosis.

To test whether the ectopic expression of RAB5A WT or S34N would affect the proliferation rate and EGF-dependency of MCF-10A cells, equal number of cells was plated in a 96-wells plate. Growth rates of un-induced and induced cells were monitored every 24 hours by MTT cell proliferation assay, a widely accepted protocol to assess cell viability and proliferation relying on the capability of the cell to metabolize and transform tetrazolium salts in purple formazane, detected by spectrophotometer (Mosmann 1983).

In control, un-induced conditions, all cell lines display the expected EGF-dependent growth profile and a similar proliferation rate (Fig. 21A). Interestingly, the expression of RAB5A WT by doxycycline treatement impaired cell growth even in EGF supplemented media (Fig. 21B, green line); on the contrary, MCF-10A RAB5AS34N cells acquired an EGF-independent growth phenotype (Fig. 21C, pink line).

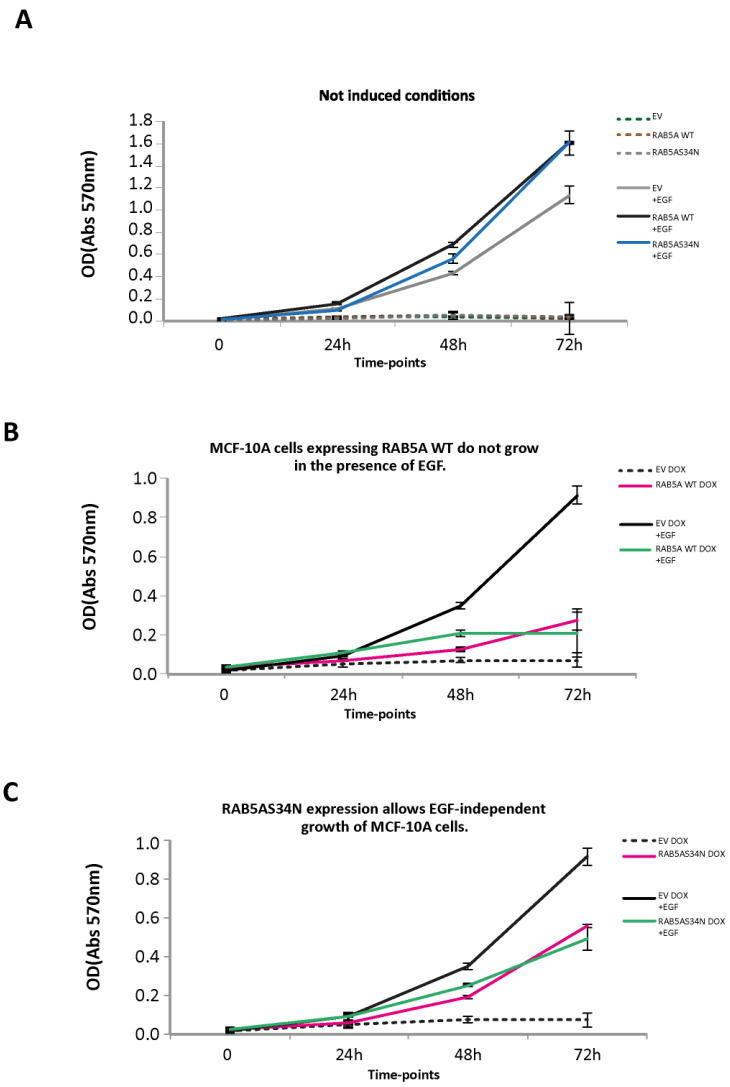

Figure 21. Cell proliferation is altered by the expression of RAB5A WT or RAB5AS34N.
(**A**) Cell growth depends on EGF in un-induced conditions (cell lines grown in media without EGF are represented with dotted lines). (**B**) MCF-10A cells expressing RAB5A WT do not grow even in the presence of EGF (green line). (**C**) The expression of RAB5AS34N allows EGF-independent growth of MCF-10A cells (pink line). The experiment was repeated 3 times with quadruplicate technical replicates. Error bars represent standard deviation for each time-point.

To better understand if the alteration in growth rate was also related to a deregulation of cell death, an AnnexinV-FITC/PI staining was performed. Through this approach, we could discriminate between viable (AnnexinV-FITC$^-$/PI$^-$), early apoptotic (AnnexinV-FITC$^+$/PI$^-$) or late apoptotic/necrotic cells (AnnexinV-FITC$^+$/PI$^+$). Compared with control MCF-10A EV cell line, FACS analysis showed no significant differences in the number of

apoptotic cells, considered as the sum of early and late apoptotic cells, ruling out that alteration in RAB5A levels and function causes programmed cell death (Fig. 22).

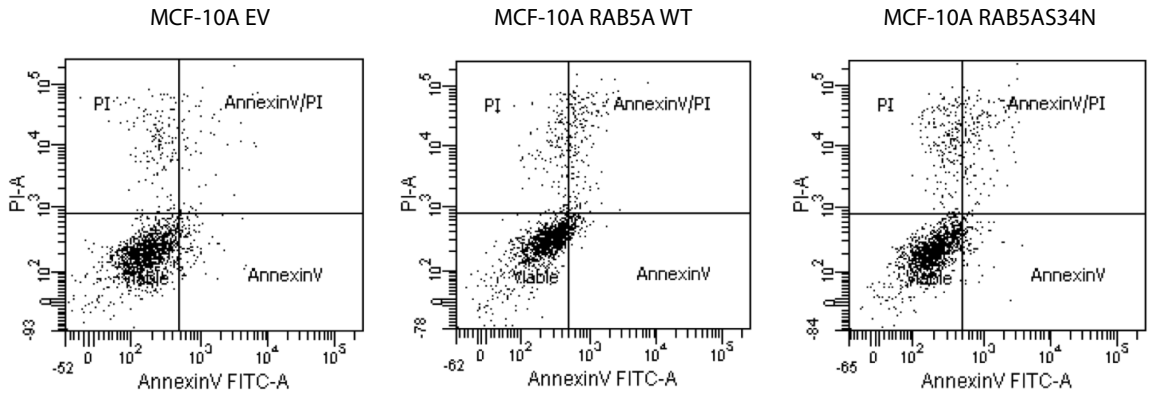

Figure 22. Cell death is not affected by RAB5A WT or RAB5AS34N expression.
Doxycycline-induced MCF-10A cells were collected in growing conditions and stained with AnnexinV-FITC and PI. FACS analysis plots revealed no significant differences between subpopulations of cells: viable (AnnexinV-FITC$^-$/PI$^-$), early apoptotic (AnnexinV-FITC$^+$/PI$^-$) and late apoptotic/necrotic (AnnexinV-FITC$^+$/PI$^+$) cells. 30,000 events were acquired for each cell line. Data analysis was performed by FACS Diva 6.1.1 software. The experiment was repeated 3 times.

RAB5A WT expression induces a delay in S-phase entry.

The expression of RAB5A WT causes impairment of MCF-10A cells proliferation; we thus explored this defect in further detail by analyzing by FACS the DNA content as a measure of the cell cycle profile. Doxycycline-treated MCF-10A EV and MCF-10A RAB5A WT cells were first grown for 48 hours in complete media without EGF to induce growth arrest in G0 by EGF-starvation. Afterwards, cell cycle re-entry was induced by an acute stimulation with EGF. Every 3 hours we evaluated cell cycle progression by FACS analysis of PI stained cells. Control MCF-10A EV cells entered into the cell cycle 12 hours after the release (Fig. 23, top panels). RAB5A WT expressing cells, instead, entered the S-phase with a nearly 3 hours delay (Fig. 23, bottom panels).

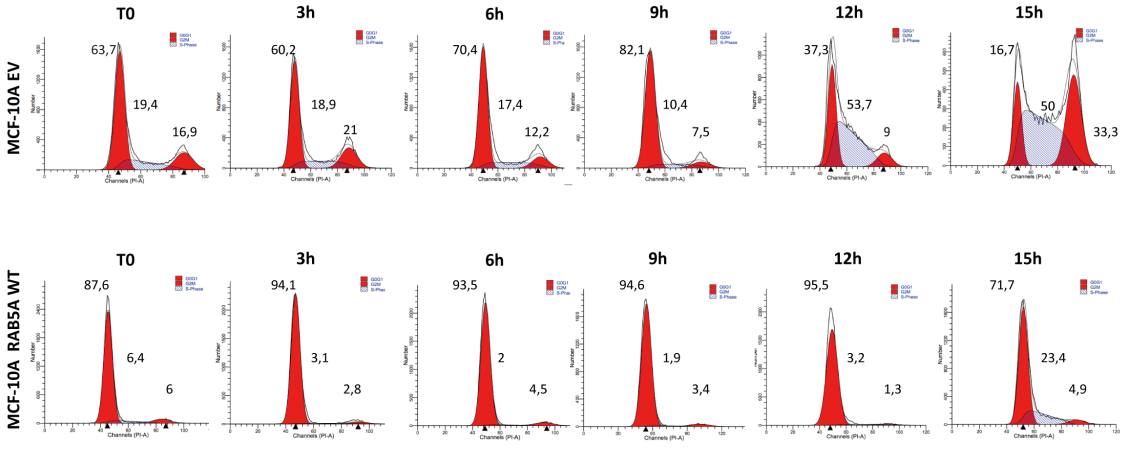

Figure 23. MCF-10A cells expressing RAB5A WT show a delay in entering in S-phase.
Doxycycline-induced MCF-10A cells were synchronized in G0 by 48 hours of EGF-starvation, and acutely stimulated with 20 ng/ml EGF to induce cell cycle re-initiation. Cells were fixed and stained with PI at different time-points to be analyzed by FACS. Graphs show cell cycle progression and relative percentages of cells throughout the different phases of the cell cycle. Top: MCF-10A EV cells clearly enter into the S-phase after 12 hours. Bottom: the expression of RAB5A WT delays the S-phase entry, cells start to cycle 15 hours after the release. 20,000 events were acquired for each time-point. Data analysis was performed by ModFit software. The experiment was repeated 3 times.

The delayed onset of S-phase was also confirmed by double thymidine block experiments. Doxycycline-induced cells were treated with a double thymidine pulse for synchronizing them at the G1/S border. Cell were then released by addition of fresh complete media and collected at different time-points to monitor DNA content and cell cycle progression by PI-staining and FACS analysis. As it is shown, cell cycle progression through S-phase and G2/M was delayed in RAB5A WT expressing cells, compared with control (Fig.24).

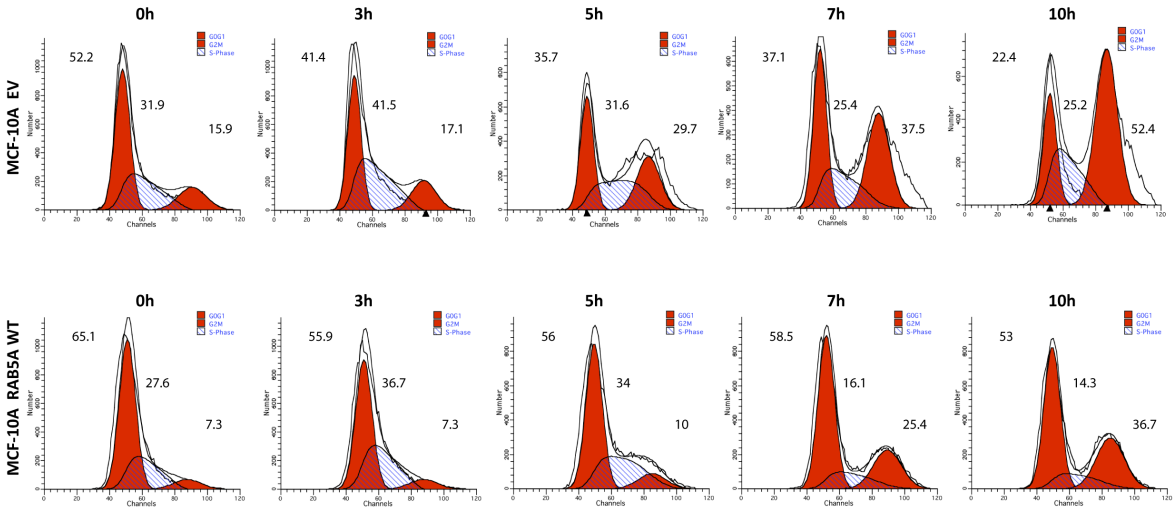

Figure 24. MCF-10A cells expressing RAB5A WT show a delay in cell cycle progression. Doxycycline-induced MCF-10A cells were synchronized at G1/S border by double thymidine treatment. Fresh media supplemented with 20 ng/ml EGF was added to induce cell cycle re-initiation. Cells were fixed and stained with PI at different time-points to be analyzed by FACS. Cell cycle progression and relative percentages of cells in the different cell cycle phases are shown. Top: MCF-10A EV cells cycles after 5 hours. Bottom: the expression of RAB5A WT delays cell cycle progression. 20,000 events were acquired for each time-point. Data analysis was performed by ModFit software. The experiment was repeated 3 times.

MCF-10A cells expressing RAB5A WT form a reduced number of acini that display a significantly larger size in 3D culture.

To test whether the expression of RAB5A WT affects MCF-10A cells ability to proliferate and to undergo a morphogenetic program in 3D culture on reconstituted basement membrane, we exploited the 3D matrix overlay assays. Cells were seeded on top of Matrigel in the presence or absence of EGF and overlaid with low concentration of soluble matrigel under conditions in which hollow acini, recapitulating mammary gland morphology, are formed (Debnath, Muthuswamy et al. 2003). As expected, both MCF-10A EV and RAB5A WT cells were not proliferating in the absence of EGF (Fig. 25, on the left), corroborating the observation obtained in 2D culture. However, RAB5A WT-expressing cells formed a significantly reduced number of acini, but unexpectedly, the few that grew had a dramatic increased size, suggesting that in those cells overcoming cell

cycle delay, RAB5A expression promotes hyper-proliferation (Fig. 25). Indeed, normal spheroids stop proliferating at day 14 from seeding, once the morphogenetic program is completed (Debnath, Muthuswamy et al. 2003). RAB5A WT acini, instead, kept on proliferating even at later time-points. The mechanisms enabling to overcome the intial RAB5A-dependent proliferation delays and the cell cycle arrest typically seen in mature and differentiated hollow acini remain unclear and would require further investigation.

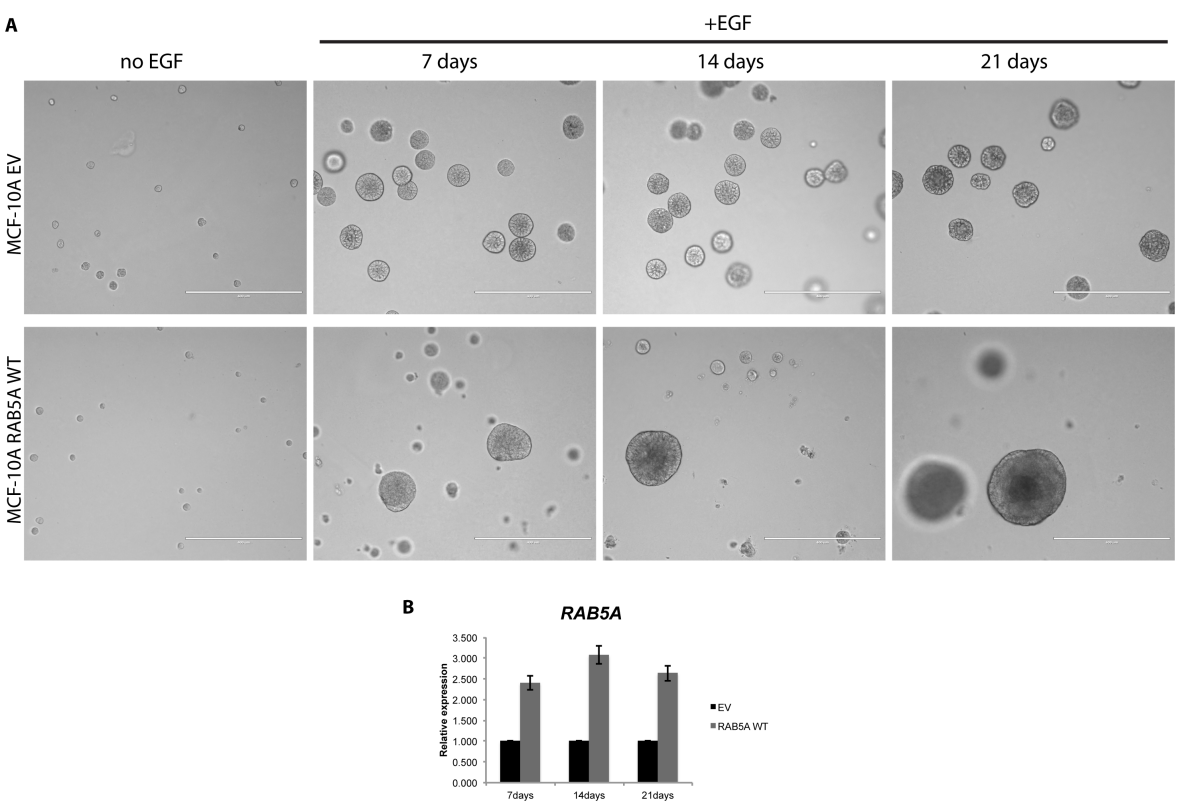

Figure 25. MCF-10A cells expressing RAB5A WT form a reduced number of 3D acini that display a significant increased size.

(A) Equal number of cells was cultured on Matrigel in the absence or presence of EGF. Top panels: both cell lines were not able to proliferate in the absence of EGF (no EGF). In growing condition (EGF), after 7 days of 3D culture RAB5A WT expressing acini (bottom panels) were fewer but bigger then control cell line (top panels). At longer time-points RAB5A WT acini, but not the control one, continue to grow. Images were collected every 2-3 days. Representative phase contrast images are shown (Scale bar, 400 μm). The experiment was repeated 5 times with 2 technical replicates. **(B)** *RAB5A* expression levels on induced-MCF-10A cells quantified by qRT-PCR at different time-points are shown. *GAPDH* was used as normalizer and EV cells relative to each time-point as calibrator. Error bars represent standard deviation.

MCF-10A cells expressing RAB5A WT show increased ERK1-2 phosphorylation both in 2D and 3D.

RAB5A WT expressing cells showed an altered EGF-dependent growth both in 2D and 3D. To characterize the involvement of EGFR signaling cascade in the process, cells were cultured either in un-induced or doxycycline-induced conditions for 72 hours and EGF-starved 9 hours. Protein lysates were collected after 5 minutes of acute stimulation with 100 ng/ml of EGF; the activation of the main signaling pathways was monitored by Western Blotting (Fig. 26A). EGFR and PI3K/Akt cascades were not affected. Conversely, RAB5A WT expressing cells showed a marked increase in the level of pERK1-2. Importantly, MAPK/ERK1-2 up-regulation was also confirmed by Western Blotting on protein lysates obtained from acini after 21 days of 3D culture, when RAB5A WT expressing acini continue to grow (Fig. 26B, C).

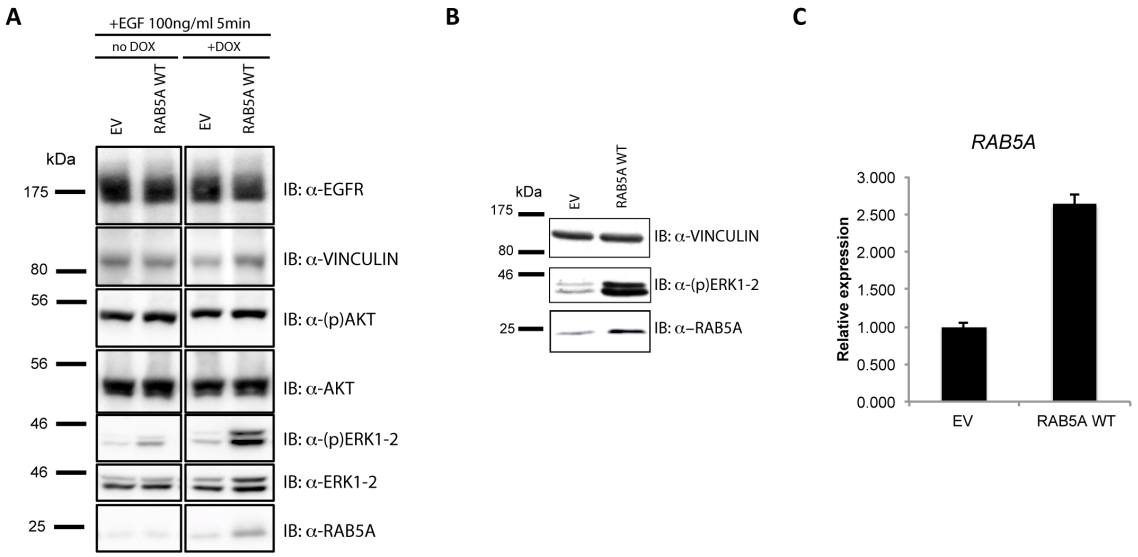

Figure 26. MCF-10A cells expressing RAB5A WT show increased activation of MAPK/ERK1-2 pathway.

(A) The indicated cell lines were cultured un-induced (no DOX) or induced (+DOX) 3 days, starved 9 hours and treated with an acute dose of EGF (100 ng/ml) to detect EGFR signaling pathway modulation. 30 μg of lysate were loaded on 8% (high molecular weight proteins) or 15% (low molecular weight proteins) polyacrylamide gels. Nitrocellulose membrane was immunoblotted as indicated and vinculin was used as loading control. **(B)** Protein lysates obtained from 3D acini cultured 21 days on Matrigel were loaded on a 8% or 15% polyacrylamide gel. Nitrocellulose membrane was immunoblotted as shown. Vinculin was used as loading control. **(C)** Induced *RAB5A* mRNA in 21 days MCF-10A EV or RAB5A WT acini, as detected by qRT-PCR, is shown. *GAPDH* was used as normalizer and EV cells as calibrator. Error bars represent standard deviation. The experiment was performed 3 times.

The results suggest that RAB5A may exert an apparently different and distinct dual function in 2D culture as compared with 3D long-term culture. On the one hand, MCF-10A expressing RAB5A WT clearly showed an impairment of 2D proliferation, caused by a delay in S-phase entry. On the other hand, when cultured in 3D, these cells develop few but giant acini. This apparently controversial data may be possibly rationalized considering that the expression of some oncogenes in normal cells cause aberrant proliferation which can trigger a stress response leading to accumulation of DNA damage responsible for the induction of either apoptosis or senescence-like growth arrest (Hills and Diffley 2014). Within this framework, RAB5A elevated expression may induce an oncogenic-like type of stress response: on one hand, the accumulation of severe DNA damages may lead to the elimination of damaged cells thus explaining first the blockade in S-phase and secondly the reduced number of acini. On the other hand, the formation of over-proliferative acini may be related to the acquisition and selection of a second mutation induced by accumulation of cell stress, enabling to overcome the cell cycle defect and sustaining an uncontrolled proliferation.

Acini derived from MCF-10A RAB5A WT cells show an increased proliferation, without any alteration in morphological architecture and polarity.

To assess whether RAB5A-dependent phenotypes could be related to an over-proliferation effect or a defect in apoptosis, a single cell suspension was seeded on 3D reconstituted basement membrane and cultured in the presence of doxycycline and EGF in order to induce the formation of 3D acinar-like structures. Acini were fixed and stained at different time-points to monitor their maturation. First, proliferation potential was assessed by Ki-67 staining, a protein easily detectable in the active S-phases of the cell cycle, but

not in G0 (Scholzen and Gerdes 2000). As previously reported, normal acini stop proliferating after 14-16 days. Accordingly, after 21 days of culture no Ki-67 positive cells were detectable in control MCF-10A EV acini. Conversely, RAB5A WT-expressing acini retained a sizable number of Ki-67 positive cells even after 21 days of culture (Fig. 27A, B).

Next we assessed whether RAB5A would affect survival under these 3D culture conditions. To this end, we measured the rate of apoptotic cell by staining for cleaved caspase 3, a prototypical marker of this cellular process. RAB5A WT expression did not significantly alter cell survival (Fig. 27A), confirming previous data obtained by Annexin V-PI staining and FACS analysis in 2D culture (Fig. 22).

Frequently, altered cell growth in 3D culture is the result of an altered epithelial cells polarity (Bilder 2004; (Partanen, Nieminen et al. 2007; Partanen, Tervonen et al. 2012). Thus, we immunostained day-14-acini with DAPI to assess the overall morphology and with antibodies against the Golgi protein Giantin (red) that in polarized epithelia displays an apical orientation toward the lumen, and Laminin V (green), a basal marker that delineate the secretion of the basement membrane components.

Neither the morphological architecture nor deposition of basement membrane and Golgi polarity were, however, altered by the expression of RAB5A WT (Fig. 27C).

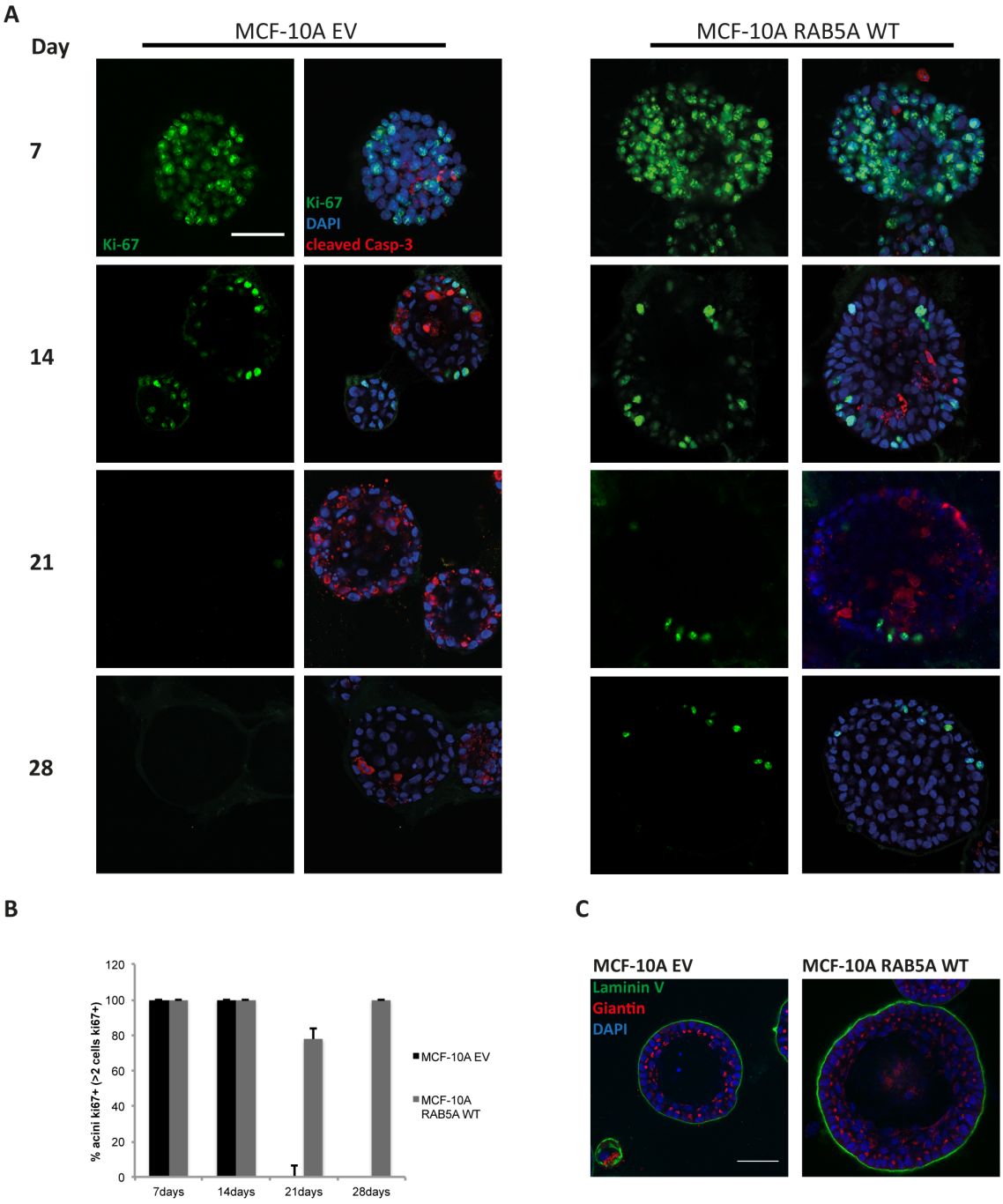

Figure 27. Acini derived from MCF-10A RAB5A WT cells show increased proliferation but no alteration in the morphological architecture or polarity establishment.

(A) MCF-10A cells were seeded on Matrigel as a single cell suspension and fed with Assay Media containing EGF and doxycycline. Acini were fixed in paraformaldehyde and stained at the indicated time-points to assess proliferation and apoptosis overtime. Samples were stained as follows: DAPI (blue), Ki-67 (green) and cleaved caspase 3 (red) and analyzed by confocal microscopy. Representative fluorescence z-stack images of Ki-67 alone or merged channels are shown (Scale bar, 50 μm). **(B)** Quantification of the percentage of acini showing at least 2 Ki-67+ cells is shown. Error bars represent standard deviation. **(C)** Acinar morphology and architecture are conserved despite the expression of RAB5A WT. Doxycycline-induced acini at day 14 were immunostained with antibodies against the Golgi protein Giantin (red), Laminin V (green) and DAPI (blue). Representative fluorescence images acquired by confocal microscopy are shown, equatorial cross sections were chosen to show the overall acinar architecture (Scale bar, 50 μm). The experiment was repeated 3 times.

The expression of RAB5A WT in MCF-10A cells alters signaling pathways involved in cell cycle control and DNA repair.

To gain some clues to signaling cascades that might be affected by RAB5A WT expression and may lead to derailed cell proliferation, we performed an Affymetrix analysis comparing MCF-10A EV and MCF-10A RAB5A WT gene profiling. Doxycycline-induced MCF-10A cells were grown in 2D in EGF-supplemented complete media for 72 hours and total RNA was extracted to compare genes expressed in control and RAB5A WT expressing cells. Genes were ranked according to the log2 ratio values and we initially focused our attention on the most up- or down-regulated genes (Tables 3-4). Gene enrichment analysis performed on these selected gene lists by DAVID Bioinformatics Resources software, revealed that a number of genes involved in cell cycle and DNA repair pathways (such as APOBEC3B and HIST1H3F) were down-regulated in RAB5A WT expressing MCF-10A cells.

up-regulated genes	down-regulated genes
log2 ratio ≥0.5 = 1156 genes	log2 ratio≤-0.5 = 1077 genes
log2 ratio ≥1 = 260 genes	log2 ratio≤-1 = 213 genes
log2 ratio ≥2 = 54 genes	log2 ratio≤-2 = 3 genes

Table 3. log2 ratio gene ranking.
Gene lists, obtained by Affymetrix gene profiling, were ranked according to the log2 ratio. Three different thresholds and relative number of genes up- or down-regulated in RAB5A WT expressing cells are shown.

		TOP 10 UP-REGULATED GENES
A_log2ratio	**Gene Symbol**	**Short description**
4.3607	FAM113A Family with sequence similarity 113, member A	It is a member of the GDSL/SGNH superfamily. Members of this family are hydrolytic enzymes with esterase and lipase activity and broad substrate specificity.
4.2221	ASMTL N-acetylserotonin O-methyltransferase-like protein	The function is unknown. The presence of the putative catalytic domain of S-adenosyl-L methionine binding argues for a methyltransferase activity. It is widely expressed.
3.6408	GPD1 Glycerol-3-phosphate dehydrogenase [NAD(+)]	It promotes the reaction sn-glycerol 3-phosphate + NAD^+ = glycerone phosphate + NADH. Involved in the hypertriglyceridemia, transient infantile (HTGTI)
3.5448	CRISP3 Cysteine-rich secretory protein 3	It is involved in the innate immune response and in neutrophils is localized in specific granules.
3.4420	IL2RG Interleukin-2 receptor subunit gamma	It is an important signaling component of many interleukin receptors, including those of interleukin -2, -4, -7 and -21, and is thus referred to as the common gamma chain. Diseases associated with IL2RG include severe combined immunodeficiency, and gamma chain deficiency.
3.4380	C1orf220 Chromosome 1 Open Reading Frame 220	Uncharacterized.
3.3882	LOC646976	LOC646976 is an RNA gene, and is affiliated with the antisense RNA class. Uncharacterized.
3.2704	IFI6 Interferon alpha-inducible protein 6	It is involved in the cytokine-mediated signaling pathway and immune response It is a negative regulation of cysteine-type endopeptidase activity involved in apoptotic process. It is induced by alpha and beta interferons.
3.1780	PDE9A High affinity cGMP-specific 3',5'-cyclic phosphodiesterase 9A	It hydrolyzes the second messenger cGMP, which is a key regulator of many important physiological processes. It is widely expressed except blood. Highest levels in brain, heart, kidney, spleen, prostate and colon.
3.0934	FGF18 Fibroblast growth factor 18	It plays an important role in the regulation of cell proliferation, cell differentiation and cell migration. Required for normal ossification and bone development. Stimulates hepatic and intestinal proliferation.

		BOTTOM 10 DOWN-REGULATED GENES
A_log2ratio	**Gene Symbol**	**Short description**
-2.2286	APOBEC3B DNA dC->dU-editing enzyme APOBEC-3B	It is a DNA deaminase (cytidine deaminase) which acts as an inhibitor of retrovirus replication and retrotransposon mobility via deaminase-dependent and -independent mechanisms.
-2.2035	S100A8 S100 Calcium Binding Protein A8	It is a calcium- and zinc-binding protein which plays a prominent role in the regulation of inflammatory processes and immune response. It can induce neutrophil chemotaxis and adhesion. Its role as an oxidant scavenger has a protective role in preventing exaggerated tissue damage by scavenging oxidants. Can act as a potent amplifier of inflammation in autoimmunity as well as in cancer development and tumor spread.
-2.0823	MIR205 MicroRNA 205	It is an RNA gene, and is affiliated with the undefined RNA class. Diseases associated with MIR205 include esophageal squamous cell carcinoma.
-1.9117	CLCA2 Calcium-activated chloride channel regulator 2	It plays a role in modulating chloride current across the plasma membrane in a calcium-dependent manner, and cell adhesion. Involved in basal cell adhesion and/or stratification of squamous epithelia. May act as a tumor suppressor in breast and colorectal cancer. Plays a key role for cell adhesion in the beginning stages of lung metastasis via the binding to ITGB4.
-1.9091	HIST1H3F Histone Cluster 1, H3f	Core component of nucleosome. Thereby plays a central role in transcription regulation, DNA repair, DNA replication and chromosomal stability.
-1.8617	TMEM156 Transmembrane protein 156	Uncharacterized.
-1.7855	STC2 Stanniocalcin-2	It has an anti-hypocalcemic action on calcium and phosphate homeostasis. It is expressed in a wide variety of tissues and the expression of this gene is induced by estrogen and altered in some breast cancers.
-1.7818	FAM72D Family With Sequence Similarity 72, Member D	It is up-regulated in gastric cancer. An important paralog of this gene is FAM72C.
-1.7344	MTSS1 Metastasis suppressor protein 1	It may be related to cancer progression or tumor metastasis in a variety of organ sites, most likely through an interaction with the actin cytoskeleton. It is classified as a tumor suppressor.
-1.6886	SLC7A11 Solute Carrier Family 7 (Anionic Amino Acid Transporter Light Chain, Xc- System), Member 11	It is a member of a heteromeric, sodium-independent, anionic amino acid transport system that is highly specific for cysteine and glutamate. It is the predominant mediator of Kaposi sarcoma-associated herpesvirus fusion and entry permissiveness into cells. The expression of this gene is increased in primary gliomas.

Table 4. Top 10 up-regulated and bottom 10 down-regulated genes in MCF-10A cells expressing RAB5A WT.

The expression of RAB5A WT in growth-arrested, polarized three-dimensional acinar structures induces re-initiation of proliferation in a MAPK/ERK1-2-dependent manner.

Most of human carcinomas, including breast cancer, are caused by the malignant transformation of epithelial cells. Our data are consistent with the expression of RAB5A in the entire MCF-10A cell population since the beginning of the morphogenetic process. However, carcinoma may arise from a secondary event within a context of an established epithelium, when disruption of tissue integrity and epithelium polarity may synergize with oncogenes and induce invasive properties (Chatterjee, Seifried et al. 2012)**.** Within this context, for example, it has been already shown that acute activation of ErbB-2, a member of EGFR family frequently amplified or over-expressed in DCIS cases, triggers re-initiation of proliferation and disruption of cell-to-cell junctions and polarity in terminally differentiated acini (Muthuswamy, Li et al. 2001).

To determine whether the expression of RAB5A WT affects well-differentiated and growth-arrested 3D acinar structure, MCF-10A EV or RAB5A WT cells were plated on Matrigel without doxycycline. After 21 days in culture we did not observe any change in size of acini derived from both cell lines, indicating a growth-arrested state was reached under these conditions. Next we added doxycycline to the media to induce the ectopic expression of RAB5A WT (Fig. 28A, Schematic of the experiment), which was verified by Western Blotting (Fig. 28B). Under these conditions, we observed a thickening of the outer polarized layer of cells in RAB5A WT-expressing acini, suggesting re-initiation of proliferation (Fig. 28C).

As previously described, MCF-10A cells expressing RAB5A WT showed an increased ERK1-2 phosphorylation both in 2D and 3D; to investigate whether re-entry into the cell cycle was dependent on MAPK/ERK1-2 pathway, post-mitotic acini media was replaced with media containing doxycycline and a MEK specific inhibitor (1 μM

PD325901). MAPK/ERK1-2 inhibition completely abolished the phenotype induced by RAB5A WT expression (Fig. 28C, right panels). The effectiveness of the specific inhibitor was detected by Western Blotting. RAB5A WT expressing acini showed increased levels of pERK1-2, not detectable in the same cells co-treated with PD325901 (Fig. 28D).

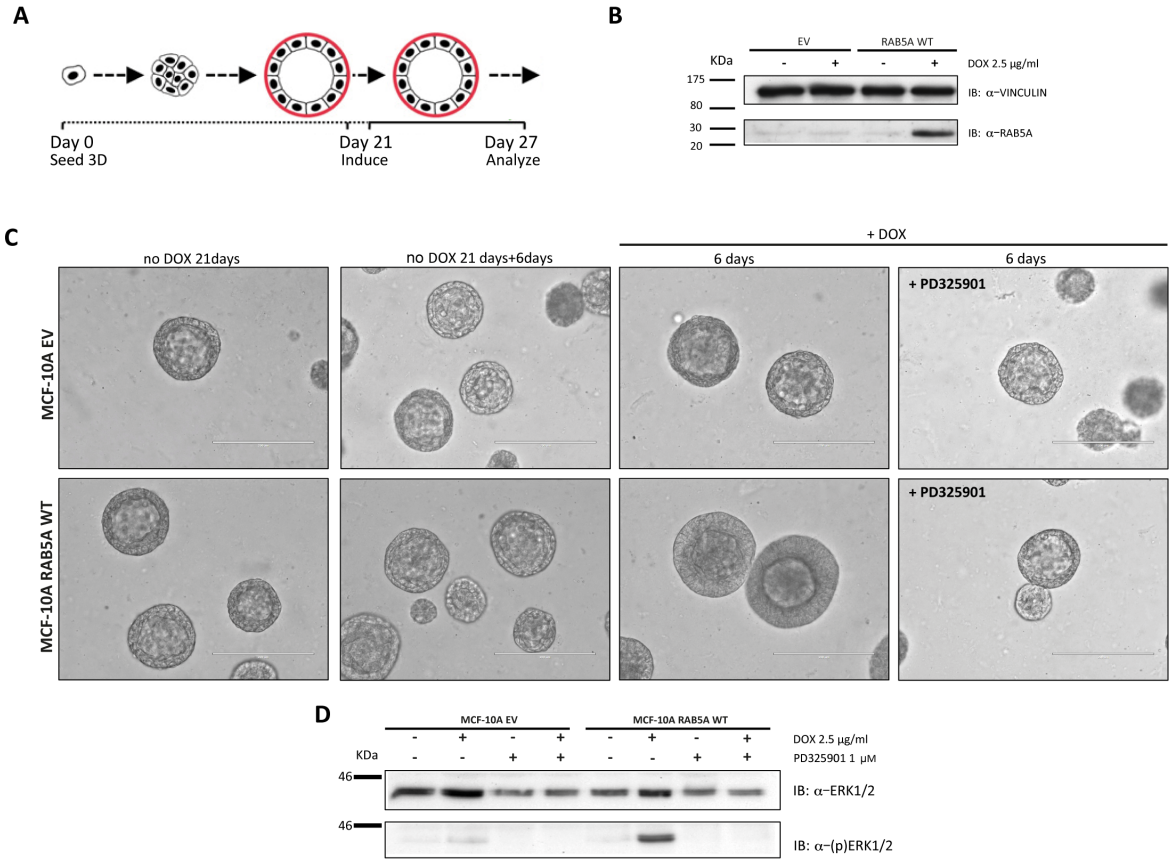

Figure 28. The re-initiation of proliferation induced by RAB5A WT expression in post-mitotic acini is MAPK/ERK1-2 dependent.

(A) Schematic of the experimental procedure, adapted from (Leung and Brugge 2012). Single cell suspension was plated on Matrigel and fed with complete media. After 21 days growth-arrested acini were doxycycline-induced 6 days. **(B)** 30 µg of lysates of the cell lines used to perform 3D experiments were loaded on a 15% polyacrylamide gel. Nitrocellulose membrane was blot by mouse monoclonal anti-human vinculin antibody or rabbit polyclonal anti-human RAB5A antibody. Vinculin was used as loading control. **(C)** As described by the experimental procedure, acini were fed 21 days till reaching of the post-mitotic state. Subsequently, they were induced 6 days by 2.5 µg/ml DOX in the presence or absence of MEK1 inhibitor (PD325901, 1 µM). Representative phase contrast images are shown (Scale bar, 200 µm). **(D)** PD325901 treatment abolished the increase in pERK1-2 level induced by RAB5A WT expression. 50 µg of lysates of MCF-10A EV or RAB5A WT cells, treated as indicated, were loaded on an 8% polyacrylamide gel. Nitrocellulose membrane was blot by mouse monoclonal anti-human pERK1-2 antibody or rabbit polyclonal anti-human total ERK1-2 antibody. Total ERK1-2 was used as loading control. The experiment was performed 3 times.

Cell cycle re-entry was confirmed by Ki-67 staining performed on these acini. Thus, upon expression of RAB5A WT, post-mitotic, growth-arrested acini re-initiated proliferation and repopulated the lumen (Fig. 29A, B).

Collectively these evidences suggest that RAB5A WT expression in post-mitotic acini induces MAPK/ERK1-2 dependent re-initiation of proliferation.

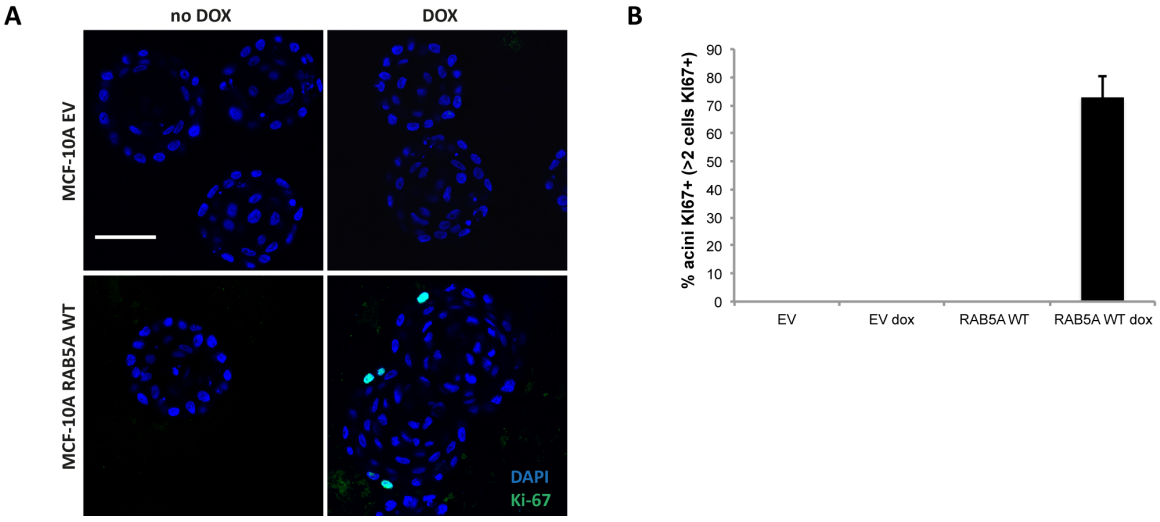

Figure 29. RAB5A expression in post-mitotic acini induces re-initiation of proliferation.
(A) Un-induced (no DOX) or induced (DOX) post-mitotic acini derived from the indicated cell lines were fixed and immunostained with DAPI (blue) and Ki-67 (green). Representative merged fluorescence images acquired by confocal microscopy are shown (Scale bar, 50 µm). **(B)** Quantification of the number of acini with at least 2 $Ki67^{+}$ cells, expressed as percentage on the total number of acini analyzed/condition. Error bars represent standard deviation. The experiment was performed 3 times.

Impaired RAB5A function promotes EGF-independent growth of MCF10-A cells both in 2D and 3D cultures.

By testing cell proliferation we uncover an unexpected phenotype following impairment of RAB5A function. The expression of RAB5AS34N induced cell proliferation in the absence of EGF both in 2 D (Fig. 21C) as well as in 3D Matrigel culture (Fig. 30).

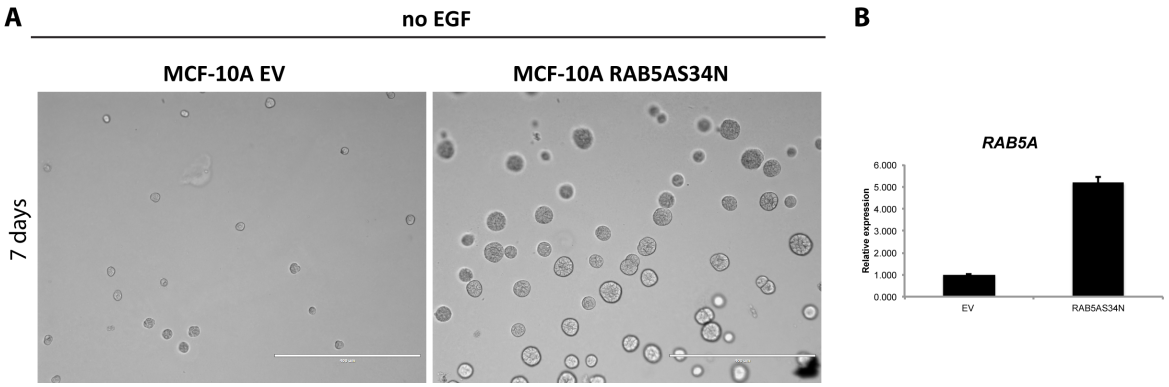

Figure 30. MCF-10A cells expressing RAB5AS34N proliferate in 3D in the absence of EGF. **(A)** Doxycycline-induced MCF10A EV (on the left) and RAB5AS34N (on the right) cells were plated on Matrigel as a single-cell suspension and fed with media without EGF. RAB5AS34N expressing cells are able to proliferate and form acini even in the absence of EGF, confirming data collected in 2D. Representative phase contrast images are shown (Scale bar, 400 μm). The experiment has been performed 5 times with 2 technical replicates. **(B)** *RAB5A* expression levels of induced-MCF-10A acini quantified by qRT-PCR are shown. *GAPDH* was used as normalizer and EV acini as calibrator. Error bars represent standard deviation.

Conditioned media derived from MCF-10A cells expressing RAB5AS34N sustain EGF-independent growth of control MCF-10A cells.

Growth factor-independent cell proliferation can be brought about either by activation of intrinsic signaling pathways or through the autocrine release of soluble growth factors. We initially tested this latter possibility. We cultured doxycycline-induced MCF-10A EV and RAB5AS34N cells in the absence of EGF for 4 days and collected supernatants, which were added to control MCF-10A cells. Strikingly, conditioned media derived from MCF-10A RAB5AS34N cells was sufficient to promote cell proliferation in the absence of EGF (Fig. 31A, right panels). As controls, cells were also plated in fresh media in the presence or absence of EGF. (Fig. 31A, left panels). Cell proliferation was monitored by acquiring images every 2 days and quantified counting the number of cells/field in each condition (Fig. 31B).

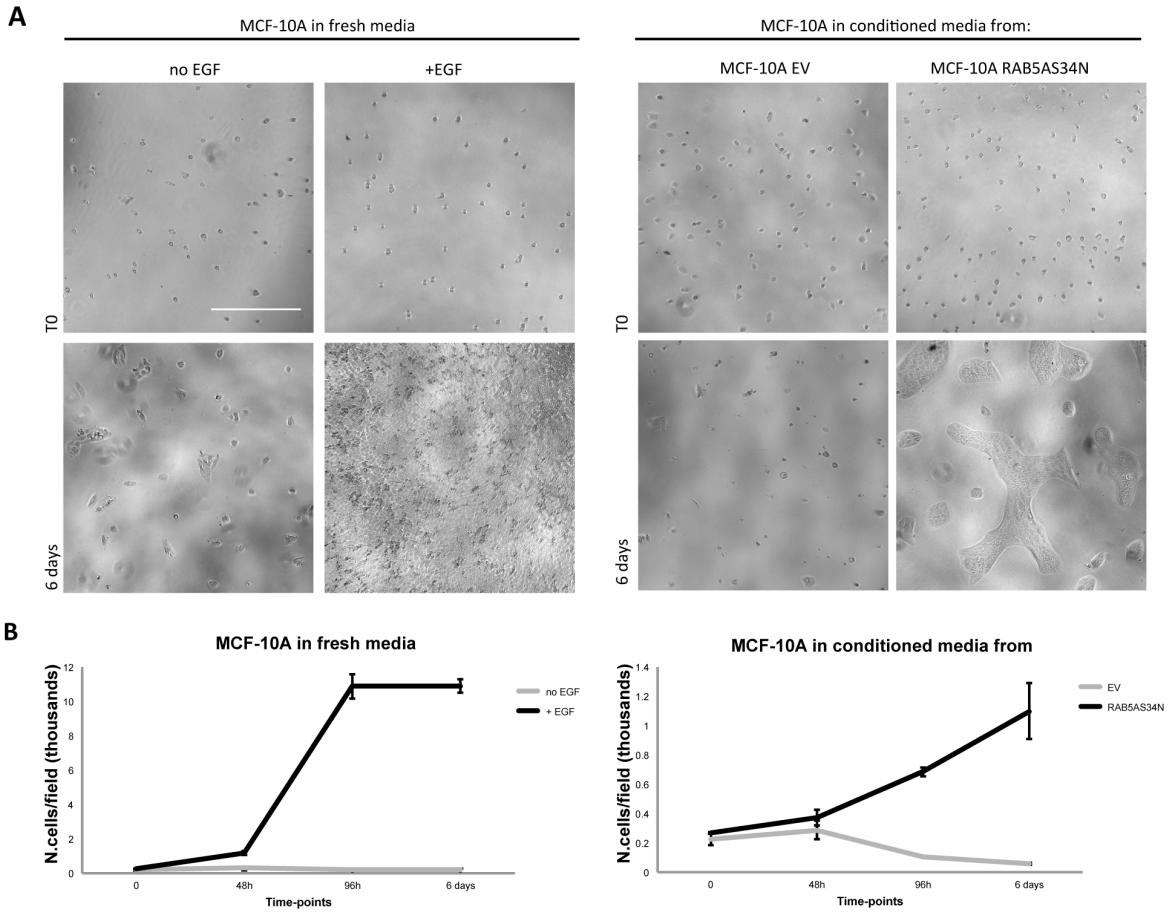

Figure 31. The supernatant derived from MCF-10A RAB5AS34N cells allows the EGF-independent growth of MCF-10A cells, suggesting the secretion of soluble growth factors.
(A) On the left, control MCF-10A cells were seeded in fresh media in the absence or presence of EGF, as proliferation control. On the right, doxycycline-induced MCF-10A EV or MCF-10A RAB5AS34N cells were cultured 4 days in the absence of EGF. Conditioned media were collected and applied onto control MCF-10A cells, plated in equal numbers. Cells were proliferating only in fresh media +EGF or in RAB5AS34N derived conditioned media. Representative phase contrast images are shown (Scale bar, 400 μm), illustrating the starting point (T0) and ending point (6 days) of the experiment. **(B)** Quantification of the number of cells/field that were counted at each time-point: control MCF-10A cells growth curves in fresh media (graph on the left) or in conditioned media (graph on the right) are shown. Error bars represent standard deviation. MCF10A cells proliferate only when cultured in RAB5AS34N derived conditioned media or in the presence of EGF. The experiment was performed 4 times with quadruplicate technical replicates.

Thus, impairing RAB5A activity triggers the release of soluble growth factors. To corroborate this finding, we performed a cell mixing experiment using GFP-positive MCF-10A EV cells. This strategy allowed us to easily distinguish the two cell populations. Cell lines were grown in the absence of EGF either separately or mixed in a 1:1 ratio. RAB5AS34N cells were able to proliferate and form acini when culture in 3D on Matrigel

without EGF, as expected. Interestingly, control cells (Fig. 32, green) also were capable of generating acini, but only when co-culture with RAB5AS34N-expressing cells, as shown by proliferation of both not-tagged RAB5AS34N and GFP-positive EV cells (Fig. 32, white dashed inset). Thus, RAB5AS34N expression in MCF-10A cells induces the expression and the release of soluble growth factors that endowed MCF-10A cells with the ability to proliferate in the absence of growth factors.

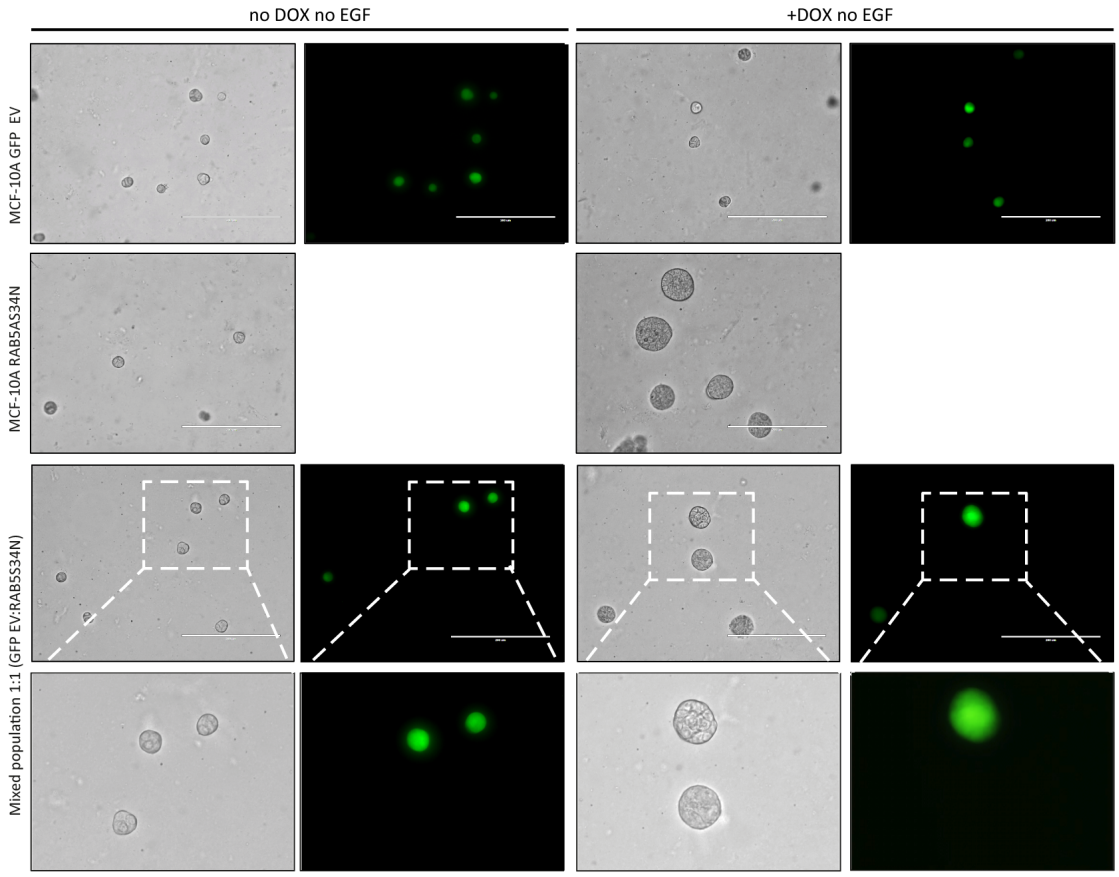

Figure 32. MCF-10A RAB5AS34N cells sustain the EGF-independent growth of control MCF-10A cells.

RAB5AS34N expressing cells enable EGF-independent growth of neighboring non-expressing cells. MCF-10A EV (GFP tagged) and MCF-10A RAB5AS34N cells (not tagged) were cultured on Matrigel either separately or as a 1:1 mixture for 7 days without EGF. Representative phase contrast and fluorescence microscopy images, and relative magnification, are shown (Scale bar, 200 μm). The experiment was performed 3 times with technical duplicate.

Identification of AREG as the candidate secreted diffusible factor in the conditioned media of RAB5AS34N expressing cells.

Amphiregulin (AREG), another known ligand of EGFR, has been recently identified as one of the soluble factors capable of sustaining EGF-independent growth in MCF-10A cells (Zhang, Ji et al. 2009; Yang, Morrison et al. 2012). Thus, we initially tested by qRT-PCR whether *AREG* mRNA was altered by RAB5AS34N expression. We plated control EV- and RAB5AS34N MCF-10A cells in the absence of EGF and extracted their mRNA at different time-points (Fig. 33A). Of note, already after 3 days of culture, a strong induction of RAB5AS34N corresponded to a strong increase in AREG transcript. This effect was completely absent in doxycycline treated control cells, suggesting a RAB5AS34N-dependent effect. To assess whether AREG was secreted into the supernatant, conditioned media of doxycycline-induced MCF-10A EV or RAB5AS34N expressing cells were collected and secreted-AREG was detected by ELISA (Fig. 33B). Remarkably, RAB5AS34N supernatant contained nearly ten times more AREG than control.

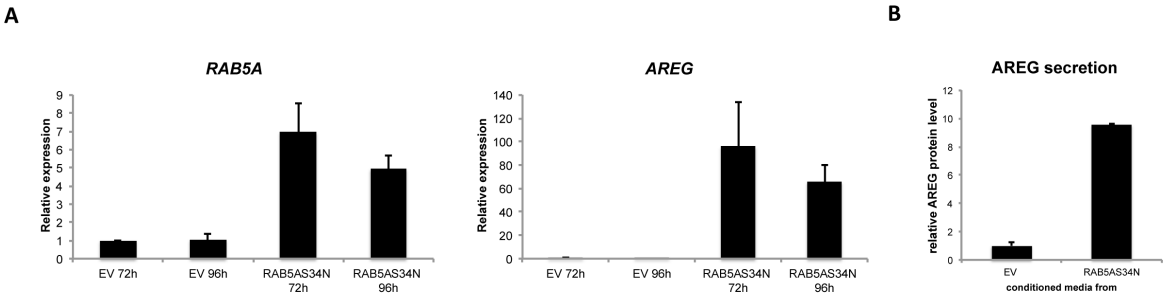

Figure 33. EGF-independent growth induced by RAB5AS34N expression relies on AREG secretion.

(A) MCF-10A EV or RAB5AS34N cells were plated without EGF and collected at different time-points. Induced *RAB5A* and *AREG* mRNAs detected by qRT-PCR are shown. RAB5AS34N expression induces an up-regulation of AREG transcript. *GAPDH* was used as normalizer. **(B)** Human Amphiregulin ELISA was performed on 4 days conditioned media collected from the indicated doxycycline-induced cell lines grown in the absence of EGF. The relative AREG secretion level referred to EV conditioned media is shown. The experiment was repeated 3 times. Error bars represent standard deviation.

To establish whether AREG up-regulation and increased secretion is necessary and sufficient to confer EGF-independent cell proliferation, firstly we added recombinant AREG (rAREG) to EGF-deprived MCF-10A EV cells. Under these conditions we showed that AREG alone was able to sustain cell proliferation (Fig. 34, left panels). Second, we tested if neutralizing antibody against AREG were able to suppress growth induced by rAREG (Fig. 34, left panels) or by RAB5AS34N induced AREG secretion (Fig. 34, right panels). Treatment with anti-AREG IgG suppressed proliferation in both the conditions. Additional controls were included into the experiment; further confirming that AREG secretion is dependent on doxycycline induced RAB5AS34N expression (Fig. 34, "Not induced" panels on the right). These phenotypes were already detectable after 3 days. The sum of these observations indicates that EGF-independent growth induced by RAB5AS34N expression relies on AREG secretion.

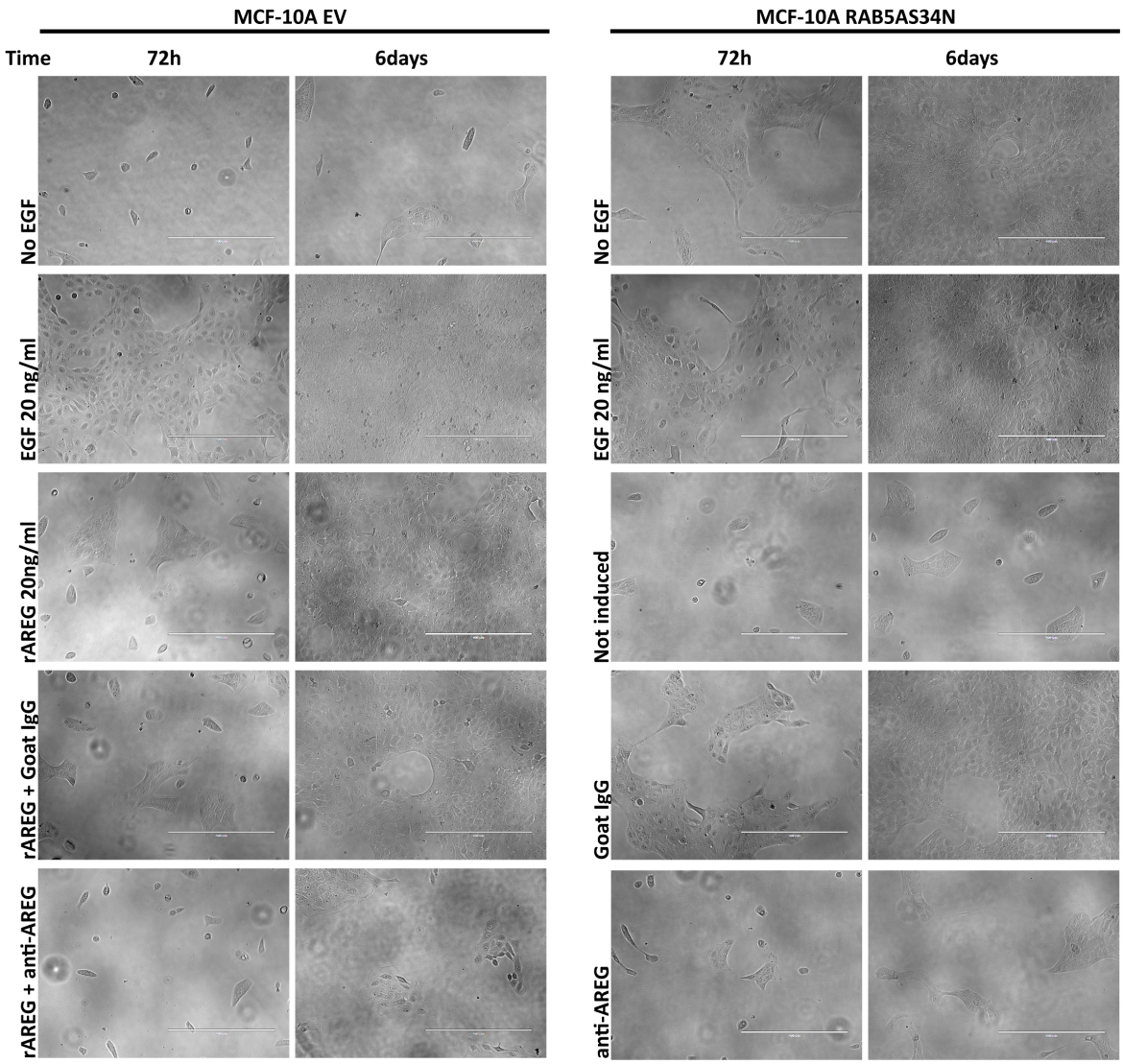

Figure 34. AREG-neutralizing antibody blocks EGF-independent growth.

Equal number of cells was plated in the indicated conditions, in the absence of EGF. Left panels: MCF-10A EV cells grow both in the presence of EGF or recombinant AREG. AREG-neutralizing antibody, but not control IgG, inhibits AREG induced growth. Right panels: RAB5AS34N expressing cells were cultured as illustrated; AREG-neutralizing antibody abolishes RAB5AS34N induced EGF-independent growth. Representative phase contrast images are shown, at 2 different time-points (Scale bar, 400 μm). The experiment was performed 3 times with quadruplicate technical replicates.

AREG sustains EGF-independent growth of MCF-10A cells through EGF receptor activation.

To test whether AREG sustains EGF-independent growth by binding and activation of EGF receptor, control EV and MCF-10A cells expressing RAB5AS34N were plated in equal number in the presence or absence of EGF. Cells were simultaneously treated with two different concentrations of the EGFR inhibitor Cetuximab. In the presence of EGF, the inhibitor impaired EGF-dependent growth in both cell lines, as expected. In EGF-deprived conditions, instead, only cells expressing RAB5AS34N were able to grow but treatment with Cetuximab inhibited their proliferation (Fig. 35A, right panels). We obtained similar results, in 3D culture of MCF-10A RAB5AS34N cells. Under these conditions, Cetuximab blocked cell proliferation and acini formation sustained by AREG secretion or by EGF supplemented media (Fig. 35B). Importantly, Cetuximab effectively inhibited EGFR activation as witnessed by impaired phosphorylation of EGFR (Fig. 35C). Collectively these evidences suggest that AREG sustains EGF-independent proliferation through canonical EGFR activation.

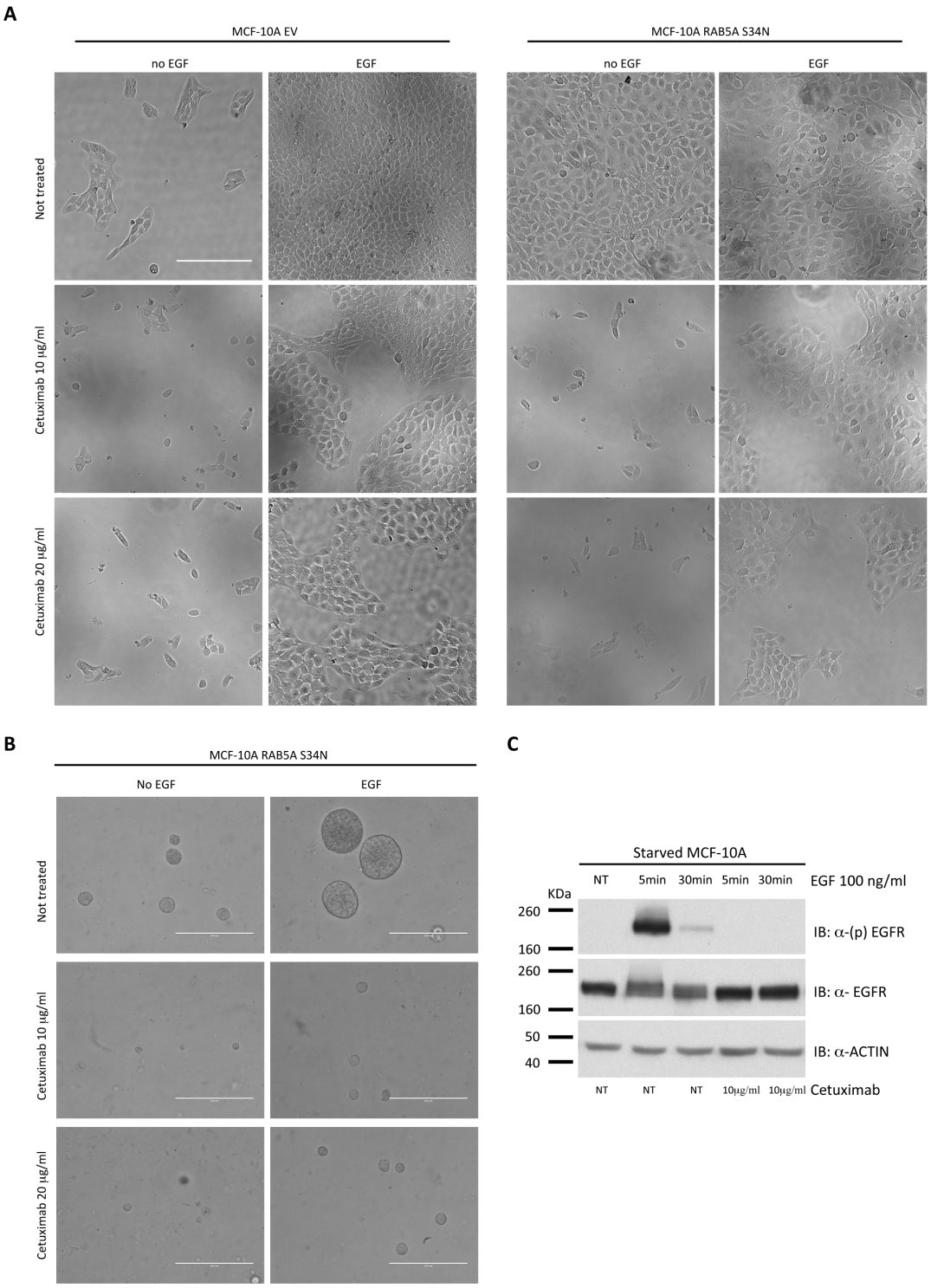

Figure 35. AREG sustains non-cell autonomous growth of MCF-10A cells through canonical EGFR activation.

(A) Doxycycline-induced cells were plated in equal number in the indicated conditions and images were acquired every 2 days to monitor cell growth. Two different concentration of Cetuximab were used to assess dose-dependent effects. RAB5AS34N expressing cells treated with Cetuximab are not able to proliferate. 96 hours images are shown (Scale bar, 200 µm). **(B)** Cetuximab treatment inhibits MCF-10A RAB5AS34N cells growth in 3D cultures. Representative phase contrast images of 3 days acini are shown (Scale bar, 200 µm). **(C)** Effectiveness of Cetuximab was assessed by starvation of control MCF-10A cells and stimulation by acute dose of EGF for the indicated time. 10 µg/ml Cetuximab was enough to abolish completely EGFR activation (pEGFR). Nitrocellulose membrane was immunoblotted as indicated. Actin was used as loading control. The experiment was performed 3 times.

RAB5AS34N-dependent AREG induction is not mediated by signaling pathways known to regulate AREG expression.

Previous studies identified AREG as a transcriptional target of different signaling cascades. Indeed, AREG was shown to be a downstream effector of the Hippo pathway either as a consequence of YAP direct binding to AREG promoter as demonstrated by Chip assay (Zhang, Ji et al. 2009) or as a target of TAZ through TEAD binding to AREG promoter (Yang, Morrison et al. 2012). In hypoxic conditions, AREG expression may also be regulated by HIF-2α, driving an autonomous breast cancer cell growth via EGF receptor family (Bordoli, Stiehl et al. 2011; Stiehl, Bordoli et al. 2012). To assess whether these pathways are similarly regulated by interference with RAB5A, doxycycline-induced control EV and RAB5AS34N-expressing MCF-10A cells were collected at different time points and processed by qRT-PCR (Fig. 36A).

We chose *CTGF* (connective tissue growth factor) as one of the main target genes of YAP/TAZ signaling pathway (Fig. 36B), *HIF-2* α for hypoxia induced AREG modulation (Fig. 36C) and *Estrogen* (Martinez-Lacaci, Saceda et al. 1995; Ciarloni, Mallepell et al. 2007) and *Progesteron Receptors* (Aupperlee, Leipprandt et al. 2013), well known mediators of mammary gland development during puberty through AREG (Fig. 36D). However, none of the screened mRNAs resulted to be significantly modulated by RAB5AS34N expression.

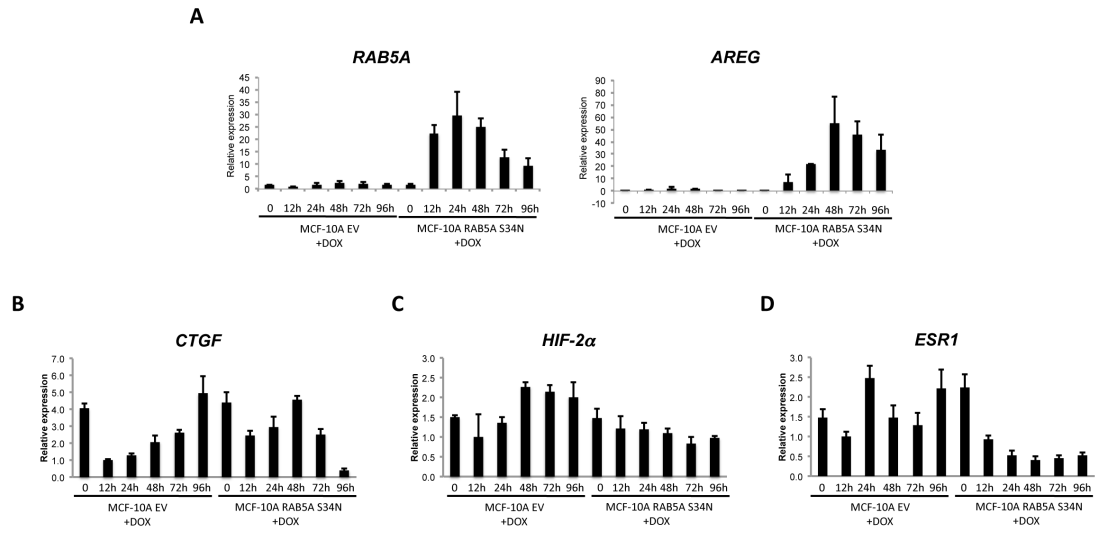

Figure 36. RAB5AS34N-induced AREG modulation is not mediated by already characterized signaling pathways that regulate AREG expression.
(A) Doxycycline-induced MCF-10A EV or RAB5AS34N cells were plated without EGF and collected at different time-points. Time-course of induced *RAB5A* and *AREG* mRNAs detected by qRT-PCR are shown. Corresponding modulation of **(B)** *CTGF*, a specific YAP/TAZ target gene; **(C)** *HIF-2α*, a mediator of hypoxia and **(D)** *Estrogen Receptor* mRNAs, detected by qRT-PCR are shown. *Progesteron Receptor* mRNA was not detectable. *GAPDH* was used as normalizer and EV 12h DOX sample as calibrator. Error bars represent standard deviation. The experiment was performed 3 times.

Genetic ablation of RAB5 does not mimic its functional impairment in AREG modulation.

We collected evidences suggesting a modulation of AREG induced by endocytosis impairment. In an attempt to confirm this observation, we assessed AREG modulation in MCF-10A cells interfered with different sets of oligos that target specifically RAB5 isoforms. Surprisingly, neither the knockdown of the single RAB5 isoforms (Fig. 37A, C) nor the simultaneous interference with all three RAB5A, B and C gene transcript recapitulated the effect of the RAB5 dominant negative (Fig. 37A, B, C).

As previously described, RAB5AS34N is locked in a GDP-bound, non-functional form. However, its over-expression may result in the sequestration of specific GEFs that may also utilize others RABs of the same subfamily of RAB5 as substrate. Thus, we

hypothesized that AREG modulation might be the result of a more complex mechanism involving also additional RABs. However, neither the single nor the combined knockdown of the closer RAB5 family member, RAB21, RAB22A and RAB31 (also known as RAB22B), was sufficient to induce AREG expression (Fig. 37 A, C).

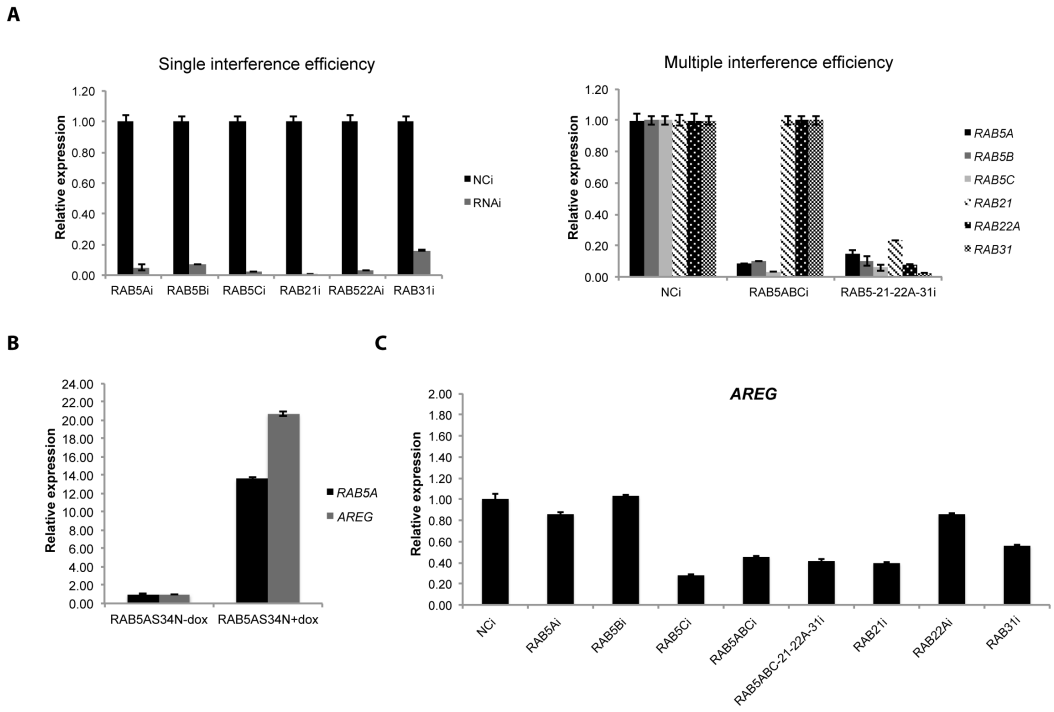

Figure 37. Genetic depletion of RAB5 and other related RABs does not phenocopy RAB5AS34N-induced AREG modulation.

(A) MCF-10A EV cells were interfered by specific siRNAs targeting the single or a combination of the indicated genes. *RABs* mRNAs levels detected by qRT-PCR 48 hours after interference are shown. **(B)** Efficiency of RAB5S34N induction and AREG modulation are shown. **(C)** Corresponding modulation of *AREG* detected by qRT-PCR in RNAi conditions is shown, *GAPDH* was used as normalizer and NCi (in **A** and **C)**, or RAB5AS34N-dox cells (in **B)**, as calibrators. The experiment has been repeated 3 times. NCi, negative control; RNAi, RNA interference; i, interference.

It is important to point out that in mouse hepatocytes, it is necessary to reduce the expression or the activity of RAB5 by more than 80% in order to impair endosome biogenesis, suggesting that this system has evolved to be extremely robust and is thus proficient even under condition that severely limits the expression of the master regulator of these organelles (Zeigerer, Gilleron et al. 2012). Thus, we hypothesized that RAB5AS34N-expressing MCF-10A cells may display a hypomorfic phenotype, that

cannot be recapitulated by the complete ablation of its function achieved through siRNAs. To investigate this possibility, we compared the impact of functional (by expression of RAB5AS34N) or genetic manipulation of RAB5 (by concomitant down-regulation of all three isoforms) on endosome biogenesis. EEA-1 staining confirmed that a complete displacement of EEA-1 from early endosomes could be achieved by knocking-down of RAB5 family members (RAB5A/B/C-RAB21-RAB22A-RAB31) or by concomitant interference with RAB5A/B/C (Fig. 38A). Conversely, the expression of RAB5AS34N caused a readily detectable, but incomplete displacement of EEA-1 (Fig. 38B). These findings indicate that the expression of the dominant negative likely cause a hypomorfic effect. They further suggest that complete loss of RAB5 wipes completely out endosomal and lysosomal activity, which is likely to impact deeply on a wide array of cell biological activity impeding the emergence of proliferation phenotypes. While further experiments are required to establish this notion firmly, it is likely that different levels of alteration of the endocytic system obtained by genetic or functional impairment of RAB5A may explain the diverse effect observed on AREG modulation.

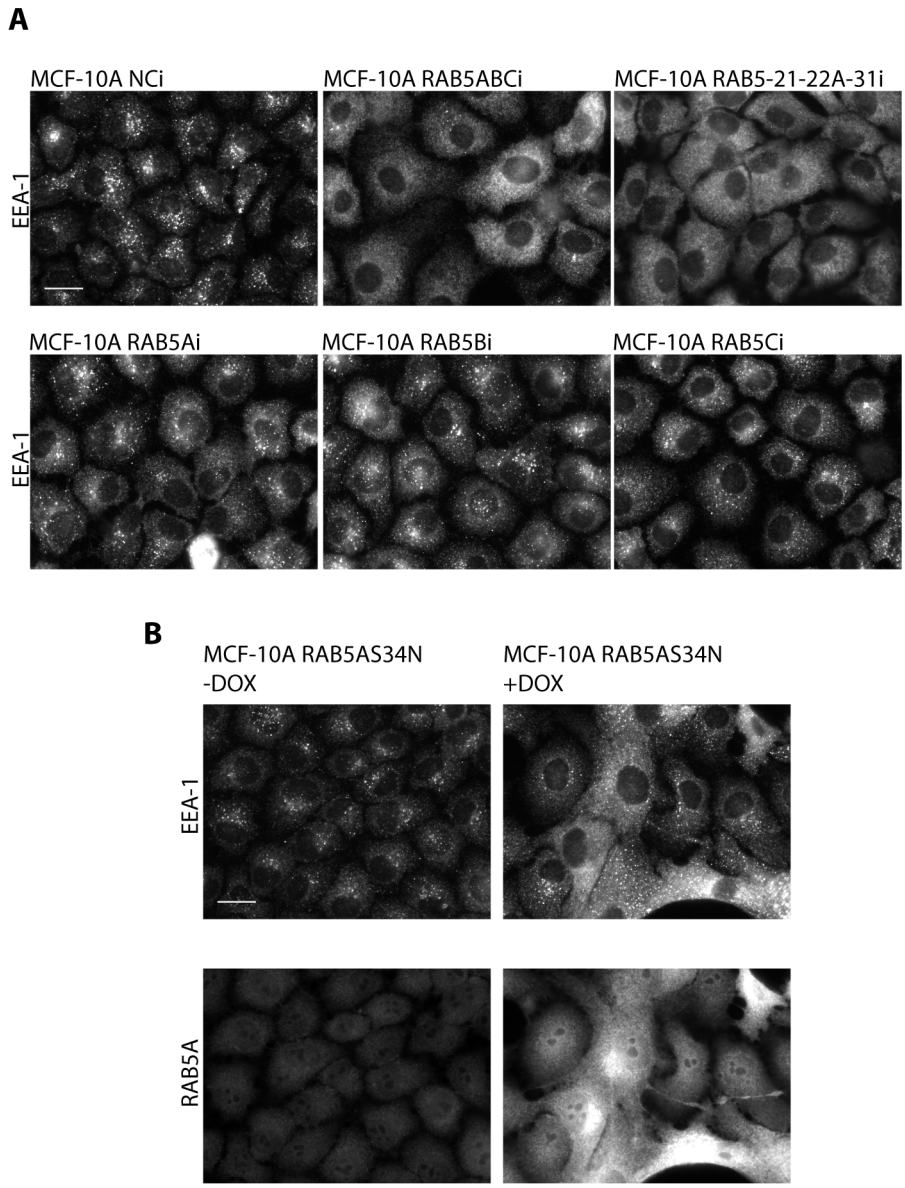

Figure 38. Genetic or functional depletion of RAB5 and other related RABs differently impact on the endosomal compartment.

Cells were seeded on coverslips and interfered for the indicated genes. **(A)** 48 hours after RNAi treatment, coverslips were fixed in 4% paraformaldehyde and stained with anti-human EEA-1 antibody, to be analyzed by wide field microscopy. **(B)** EEA-1 displacement was compared with un-induced or induced MCF-10A RAB5S34N cells. Representative images are shown (Scale bar, 20 μm). The experiment has been performed 3 times.

RAB5A expression increases collective cell migration in MCF-10A cells.

Clinical data and *in vitro* studies collected by other and by our lab concordantly demonstrates that RAB5A is required for invasion and metastasis, suggesting that in certain pathological conditions, RAB5 may act as promoter of tumor progression rather

than as tumor suppressor. Tumorigenesis is a multistep process; cancer cells progressively acquire different properties that transform a normal cell into a neoplastic cell. Among the typical hallmarks of cancer, cell migration and tissue invasion are specific traits correlated with tumor progression and metastasization (Hanahan and Weinberg 2000; Hanahan and Weinberg 2011). Notably, RAB5A has been shown to promote the formation of migratory protrusion as well as of invasive structures, that are required and instrumental to induce a mesenchymal program of individual cell invasion (Palamidessi, Frittoli et al. 2008; Frittoli, Palamidessi et al. 2014). To extend and explore a potential pro-metastatic role of RAB5A, we investigated the impact of deregulation of the expression of this GTPase on a form of locomotion that is typically used by tumor of epithelial origin. In addition to disseminate as individual cells that detach from the tumor mass, frequently epithelial-derived tumors can invade as collective entities (Theveneau and Mayor 2013). Under these conditions, cell-to-cell junctions are dynamic and constantly remodeled, but remain functionally proficient in keeping cell together and in promoting a coordinated mode of cell motility. One *in vitro* assay that recapitulates certain aspect of this mode of locomotion is the wound healing assay, whereby confluent monolayers of epithelial origin are induced to migrate into the void created by a scratch into the epithelial sheet. We initially utilized normal mammary epithelial cells in an effort to understand and capture fundamental, physiological role of RAB5A. To this end, control and RAB5A WT expressing MCF-10A confluent monolayers were scratched with a pipette tip to induce epithelial collective cell migration. Wound closure was monitored overtime by time-lapse microscopy. Strikingly, compared with control MCF-10A EV cells, RAB5A expression enhanced the speed of migration of the epithelial cell sheet (Fig. 39 and Movie 1).

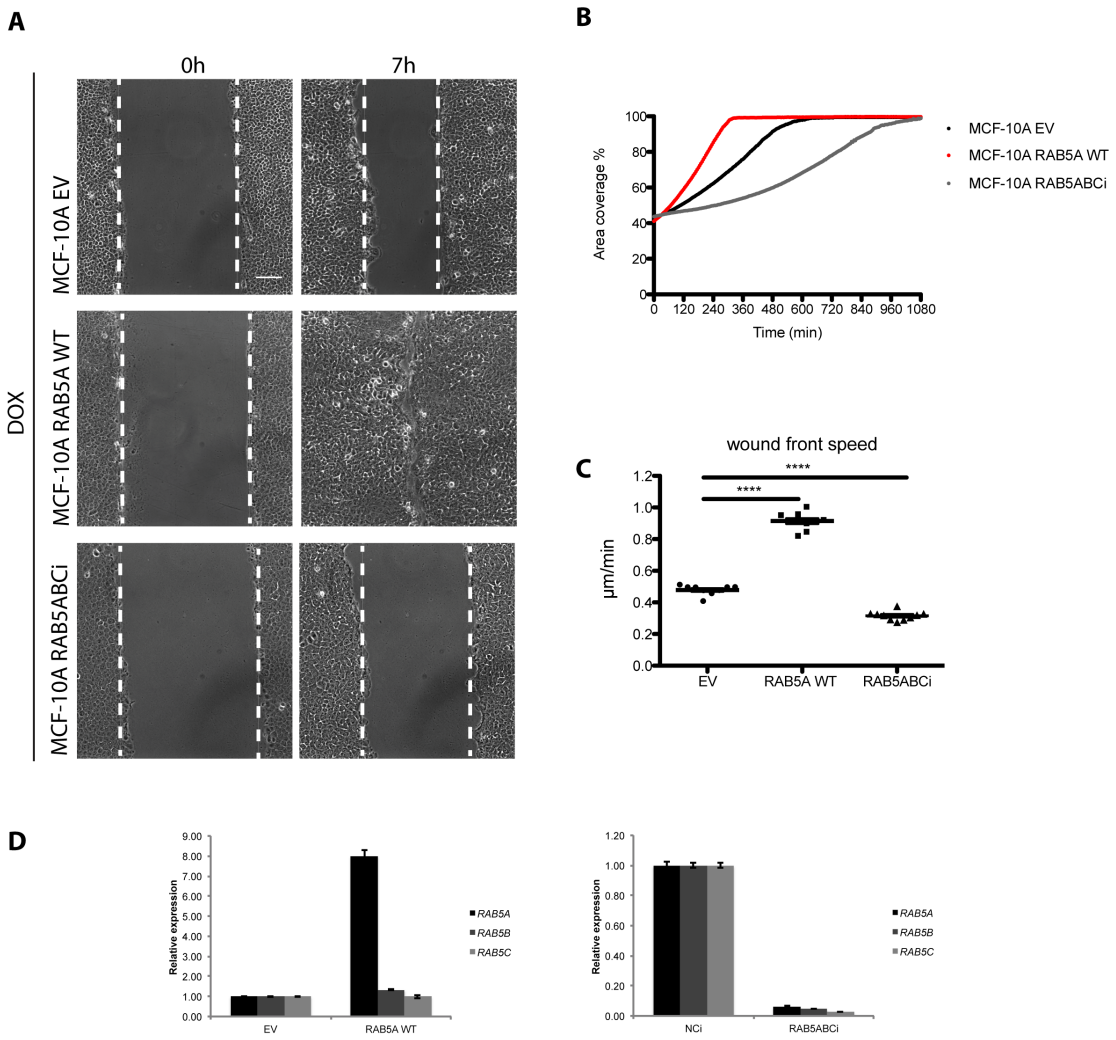

Figure 39. Collective migration of MCF-10A epithelial layer is increased by RAB5A expression and impaired in RAB5 knockdown cells.

(A) Wound-healing assays. MCF-10A cells were grown at confluency and doxycycline induced 16 hours before the experiment. Induced-monolayers were mechanically scratched by a pipette tip and cell migration was monitored by time-lapse phase contrast microscopy. Images were recorded every 5 minutes using a 10x objective. Representative images just after the scratch (0 hour) and at 7 hours from the incision are shown. Dashed lines represent the wound edge. Scale bar, 100 µm. **(B)** Motility was quantified by measuring the increase in the percentage of area covered by cells overtime (MatLab software) **(C)** The distribution around the value of mean wound front speed for each cell line is shown. MCF-10A RAB5A WT cells were significantly faster than control EV cells. Conversely, RAB5ABCi cells were less motile. Data are the mean -/+ SEM. ****p<0.0001. **(D)** *RAB5A*, *RAB5B* and *RAB5C* mRNA levels in the indicated cell lines and in the same experimental conditions used for the experiment, are shown. *GAPDH* was used as normalizer and control EV or NCi cells as calibrators. The experiment was performed 3 times in duplicate.

To exclude any contribution of cell proliferation to wound healing, we interfered with cell division. Inhibition of cell division with Mitomycin C did not alter the effect of RAB5A on collective locomotion (Fig. 40A). Wound healing assay was also performed on un-induced

cells, to confirm the two cell lines have a comparable behavior when not induced. Both EV- and RAB5A WT-MCF-10A cells migrate with comparable speed, in the absence of doxycycline, further confirming the role of RAB5A in promoting collective cell migration (Fig.40B).

Conversely, when RAB5A, B and C were genetically silenced by small interfering RNAs (siRNAs), collective cell migration was impaired and wound closure was severely delayed as compared with cells interfered with scrambled siRNAs (Fig.39 and Movie 1).

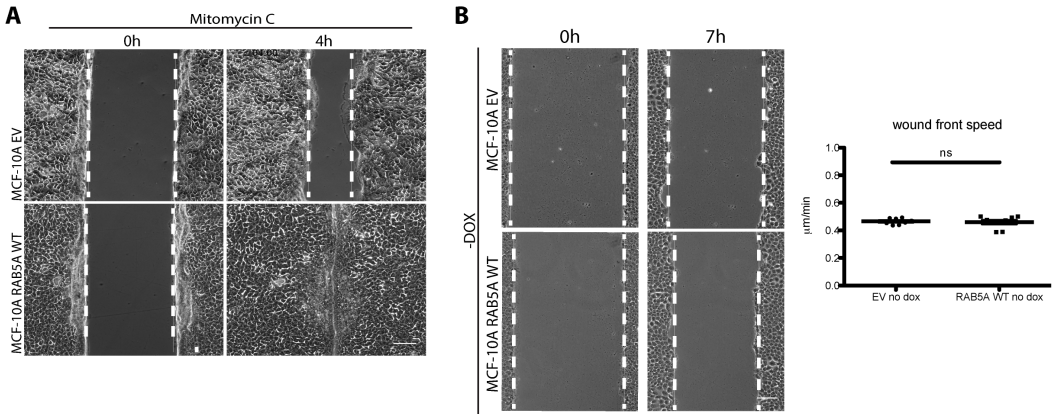

Figure 40. The increase in wound healing velocity is dependent on RAB5A expression, without any contribution of cell proliferation.

(**A)** Wound-healing assays on induced MCF-10A cells treated with Mitomycin C. Representative images just after the scratch (0 hour) and at 4 hours from the scratch are shown. Scale bar, 100 µm. **(B)** Wound-healing assays of un-induced MCF-10A cells. Representative images just after the scratch (0 hour) and at 7 hours from the incision are shown. Dashed lines represent the wound edge. The distribution around the value of mean wound front speed for each cell line is shown. Data are the mean -/+ SEM. ns, not significant. Scale bar, 100 µm.

RAB5A selectively enhances collective cell migration.

RAB5A has been shown to impact on the migration of different kind of tumor derived cells moving as single entities. To exclude the possibility that the collective motility phenotype resulted from alteration of single cell motility within the epithelial monolayer, we directly measured a number of parameters of locomotion by plating sparse cells and monitoring their single cell motility upon deregulation of RAB5A expression.

Single cells were seeded sparsely in complete media in the absence of added chemotractants and monitored for 24 hours by time-lapse microscopy. Random migration was quantified by single cell tracking and analyzed by ImageJ software. Notably, RAB5A WT expression in MCF-10A cells was insufficient to alter single cell migration. Conversely, as expected, RAB5 depletion abrogates cell motility (Fig. 41 and Movie 2). These finding indicates that while RAB5A is essential for optimal cell motility regardless of the mode of locomotion, it elicit cell locomotion only when cell are forced to move in a coordinated and directional fashion, such as during wound sheet closure. These evidences further suggest that the topographical constrain of an epithelial sheet may be instrumental to cooperate with altered endosomal function that is brought about by elevation of RAB5 expression.

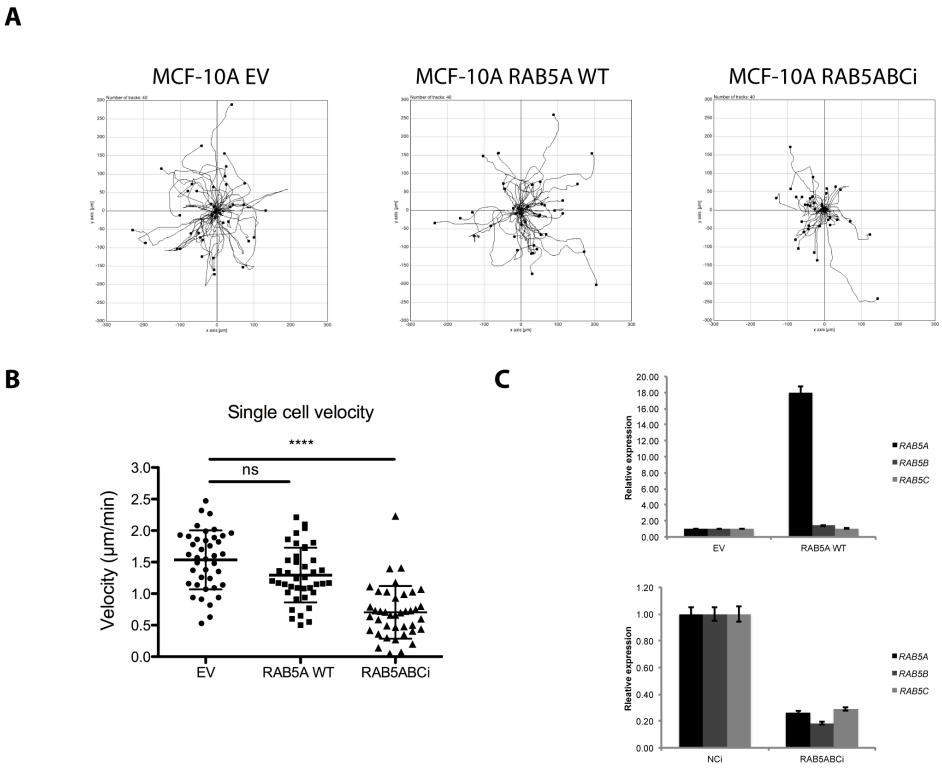

Figure 41. RAB5A does not increase the velocity of randomly migrating single cells.
(A) MCF-10A cells were seeded sparsely in the absence of any diffusible gradient. Random cell migration was recorded by time-lapse phase contrast microscope every 5 minutes over a 24 hours period. Cell tracking was performed manually and analyzed by Chemotaxis Tool ImageJ software plugin. Single cells per each condition were tracked for 3 consecutive hours and plotted in the correspondent graph. **(B)** Single cell velocity is not affected by RAB5A expression but its knockdown strongly decreases migration speed. The analysis was conducted on 40 single cells/experiment/genotype of three independent experiment; data are the mean ± SEM. ns not significant; ****p < 0.0001. **(C)** *RAB5A*, *RAB5B* and *RAB5C* mRNA levels in the indicated cell lines used for the experiment, are shown. *GAPDH* was used as normalizer and control EV or NCi cells as calibrators.

Cell coordination is increased in migrating epithelial sheets expressing RAB5A.

Collective locomotion is the result of a tightly regulated set of processes that strictly depends on complex and dynamic cell-to-cell interactions occurring during the migration of epithelial sheet. To further characterize the phenotype induced by RAB5A WT expression in MCF-10A cells, we analyzed movies recorded in wound healing assay by Cell Image Velocimetry software (Milde, Franco et al. 2012). Exploiting this bioinformatic approach, we determined cell position overtime within a monolayer, detecting the progression of migrating cells in consecutive frames (Fig 42A). As it is shown by the specific color-coding that reveals the direction of migration of group of cells, relative to the orientation of the wound, RAB5A expression greatly enhanced cell coordination (Fig. 42B, C and Movie 3). Furthermore, the increase in mean angular correlation, a specific measure of the coherence in cell movement, indicated that neighboring cells move in a highly coordinated fashion (Fig. 42D, E). On the contrary, genetic ablation of RAB5 impairs not only wound healing speed, but also cell coordination, as it is shown by a decreased mean angular correlation value (Fig. 42 and Movie 3).

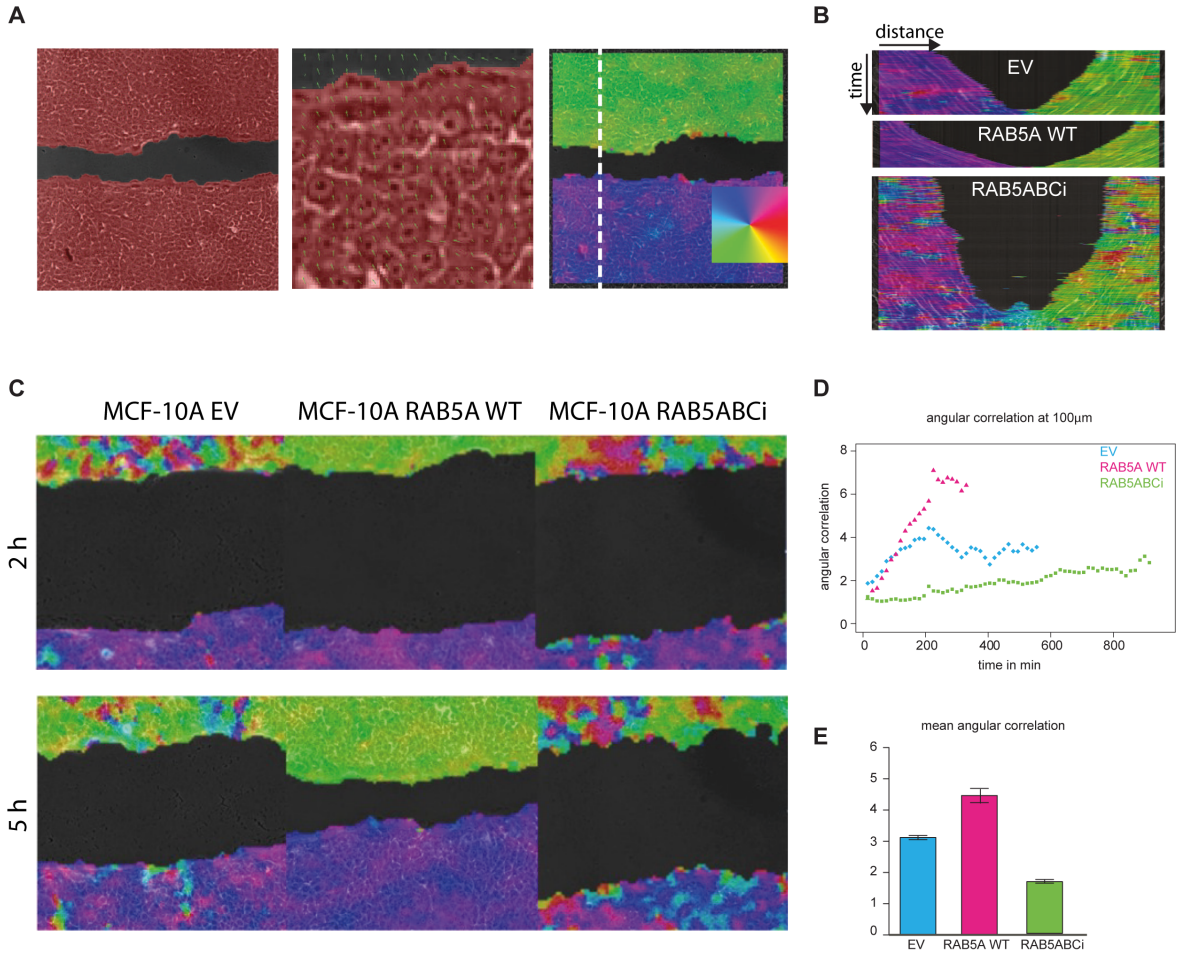

Figure 42. RAB5A levels affect collective migration dynamics of MCF-10A cells.
(A) Overview of the CIV (Cell Image Velocimetry) analysis (Milde, Franco et al. 2012). Wound edges are detected in a segmentation step and cell layers are masked. PIV (Particle Image Velocimetry) is used to quantify the dynamics of the cell monolayer. Coherence plots are obtained by comparing the movement of few cells to the neighboring regions. Color code indicates direction of movement. **(B)** Kymographs taken perpendicular to the wound (as indicated by the white line in **A**) are shown. Homogeneous colors indicate high coherence; in-homogeneous colors indicate less coeherent dynamics. **(C)** Cell coherence of the indicated cell lines are shown at 2 and 5 hours after wound. **(D)** Angular correlation of the cell movements for the different phenotypes overtime (bin distance: 100µm) and **(E)** mean angular correlation during entire wound closure are shown.

RAB5A promotes collective cell streaming in the epithelial monolayer

Collective cell movement is an important strategy in several physiological processes, including development, morphogenesis and regeneration. Furthermore, it also plays a central role in pathological events such as tumor progression and metastasis. To further characterize the role of RAB5A in collective locomotion, we plated control (EV)

and RAB5A WT expressing MCF-10A cells at confluency in order to generate a tight monolayer that recapitulate epithelial tissues in vivo, and monitored cell behavior within the monolayer by time-lapse microscopy. Indeed, fully confluent monolayers closely resemble the situation in mature epithelia with stable adhesive contacts.

Interestingly, un-wounded MCF-10A cell sheets underwent steaming like locomotion only when RAB5A WT expression was induced (Fig. 43A and Movie 4). Single cells were manually tracked and the analysis of migration parameters demonstrates that in cells expressing RAB5A both migration speed and directionality are improved, resulting in a higher accumulated distance (Fig. 43B).

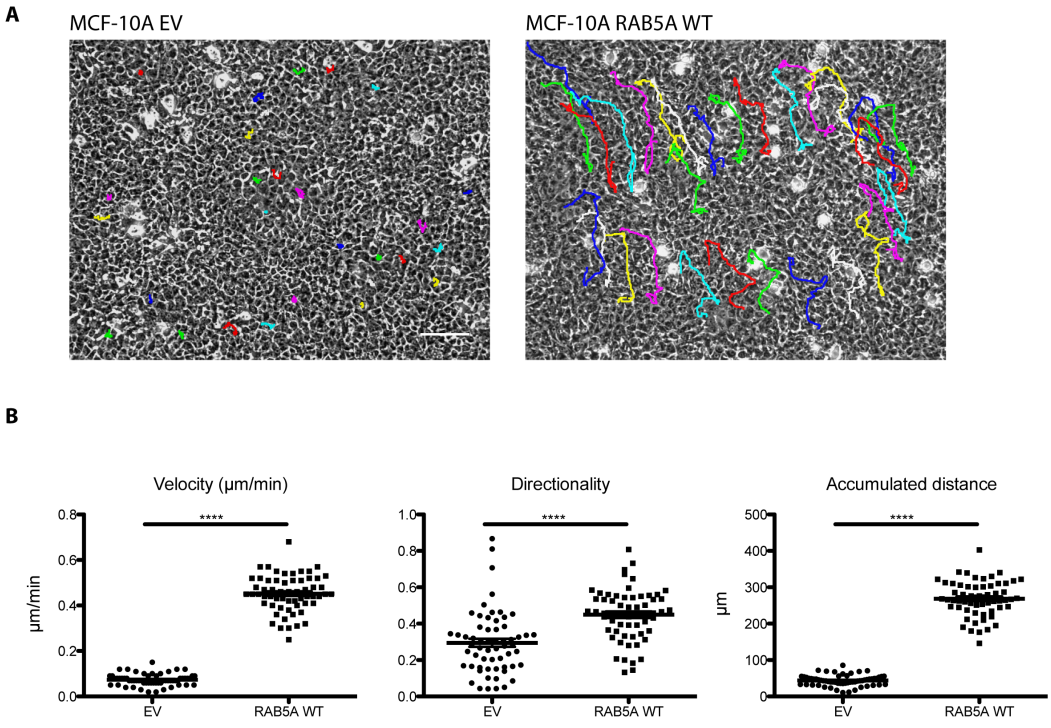

Figure 43. RAB5A promotes collective cell streaming in un-wounded MCF-10A cells monolayer.

(A) Stable MCF-10A monolayers were doxycycline induced 16 hours before the experiment. Cell migration was monitored by time-lapse phase contrast microscopy. Images were recorded for 12 hours with a 5 minutes interval using a 10x objective. Single cells within the monolayer were manually tracked by ImageJ plugin software. Representative overlay of 30 cell tracks/condition are shown. Scale bar, 100 µm. **(B)** Quantification of migration parameters was performed by Chemotaxis tool ImageJ software plugin, to determine single cell velocity, directionality and accumulated distance. The distribution around the mean is shown. The experiment was performed 3 times. Data are the mean -/+ SEM. ****p<0.0001.

RAB5A alters E-cadherin pattern in the epithelial monolayer, without affecting its expression levels.

So far, we showed a specific role of RAB5A in promoting cell streaming in un-wounded monolayer as well as the speed and coherence of migrating cells in wound closure. Previous works on collective wound locomotion, revealed the relevance of cell-to-cell adhesion and of adhesion molecules in sustaining and coordinating sheets migration (Simpson, Selfors et al. 2008). Indeed, cadherins perturbation by siRNA-mediated knockdown or by calcium chelation was shown to cause strong alteration of coordinated motion in epithelial sheets (Ng, Besser et al. 2012; Czirok, Varga et al. 2013).

Thus, we chose to investigate the possible involvement of E-cadherin, specific of epithelial tissues, in our system. Although E-cadherin expression level was not affected by RAB5A WT expression, E-cadherin staining of MCF-10A cells monolayers revealed different patterns of adherens junctions (Fig 44A,B). Compared with control MCF-10A cells, RAB5A WT expressing cells show straighter and more delineated cell-to-cell contacts, suggesting a possible increase in cell-to-cell adhesion strength. Cell images were quantified by measuring the straightness index of the junction, considered as the ratio between the junction length and the junction tracking obtained by ImageJ software (for more details refer to Materials and Methods). RAB5A WT-expressing cells show a mean index value closer to one (Fig 44C).

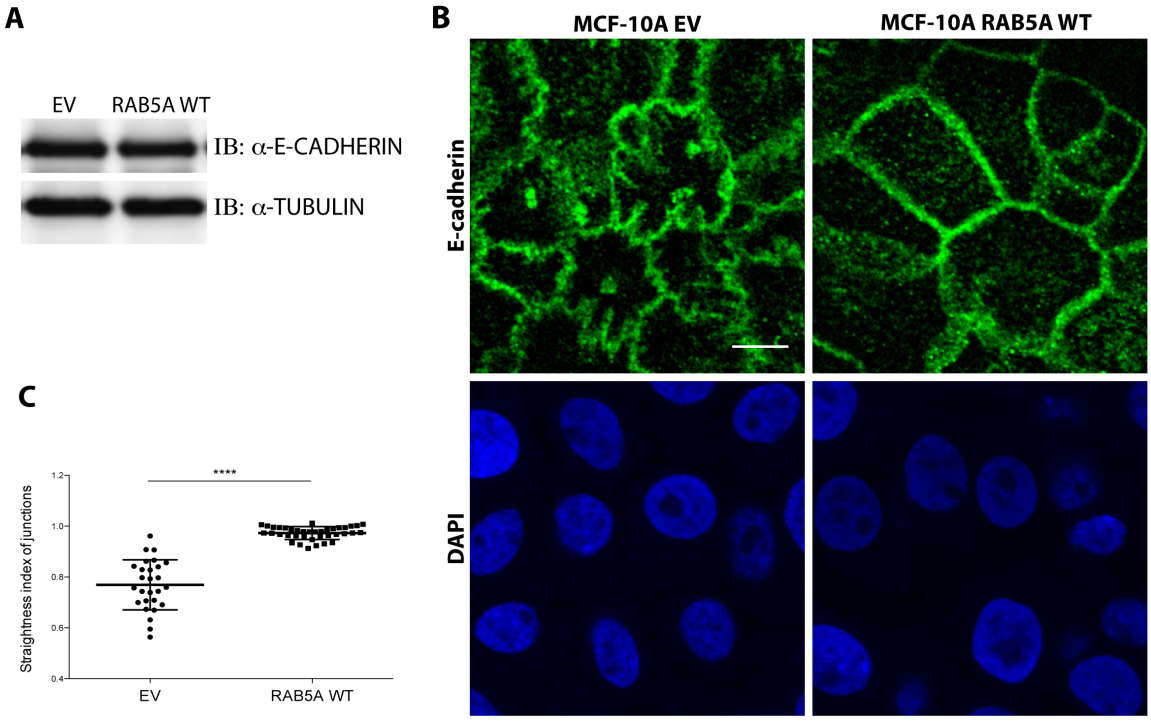

Figure 44. RAB5A expressing cells show higher organization of E-cadherin mediated homotypic adherens junctions.

(A) Equal amount of protein lysates derived from 16 hours doxycycline-induced monolayers of MCF-10A EV and RAB5A were loaded on 8% polyacrylamide gel. Nitrocellulose membrane was blot by mouse monoclonal anti-human E-cadherin antibody or mouse monoclonal anti-human tubulin antibody, as loading control. **(B)** Cells were seeded as a monolayer and doxycycline-induced for 16 hours. Samples were fixed in 4% paraformaldehyde and stained as indicated. Representative confocal microscopy images are shown (Scale bar, 10 μm). **(C)** Confocal images were analyzed by ImageJ software. The straightness index of the junction has been quantified as the ratio of the junction length and the manual tracking of the junction. The experiment was performed 3 times. Data are shown as the mean ± SEM. ****$p < 0.0001$.

RAB5A induces the formation of bigger and more persistent protrusions in cells at the leading front.

Lamellipodial protrusions are essential in guiding cell motility (Small, Stradal et al. 2002; Ridley, Schwartz et al. 2003). It has been shown that RAB5A promotes the activation and spatial restriction of RAC1 to the plasma membrane, leading to the formation of polarized actin signaling which fuels the formation of migratory cellular protrusions (Nobes and Hall 1995; Palamidessi, Frittoli et al. 2008).

We thus performed a wound healing assay to monitor at higher magnification and with a shorter time-frame the morphology and dynamic of the protrusion at the leading front of

the migrating epithelial sheet. Strikingly, RAB5A WT-expressing monolayer showed larger and longer-lived protrusions, characterized by an altered protrusion dynamics (Fig. 45A, B and Movie 5). We quantified these dynamic behaviors by kymograph analysis. Although the rate of protrusion extension was nearly identical between control and RAB5A WT expressing cells, elevation of RAB5A was sufficient to significantly decrease the rate of retraction and increase the persistence of migratory protrusion extension (Fig. 45C, D).

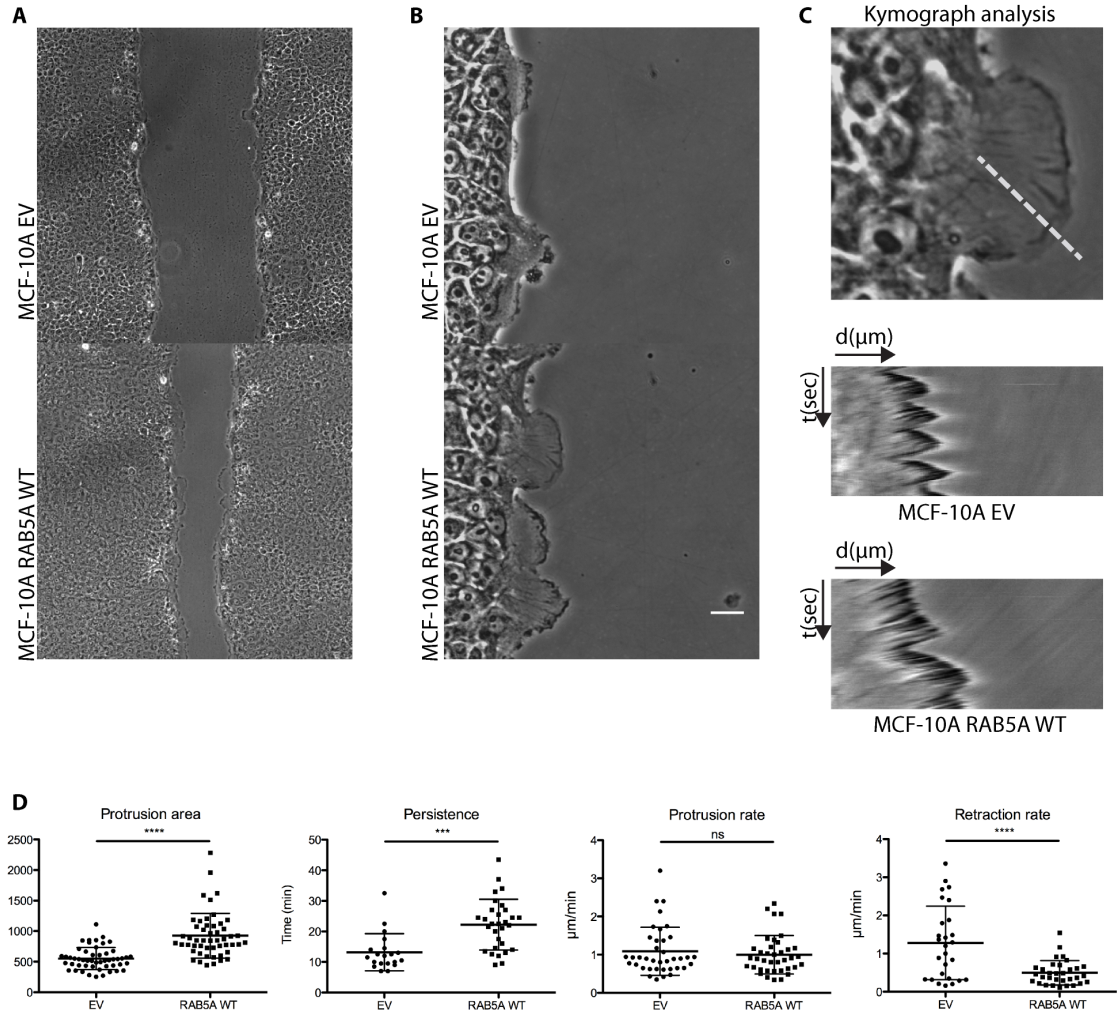

Figure 45. RAB5A expression increases protrusion area and persistence.
Snapshots of the leading front of control EV- or RAB5A WT- expressing MCF-10A cells at 10x **(A)** and 32x **(B)** magnification. Scale bar, 20 µm. **(C-D)** Cell migration was monitored for one hour with 30 seconds timeframe. Quantification of protrusion dynamics was performed, by kymograph ImageJ software plugin, to determine the rate of protrusion extension, the rate of retraction and persistence. The distribution around the mean values of protrusion parameters of each of at least 20 cells/genotype is shown. Protrusion area was measured manually by ImageJ software. The distribution around the mean values of protrusion parameters is shown. The experiment was performed 3 times. Data are the mean -/+ SEM. ***p < 0.001; ****p<0.0001; ns not significant.

Focal Adhesions morphology is affected by RAB5A expression in polarized migrating MCF-10A cells.

Migrating cells interact with the extracellular matrix to anchor their cytoskeleton to the substrate and sustain locomotion. Focal adhesions are signaling platform that sense biochemical and physical properties of the surrounding microenvironment allowing cells to respond and adapt to different matrices. The dynamic assembly and disassembly of these structures plays an important role in cell locomotion and RAB5 activation controls focal adhesions turnover (Mendoza, Ortiz et al. 2013) (Palamidessi, Frittoli et al. 2013). Importantly, in cell protrusions, FAs undergo rapid dynamic remodeling. They form as focal contacts near the advancing leading edge, to mature in FAs as the edge advances and actomyosin contractility builds up just behind the lamellipodia periphery. Since RAB5A WT-expressing cells display altered protrusion dynamics we explored whether these was mirrored by a concomitant alteration of focal adhesions size, as one would expect.

To this end, we wounded control and RAB5 WT-expressing MCF-10A monolayers and fixed them 5 hours after the scratch. Control and RAB5A WT-epithelial sheets were stained with antibodies recognizing vinculin and paxillin, fundamental components of these adhesive structures (Fig. 46A, B, C). Focusing the attention on cells at the leading front, RAB5A WT-expressing cells showed EEA-1 positive enlarged endosomes accumulated at the leading front, resulting from the RAB5A-induced fusion of early endosomes (Fig. 46D), and smaller focal adhesions compared to the control. This latter observation suggests that the enlarged and persistent protrusions brought about by RAB5A are accompanied by smaller FAs that resemble focal contacts. Whether such alteration in FAs size is a consequence or a cause of altered protrusion dynamics remains to be further explored.

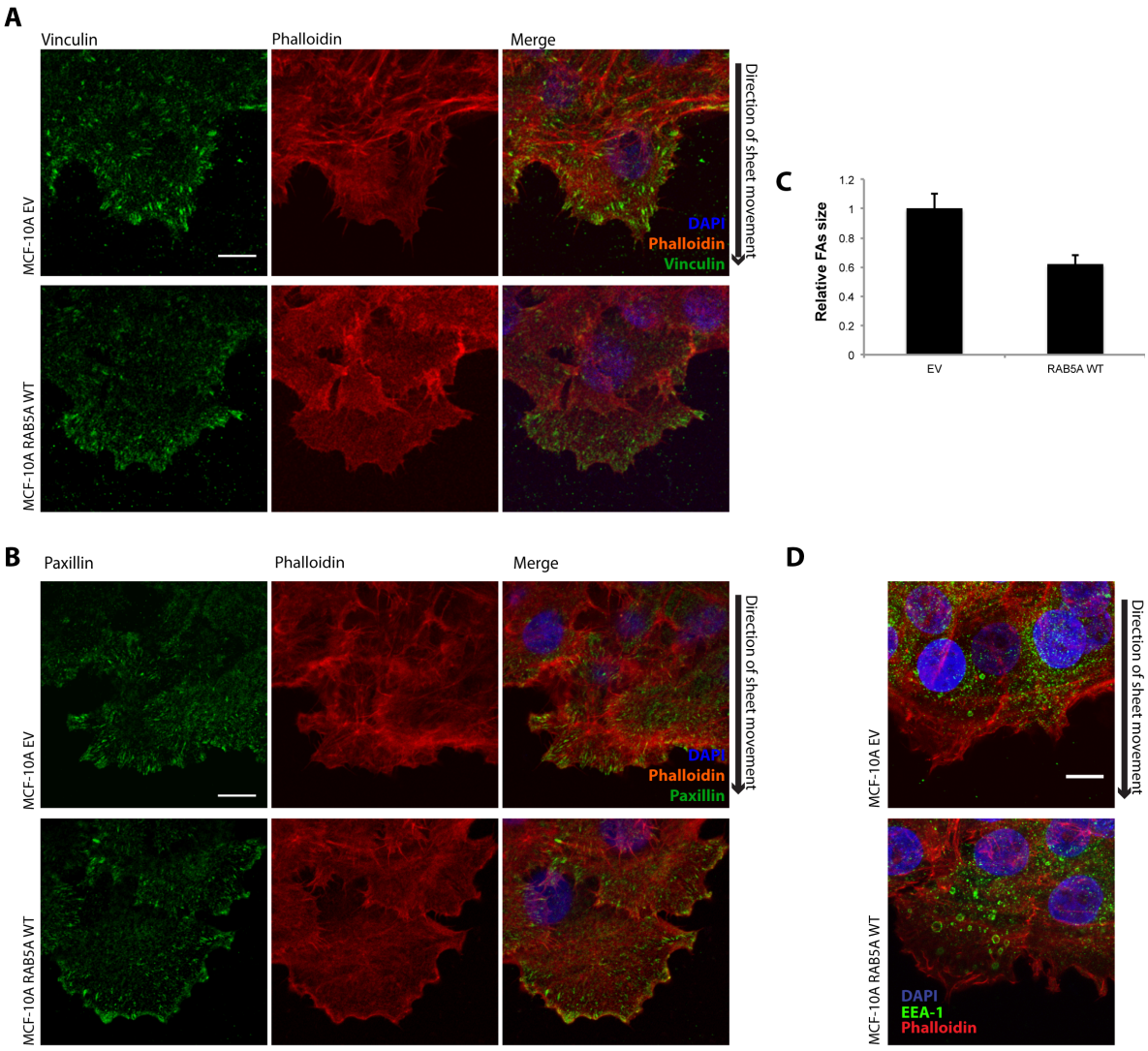

Figure 46. RAB5A expressing cells at the leading front show smaller focal adhesions and enlarged endosomes.

MCF-10A cells were grown as monolayer and scratched with a pipette tip. Samples were fixed in 4% paraformaldehyde and stained with specific antibody combinations: **(A)** DAPI for nuclei (blue), vinculin for focal adhesions (green) and TRITC-phalloidin for actin (red); **(B)** DAPI (blue), paxillin for focal adhesions (green) and TRITC-phalloidin (red) and analyzed by confocal microscopy. (**C**) Quantification of focal adhesions size was performed by ImageJ software plugin and it is shown as relative focal adhesions size referred to control cells. (**D**) Staining with DAPI for nuclei (blue), EEA-1 for early endosomes (green) and TRITC-phalloidin for actin (red) revealed enlarged endosomes in migratory protrusion of RAB5A WT-expressing cells. Representative confocal fluorescence images and merged signals are shown (Scale bar, 10 μm).

Generation and characterization of stable inducible MCF-10.DCIS.com cell lines expressing RAB5A WT or RAB5AS34N.

Our findings indicate that RAB5A specifically alters collective locomotory behavior of normal mammary human cells. Given the potential pro-tumorigenic role of RAB5A, we next tested whether the increase collective locomotory activity could also be observed in the tumorigenic variant of MCF10A cells.

MCF-10.DCIS.com cells, a well-characterized H-Ras transformed cell line (Miller, Santner et al. 2000), expressing ectopic RAB5A WT or RAB5AS34N were generated and characterized with the same strategy described for the generation of inducible MCF-10A cells: both the efficiency of the inducible system (Fig. 47A), and the expected alteration of the endosomal compartment induced by manipulation of RAB5A (Fig. 47B) were confirmed.

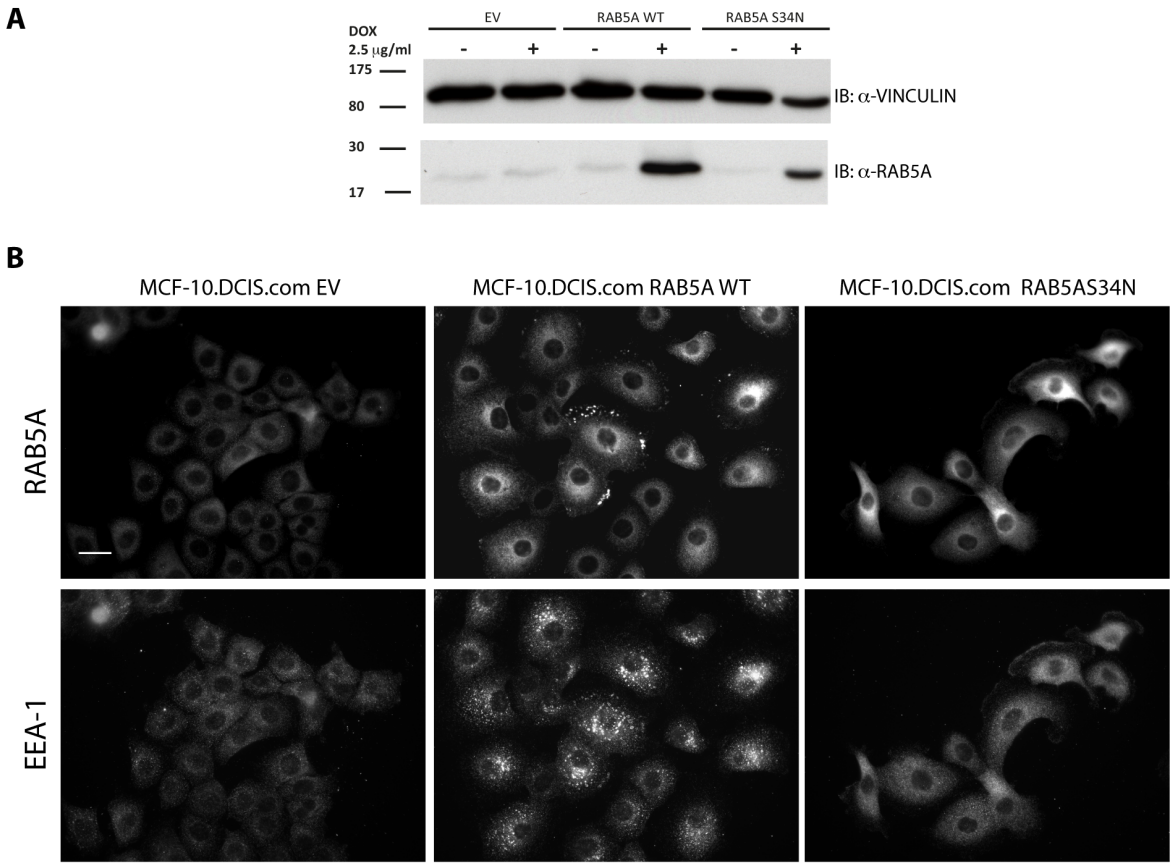

Figure 47. RAB5A WT or RAB5AS34N expression in MCF-10.DCIS.com alters the endosomal compartment.

(**A**) 30 μg of protein lysates of the indicated cell lines were loaded on a 15% polyacrylamide gel. Nitrocellulose membrane was blot by rabbit polyclonal anti-human RAB5A antibody or mouse monoclonal anti-human vinculin antibody, as loading control. (**B**) Cells were seeded on coverslips and induced 72h by 2.5 μg/ml doxycycline, fixed in 4% paraformaldehyde and stained as indicated, to be analyzed by wide field microscopy. Representative images are shown. Scale bar, 20 μm.

RAB5A promotes collective cell locomotion in MCF-10.DCIS.com cells.

RAB5A role in collective cell locomotion was further confirmed performing a wound healing assay on this oncogene-transformed cell line, MCF-10.DCIS.com. Control and RAB5A WT-expressing cells were seeded as monolayer and scratched by a pipette tip. Cell migration of doxycycline-induced cells was monitored overtime by time-lapse microscopy (Fig.48A and Movie 6).

MCF-10.DCIS.com cells showed an evident increase in wound front speed when RAB5A expression was induced (Fig. 48B).

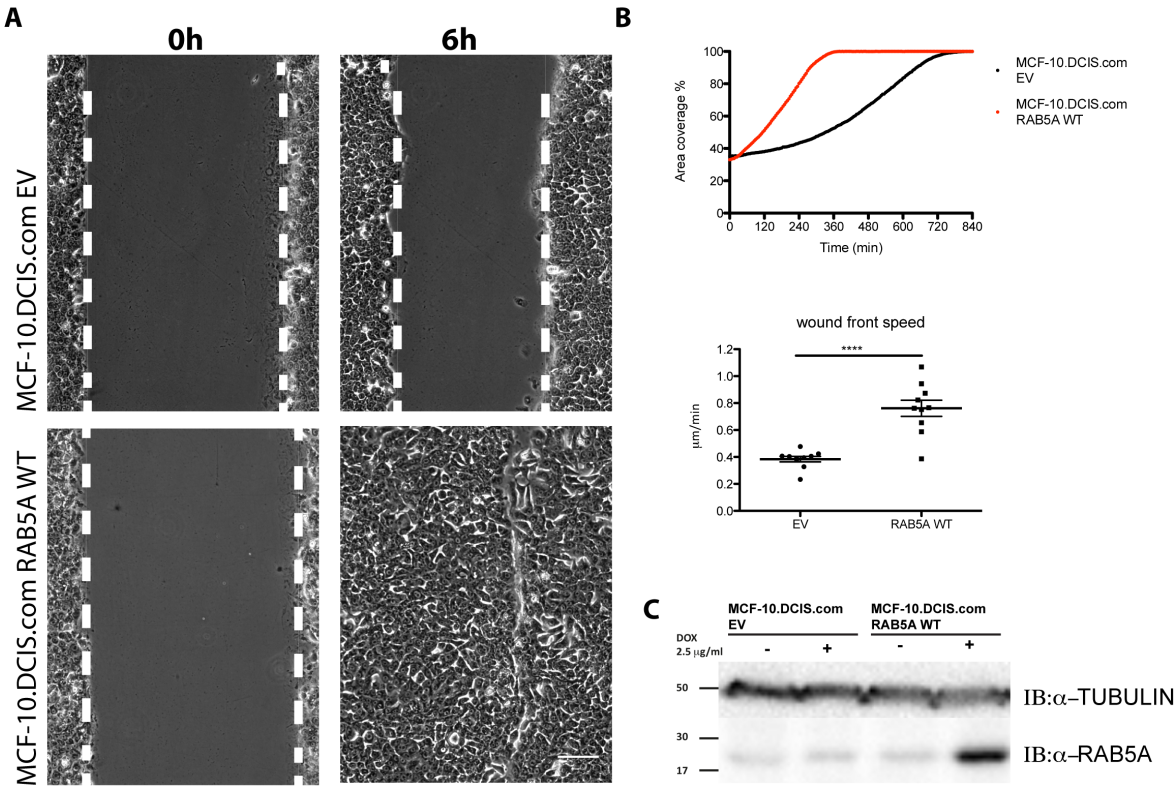

Figure 48. RAB5A expression enhances collective cell migration in the oncogene-transformed cell line MCF-10.DCIS.com.

(A) MCF-10.DCIS EV or RAB5A WT cells were seed as monolayer and analyzed for migration by wound healing assay. Images were recorded every 5 minutes using a 10x objective; scale bar, 100 μm. Representative images acquired just after the scratch (0 hour) and at 6 hours from the incision are shown. Dashed line represents the wound edge. **(B)** Wound closure speed was measured by MatLab software, calculating the percentage of area coverage overtime. Mean wound front speed is represented for each condition. 10 movies were analyzed for each condition and the experiment was repeated 3 times. **(C)** RAB5A expression was detected by Western Blotting. 70 μg of lysates of MCF-10.DCIS.com EV or RAB5A WT cells treated as indicated were loaded on a 15% polyacrylamide gel. Nitrocellulose membrane was blot by mouse monoclonal anti-tubulin and rabbit polyclonal anti-human RAB5A antibody. Tubulin was used as loading control.

CIV analysis showed an improvement in cell coordination in RAB5A WT-expressing cells (Fig. 49 and Movie 7). Data collected in the tumorigenic variant of MCF-10A cells further confirm the role of RAB5A in promoting collective cell migration.

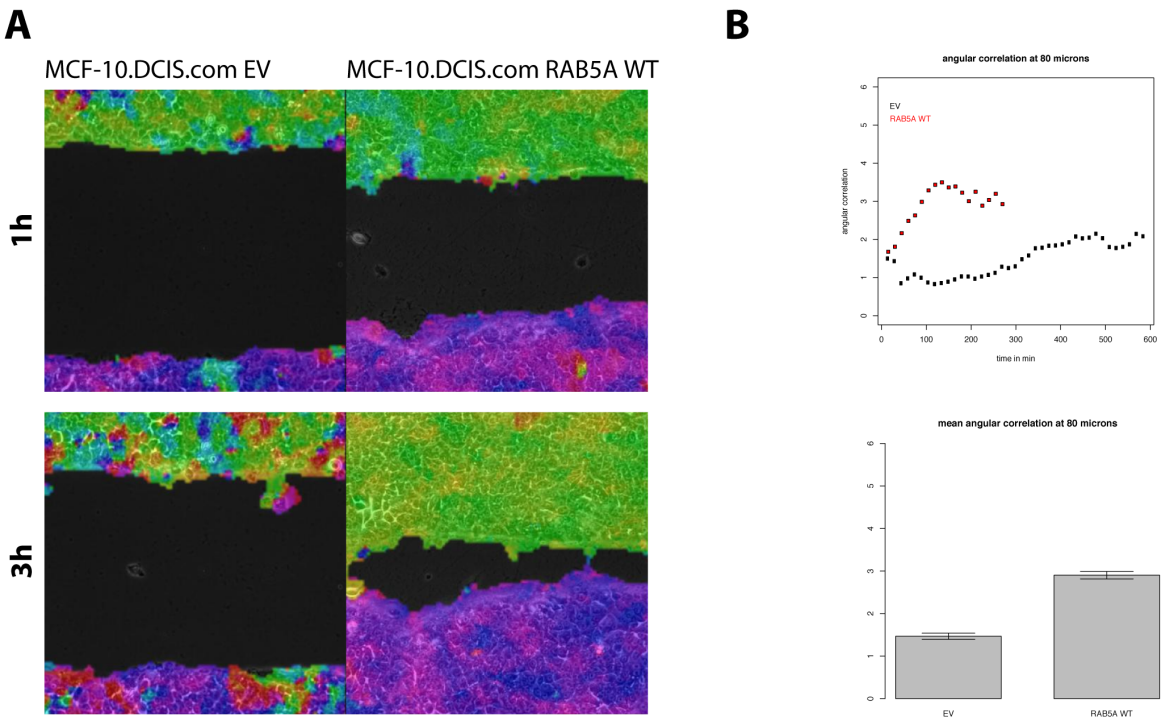

Figure 49. RAB5A promotes cell coordination of collectively migrating MCF-10.DCIS.com cells.
(A) Cell coherence of the indicated cell lines are shown after 1 hours or 3 hours after the wound. **(B)** Angular correlation of the cell movements for MCF-10.DCIS.com EV or RAB5A WT cells overtime (bin distance: 80μm) and mean angular correlation during entire wound closure are shown.

Perturbation of RAB5A function impairs the formation of HGF-induced invasive outgrowth.

We collected evidences showing the role of RAB5A in promoting collective migration and tumor progression. To further confirm the involvement of RAB5A in the process of tumorigenesis, we investigated its effect on cancer invasion. Thus, MCF-10.DCIS EV and RAB5AS34N cells were seed into a Matrigel/Collagen matrix to monitor their invasive potential, when treated with HGF (Edakuni, Sasatomi et al. 2001; Jedeszko, Victor et al. 2009). We observed that DCIS EV cells developed invasive outgrowth when stimulated with HGF, on the contrary RAB5AS34N expressing cells did not form any protrusion, even in the presence of HGF (Fig. 50). Thus, perturbation of RAB5A function

in an oncogene-transformed context impairs the formation of HGF-induced invasive outgrowth, corroborating the hypothesized pro-metastatic role of RAB5A.

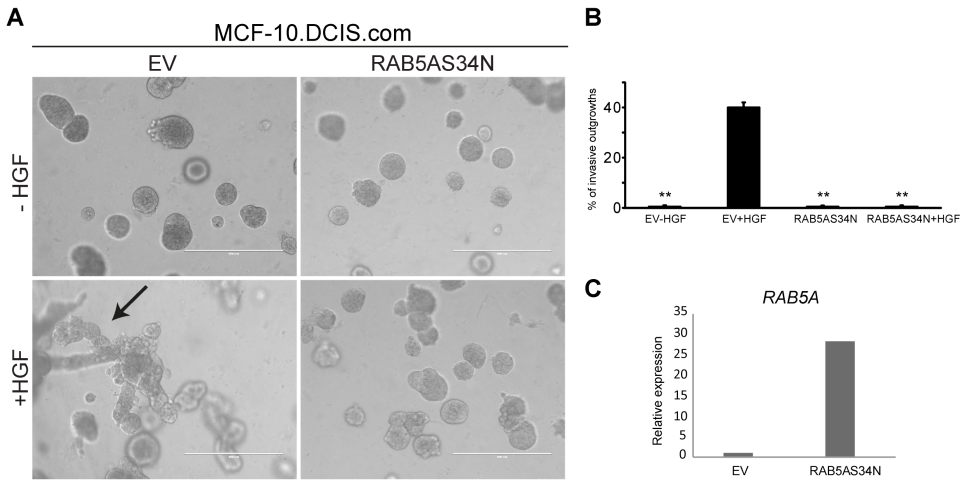

Figure 50. RAB5AS34N expression in an oncogene-transformed cell line impairs the invasive growth induced by HGF.

(A) Equal number of MCF-10.DCIS EV or RAB5AS34N cells was cultured in 3D into Matrigel/Collagen matrix, in un-induced condition. After 4 days, cells were doxycycline-induced in the absence or presence of HGF. RAB5AS34N expression inhibits the formation of invasive protrusion in MCF-10.DCIS stimulated by HGF. Representative phase contrast images, after 4 days from the induction, are shown. The arrow indicates a typical invasive protrusion (Scale bar, 400 μm). **(B)** Quantification of the percentage of invasive outgrowths in each condition. Data are mean -/+ SEM. **(C)** Induced *RAB5A* mRNA levels in MCF-10.DCIS EV or RAB5A S34N cells, as detected by qRT-PCR are shown. *GAPDH* was used as normalizer and EV cells as calibrator. The experiment was performed 3 times with 2 technical replicates.

DISCUSSION

1. RAB5A as a tumor suppressor.

A critical hallmark of tumorigenesis is the acquisition of growth factor independent proliferation. In the first part of the present study, we provide evidences that alteration of endocytosis brought about by interference with RAB5A activity induces an EGF independent growth phenotype in MCF-10A cells. We have identified Amphiregulin (AREG), a ligand of the EGFR, as the specific secreted factor that is responsible for proliferation in the absence of EGF. Both the conditioned media collected from RAB5AS34N-cells and recombinant AREG are capable of sustaining EGF-independent proliferation of parental MCF-10A cells. Conversely, the phenotype is reverted by the concomitant presence of a specific AREG-neutralizing antibody. Finally, the EGF-independent growth achieved by the autocrine or paracrine production and secretion of AREG is dependent on the ability of this ligand to bind and activate the EGF receptor.

In physiological conditions, Estrogen and Progesteron Receptor dependent up-regulation of AREG has been shown to be an indispensable mechanism to sustain pubertal development of mouse mammary gland (Martinez-Lacaci, Saceda et al. 1995; Ciarloni, Mallepell et al. 2007; McBryan, Howlin et al. 2008; Aupperlee, Leipprandt et al. 2013). In pathological conditions, AREG expression appears, instead, to be modulated by other signaling pathways, including those triggered by hypoxia (Bordoli, Stiehl et al. 2011; Stiehl, Bordoli et al. 2012) and by the YAP/TAZ signaling cascades (Zhang, Ji et al. 2009;

Yang, Morrison et al. 2012). Quantitative RT-PCR analysis, however, indicated that the expression of RAB5AS34N does not significantly alter the expression of genes that are typically regulated by these signaling cascades, suggesting that AREG expression is controlled by RAB5A through alternative mechanisms, the molecular nature of which remains to be further investigated.

In *Drosophila,* genetic interference with RAB5 expression or activity has been shown to induce a hyper-proliferative phenotype, suggesting that RAB5 may possess tumor suppressor-like function during normal, physiological developmental processes of certain epithelial tissues (Lu and Bilder 2005; Robinson and Moberg 2011). Mechanistically, alterations of the endocytic machinery by RAB5 null mutant or RAB5 deletion was shown to cause abnormal membrane trafficking and aberrant delivery of various proteins, such as the polarity determinant Crumbs and the Notch signaling receptor. Both eye discs and follicle cells homozygous for RAB5-null deletion mutant showed multilayered, overproliferative phenotypes and accumulation of these proteins at the cell surface, induced by a failure in endosomal entry and progression to lysosomal degradation (Lu and Bilder 2005). Furthermore, loss-of-function mutants of RAB5 and other key endocytic mediators have also been reported to promote the deregulated activation of Yorkie (YAP/TAZ in vertebrates) and JNK (Rodahl, Haglund et al. 2009; Robinson and Moberg 2011). The former co-transcriptional regulator, in particular, has emerged as a factor of paramount importance in the control of tissue homeostasis, sitting at the core of complex networks of biochemical as well as mechanical cues that all converge in fine tuning its activity, ultimately dictating the proliferation, survival and differentiation fate of cells (Yu and Guan 2013). JNK pathway, among the numerous functions it controls, may, instead, act upstream of Yorkie in cells with alteration in polarity (Robinson and Moberg 2011), suggesting that the apparently disparate, biological functions of RAB5 may all be rationalized within its originally described role as a central hub in membrane

trafficking. Indeed, the acquisition and maintenance of polarity, which represents a defining distinguishing property of epithelial cells and tissues, strictly depends on the appropriate delivery through membrane trafficking of various polarity determinants (Lu and Bilder 2005). Hence, disruption of endocytic networks may not only causes loss of epithelial tissues identity, but may also liberate proliferation-inhibitory signals and trigger differentiation programs, that can culminate into a change of identity, typified by the epithelial to mesenchymal transition process. Whether the functional consequences linked to RAB5 perturbation are also relevant in the development of mammalian cancer remain, however, entirely unclear. In particular, no evidence has so far been provided of loss of RAB5 neither in mammalian tumors nor in experimental models of tumor cell lines in culture. Notwithstanding this, a conserved potential onco-suppressive role of RAB5 remains plausible.

Our finding, in mammary epithelial cells are somewhat in line with the notion outlined above and lend support to the general paradigm that disruption of RAB5 in the context of a normal epithelium may lead to the acquisition of growth factor-independent proliferation, a distinctive hallmark of tumor development. Whether similar altered auto/paracrine secretion of growth factor may also account for the hyper-proliferation that accompanies RAB5 disruption in *Drosophila* or in murine liver remain to be firmly assessed. Conversely, while in epithelial tissues of the fly *Drosophila* and in murine hepatocytes disruption of RAB5 and some of its interaction partners is sufficient to cause loss of polarity and to promote neoplastic-like hyper-proliferation, this does not appear to be the case in mammary epithelial MCF-10A cells in culture, suggesting that additional events may be required to unleash a full pro-proliferating role caused by the disruption of endocytic pathways.

2. RAB5A as a tumor promoter.

In normal mammary epithelia, we also observed that RAB5A expression induces S-phase entry delay, impairing MCF-10A cells proliferation when cells are grown in 2D. Intriguingly, this phenotype was accompanied by a robust increase in ERK phosphorylation that was observed both in 2D and in 3D cultures, pointing to the involvement of MAPK/ERK1-2 pathway in the regulation of G1/S transition. Previously, numerous studies have reported of a possible correlation between cell cycle defects and ERK signaling pathway (Chambard, Lefloch et al. 2007). In normal conditions, the proper attachment to ECM is fundamental for cell survival, while loss of contact with the substrate induces a BH3-only protein Bim-mediated cell death by anoikis. The direct association of Bim expression with ERK inhibition identifies this signaling pathway as a key regulator of Bim and may account for the observation that these proteins might be hijacked under pathological conditions. Indeed, the expression of certain oncogenes confers anoikis resistance by inducing cell cycle arrest in G1/S stage and sustaining ERK activation. This mechanism protects metastatic cells from anoikis and promotes cell survival outside of the natural microenvironment. More specifically, G1/S-arrested, MCF-10A cells either growing attached to a substrate or kept in suspension were shown to display elevated ERK phosphorylation, which, in turn, is essential to bypass anoikis through the suppression of the pro-apoptotic Bim (Collins, Reginato et al. 2005). This mechanism may also provide protection from apoptosis induced in response to growth factor withdrawal and ERK–mediated modulation of Bim is predicted to be essential for cells that must detach from their basement membrane in order to undergo normal morphogenetic processes, such as during the formation of a lactating gland (Debnath, Mills et al. 2002). Notably, the same mechanism may also be harnessed by certain oncogenes, first and foremost activated ErbB-2 (Reginato, Mills et al. 2005), which, in addition to deregulating cell proliferation, also disrupt cell polarity and ECM attachments virtually

generating pro-apoptotic conditions that must be overcome in order to achieve full transformation.

In this context, RAB5A elevation of ERK pathway may be a way to enable cells to resist anoikis occurring during the morphogenesis of mammary cells in 3D. However, we found that: i) the morphogenetic program of 3D acini is not drastically perturbed by elevation of RAB5A expression as RAB5A-expressing cells invariably form hollow acini. ii) Furthermore, the few but large RAB5A-MCF10A acini show no alteration in the extent of activated caspase-3 positivity, indicating that anoikis induced by ECM detachment of the inner subpopulation of cells is not impaired. Clearly, further investigations are required to identify the molecular mechanisms through which RAB5A modulates ERK phosphorylation and assess its biological consequences. This latter point is particularly challenging considering the complexity and the temporal dynamics of the regulation of this signaling cascade. Indeed, both the frequency and intensity of ERK activity pulses have been recently shown to be important for the regulation of cell responses to proliferation signals, such as EGF. For example, dynamic analysis of ERK activity in MCF-10A cells revealed that the decision to enter S-phase in response to EGF addition is determined by the duration, rather than by the frequency of its activity pulses (Albeck, Mills et al. 2013). In keeping with these considerations, RAB5A may play a role in the control of cell cycle progression by impinging on ERK signaling dynamics or affecting cell sensitivity to EGF, as it has already been shown for other oncogenes. How these signaling are temporally associated and the molecular mechanisms underlying this correlation remain to be further investigated.

Intriguingly, our data show that RAB5A expression in 2D cultures delays S-phase entry and cell proliferation, while in 3D assay on reconstituted basement membrane RAB5A reduces the number of acini, but the one that grow are significantly larger, reflecting the fact that they do not cease proliferation, which is invariably observed in acini

that have completed the morphogenetic differentiation program. One possibility to rationalize these finding is to hypothesize that RAB5A expression elicits a cell stress response possibly accompanied by alterations in DNA repair processes, somewhat resembling the situation observed with certain oncogenes, which, when introduced into primary cells, can cause proliferation-dependent stress that ultimately results in accumulation of DNA damage and a blockade in cell expansion (Hills and Diffley 2014). It is interesting in this respect that gene profiling obtained by Affymetrix analysis of RAB5A expressing cells revealed that genes involved in DNA repair are significantly down-regulated, suggesting that RAB5A may impair such a process and thereby lead to the accumulation of DNA damage that in most cases would be so detrimental to cause the elimination of the damaged cell, accounting for the reduced acini number. In few instances, however, RAB5A-dependent DNA repair-defective cells may acquire mutation that are positively selected enabling the emergence of single clones of cells that have lost their differentiation-induced proliferation arrest and keep on growing to a large size.

Alternatively, once acini has reached a minimal size and cell-number, the cell cycle defect may be overcome in a cell-context dependent manner, with a mechanism similar to the one observed in cell-competition. In *Drosophila*, for example, it has been shown that mutant cells are viable and continue to proliferate only when surrounded by other mutant cells, conversely they are eliminated by cell-competition if surrounded by normal cells (Ballesteros-Arias, Saavedra et al. 2014). The importance of the interface between normal and mutant cells has been also confirmed in mammalian: RAS^{V12}-transformed MDCK cells when surrounded by normal cells are apically extruded or invade the basal matrix through the formation of basal protrusion (Hogan, Dupre-Crochet et al. 2009). Thus, cell displacement has been proposed as a protective mechanism to remove aberrant cells from the epithelia, likely hijacked by cancer cells to facilitate clonal outgrowth (Leung 2013). RAB5A cells, in this framework, would need a minimal number of surrounding cells to overcome the cell cycle defect and proliferate. Our data on re-initiation of proliferation in

post-mitotic acini when RAB5A is expressed, further suggest that the cell-context may play an important role in the control of RAB5A-dependent cells proliferation. In post-mitotic acini, the critical cell number composing the structure may be sufficient to sustain cell proliferation and induce the repopulation of the lumen that we observed in RAB5A expressing acini.

In summary, on one hand we observed that RAB5A expression delays S-phase entry and impairs MCF-10A cells proliferation. On the other hand, in oncogenic mammalian epithelial tumor cell line and tissues, elevated expression of RAB5A is frequently selected to confer pro-invasive and metastatic propensity (Lanzetti, Palamidessi et al. 2004; Palamidessi, Frittoli et al. 2008; Torres and Stupack 2011). Consistently with this latter notion, elevated RAB5A expression levels have been correlated to the increased migration potential of hepatocellular carcinomas (Fukui, Tamura et al. 2007), with ovarian cancer (Zhao, Liu et al. 2010), and with the metastatic potential of lung (Yu, Hui-chen et al. 1999), breast (Yang, Yin et al. 2011; Frittoli, Palamidessi et al. 2014) and gastric cancer (Li, Feng et al. 1999).

This apparently contradictory observation may be reconciled within the notion that frequently oncogene expression in normal tissues elicits a stress response that leads to growth proliferation delays and in some occasion to apoptosis or senescence. Conversely, in a pre-tumorigenic setting the same oncogene promotes neoplastic transformation. Whether this notion is applicable also to RAB5A remains to be established and the dissection of the molecular mechanisms through which this master regulator of endocytosis act may provide clues to answer this *conundrum*.

3. RAB5A plays an essential role in cell locomotion and tumor progression.

Besides the well-characterized role of RAB5A in endosome biogenesis and trafficking (Zerial and McBride 2001), a substantial amount of evidences identified additional non-canonical functions of this small GTPase. Most notably, RAB5 has been implicated in controlling cell migration where it may act at different steps of the process, including the control of FAs turnover (Mendoza, Ortiz et al. 2013; Palamidessi, Frittoli et al. 2013), integrins trafficking (Frittoli, Palamidessi et al. 2014) and actin cytoskeleton remodeling. In this latter case, our lab showed that RAB5A is necessary for spatial restriction of RAC1 activity to the plasma membrane, in turn required for the acquisition of polarized membrane protrusion driving cell locomotion (Palamidessi, Frittoli et al. 2008). Consistent with its central role in directed cell migration, RAB5A has also been shown to promote cancer progression, by enhancing the dissemination potential of different cancer types, including stomach (Li, Feng et al. 1999), lung (Yu, Hui-chen et al. 1999) and breast cancer (Yang, Yin et al. 2011; Frittoli, Palamidessi et al. 2014).

3.1. Epithelial collective locomotion is sensitive to RAB5A expression levels.

Cancer progression and metastatization is accompanied and promoted by the acquisition of cell locomotory ability that allows tumor cells to detach from the primary tumoral mass and disseminate into the organism toward a distant cancer *niche*, where proliferation is reinstalled leading to the generation of metastatic clones (Hanahan and Weinberg 2000). Indeed, cancer metastatization is best described as a multistep process or metastatic cascade, that include rupture of the confining basement membrane, interstitial stromal, local dissemination, intravasation and survival into the lymphatic and blood

stream, extravasation and growth at distant "niche" site (Hanahan and Weinberg 2000). In carcinoma arising from epithelial tissues, the first of these steps leading to metastasis involves local invasiveness and the acquisition of major phenotypic changes in a subset of cells within the primary tumor.

The morphological phenotypic changes that enable a sessile epithelial cell to become highly migratory can be extremely diverse and flexible. Indeed, multiple migratory modes are utilized by tumors cells. These modes are: i) morphologically distinct, ii) bio-mechanically diverse and iii) respond and are driven by a variety of different biochemical circuitries. The ability of tumors cells to plastically change their mode of cell locomotion enables them to adapt to diverse micro-environmental conditions and represent a prerequisite for stromal dissemination. Among the diverse migratory strategies, cell motility has been classified into two main broad categories: i) in collective locomotion, cancer cells migrate as whole "clumps" of tightly adherent cells advancing as an invasive front; alternatively, ii) individual cells can detach from the tumor mass and adventure into the surrounding tissues adopting either a round, blebbing, amoeboid motility mode strictly dependent on actomyosin contractility; or a mesenchymal migration associated with RAC1-dependent, F-actin-rich protrusions that drive directional motility coupled with pericellular proteolysis (Friedl 2004).

Our lab previously showed that RAB5A, in a variety of tumor, promotes a single cell program of proteolytically-dependent mesenchymal dissemination. Indeed, RAB5A expressing cells, autonomously, rewire trafficking circuitries so as to couple RAC1-dependent cell protrusion and pericellular proteolysis, which is essential in the initial phase of cancer dissemination (Palamidessi, Frittoli et al. 2008). However, epithelial tumors cells frequently utilized a collective mode of cell migration where cell-to-cell junctions are not broken apart, but rather exploited to coordinate the motility of entire sheets of isolated clusters that in highly coordinated manner invade the space of least resistance, enabling effective local invasion into surrounding tumor stroma. Based on this latter observation,

we initially elected to investigate whether deregulation of RAB5A in normal mammary epithelial cells would impact, not only on single cell locomotion, but also on collective motility mode. The normal genetic background of MCF10A cells allowed us to exclude any potential confounding contribution of other transforming hits and to further explore fundamental mechanisms that RAB5A may control in physiological setting that may be deranged in late tumorigenic stages.

The data we collected in this study, using a non-transformed model system, are consistent with the notion that RAB5A plays an important function in promoting cancer progression. We showed that RAB5A elevated expression increases significantly cell speed, directionality and coordination of un-wounded sheets of motile cells. When a directional cue is generated by scratching a wound into an otherwise intact monolayer, RAB5A elevation is sufficient to promote a highly coordinated mode of collective locomotion; whereas, migration is impaired by genetic ablation of the three isoforms of RAB5. These results support a role of RAB5A in promoting collective epithelial locomotion, and provide a rational base to account for the potential pro-metastatic role exerted by this GTPase in human invasive breast cancer.

Importantly, sparsely seeded cells migrating randomly in the absence of any chemoattractant did not show alterations in single cell velocity when RAB5A expression was induced by doxycycline. The observation that RAB5A elevation is sufficient to promote an increase in the wound front speed without significantly affecting single cell velocity, provides a solid evidence that RAB5A plays a specific role in collective cell migration, presumably affecting molecular and cellular mechanisms that become absolutely needed during collective motility, i.e. under conditions where cells are mechanically linked through cell–to-cell junctions, and thus their movement must be coordinated for efficient locomotion to occur.

Interestingly, an improvement in collective cell locomotion has also been observed in RAB5A expressing MCF-10A cells when plated as a confluent but un-wounded monolayer

that display a cell movement reminiscent of viscous flow in fluid dynamics. This latter observation suggests a role of RAB5A in collective locomotion, even in the absence of a directional cue that promotes cell polarization and directional motility.

3.2. RAB5A promotes cell coordination of the migrating epithelial sheet possibly by cadherin-mediated transmission of migratory cues.

In vivo, when epithelial sheets are damaged, surrounding cell layers migrate to heal the open space and restore the initial integrity of a tissue, furthermore the coordinated movement of the epithelium plays vital roles in embryogenesis and development of complex tissues. Our observations and previous studies demonstrate the importance of coordination of cells migrating as collective entities to ensure their efficient movement. CIV analysis on wound healing assay performed on MCF-10A cells, confirmed this hypothesis. We showed that RAB5A enhances cell velocity by promoting coherent and directional cell migration within the epithelial sheet. On the contrary, RAB5 ablation dramatically impairs sheet cohesiveness and the correspondent mean angular correlation value, a measurement of how coordinated is the cell motility, is decreased, compared with control cells.

Epithelial sheets are kept together by cell-to-cell adhesion structures. A key component of epithelial junctions in vertebrates is the transmembrane protein E-cadherin, which defines the so-called adherens junctions (AJs). Within these structures, E-cadherin connects adjacent cells through homophilic interactions and associates with the cytoskeleton through a multiprotein complex (Reynolds and Roczniak-Ferguson 2004; Cavey and Lecuit 2009). AJs are not immobile, unflexible, glue-like structures; rather these junctions undergo rapid assembly and disassembly to enable epithelial tissue morphogenesis and rearrangement, as well as the acquisition of cell motility during epithelial-to-mesenchymal

transition (Cavey and Lecuit 2009; Thiery, Acloque et al. 2009). Previous works demonstrated the importance of AJs in promoting the coordination and the transmission of motogenic stimuli during collective cell locomotion (Vitorino and Meyer 2008; Ng, Besser et al. 2012). The importance of adhesive junctions in the mechanical cohesion of a monolayer has been documented not only in epithelial tissues but also in the endothelium, and the observation that the excessive reinforcement of cell-to-cell adhesions slows down wound closure underlines the importance of a tight control of AJs dynamics (Vitorino, Hammer et al. 2011). For example, fine modulation of the mechanical adhesion between endothelial cells, mediated by the member of cadherin family Vascular Endothelial Cadherin (VEC) was shown to be critical to sustain collective locomotion together with the integrity of the monolayer (Franco, Milde et al. 2013).

Recent studies on the motility of endothelial and kidney epithelial cells within monolayers have highlighted the existence of peculiar motility behavior, in which groups of cells, that compose the intact monolayer, move together as a unique element that exhibit a globally undirected but locally correlated streaming behavior. In collective cell streaming indeed, transient cell chains move together as groups with similar direction and persistence, and their velocity correlations extend over several cells that compose the whole cell sheet (Vitorino and Meyer 2008; Szabo, Unnep et al. 2010). Interestingly, while the direction of cell migration in the monolayer was random because of the absence of any directional cue, the relative movement between neighboring cells was highly coordinated. Such a collective flow within a monolayer has been shown to be strongly influenced by cell-to-cell adhesions and the dynamics of the cohesive interactions between cells are reminiscent of the typical reversible interactions connecting individual molecules in fluids. Hence, the coordinated flow-like movement detected in MCF-10A cells monolayers can be understood and interpreted using fluids dynamics, which is influenced primarily by the dynamics and coordination of AJs. Consistently, perturbation of adherens junctions by calcium chelation or genetic ablation of cadherins reduce spontaneous collective cell

streaming in confluent epithelial monolayer and compromised cell adhesions lead to cells movements in opposite and anisotropic directions (Czirok, Varga et al. 2013).

Based on these considerations, we hypothesized that RAB5A-dependent increase in coordination of collective cell migration would be provided by increased mechanical connection mediated by adherens junctions. Of note, E-cadherin expression levels were not affected by RAB5A expression. Thus, we investigated whether RAB5A may affect the cellular distribution of E-cadherin in MCF-10A monolayers. Strikingly, RAB5A-positive confluent cells showed a narrower localization of E-cadherin along the periphery of the cell. In addition, AJs were linear and significantly straighter than in control cells, which display a more diffuse and a wavy distribution of E-cadherin along cell contacts. These results suggest that RAB5A increases adhesion strength, and thus improves cell cohesion, accounting, at least in part, both for the enhanced collective locomotion of wounded monolayer as well as for the increased cell streaming in intact epithelial sheets.

The involvement of endocytosis in the control of E-cadherin turnover and adherens junction dynamic is well established. For example, we recently identified CDC42-Interacting Protein 4 (CIP4), a member of the FCH-Bin-Amphiphy-sin-Rvs (F-BAR)-domain containing proteins family, as a key endocytic molecule in the control of E-cadherin trafficking and junctional stability (Rolland, Marighetti et al. 2014). Although E-cadherin levels were not significantly different between control and CIP4-depleted cells, the amount of junctional E-cadherin was controlled by CIP4 through endocytosis and SRC-dependent regulation of junctional tension, an important event to promote adherens junctions disassembly and subsequent endocytosis of E-cadherin. At the cell biological level, removal of CIP4, but not of the other two family members FBP17 (formin-binding protein 17) and TOCA1 (transducer of CDC42-dependent actin assembly 1), induces compaction of MCF10A breast epithelial cells into tightly organized cell clusters. We further demonstrated that EGF-induced cell scattering, motility and invasion are impaired

in CIP4-depleted cells. These latter cell biological phenotypes are mirrored by the finding that CIP4 elevated expression is selected in ErbB-2 positive breast cancer tumors and correlates with increased distant metastasis (Rolland, Marighetti et al. 2014).

The maintenance of junctional stability is a dynamic process ensured by a fine balance of internalization and recycling of adherens junction components, a mechanism already described in *Drosophila* where RAB11 recycling is required for epithelial integrity (Roeth, Sawyer et al. 2009). Multiple routes mediate E-cadherin entry into cells, including clathrin-dependent and clathrin-independent pathways, both converging to early endosome compartment, as confirmed by EEA-1 and RAB5 enrichment in E-cadherin-positive vesicles after internalization through one of these pathways. From this sorting station, E-cadherin may than be directed either to lysosomal degradation, or recycled back to the plasma membrane *via* RAB11-dependent recycling (Paterson, Parton et al. 2003; de Beco, Gueudry et al. 2009).

The role of CIP4 in promoting E-cadherin trafficking and actomyosin contractility, thus sustaining cell migration and invasion, points to the fundamental function of endocytosis in intracellular trafficking and signaling. Additionally, the observations that RAB5A, similarly to CIP4, drives tumor progression and improves collective locomotion affecting adherens junctions distribution and possibly dynamics, rise the possibility of a similar process involving RAB5A-mediated endocytosis in the control of AJ remodelling.

Despite further work is required to address the precise molecular mechanism linking RAB5A expression and E-cadherin, our current data reinforce the notion of a central role of endocytosis in the control of E-cadherin internalization and dynamics, and thus of AJs remodeling mediated by this small GTPase. Whether RAB5A-dependent circuitry that modulates epithelial cell-to-cell adhesions relies on a fast RAB4 recycling route, similarly to what we have recently shown in the case of metalloprotease MT1-MMP (Frittoli, Palamidessi et al. 2014), it is an intriguing possibility that remains to be investigated.

It is also of note that in the MCF-10.DCIS.com model system, we observed similar RAB5A-induced phenotypes as the one observed in the non-transformed cell counterpart. Indeed, collective cell migration toward the artificial gap created by scratching of the monolayer was enhanced by RAB5A expression in MCF-10.DCIS.com. This phenotype was also mirrored by an increase in the wound front speed and cell-cell coordination, similarly to what we observe in normal MCF-10A cells. Although further investigation would be needed to better characterize how RAB5A modulates E-cadherin pattern and localization, this latter finding suggest that RAB5A promotes collective cell migration and cell coordination also in a relevant breast cancer model system. Of note, MCF-10.DCIS.com cells are known to display an altered distribution of junctional E-cadherin with respect to MCF-10A cells that renders these cells more prone to undergo individual cell locomotion (Li and Mattingly 2008). Whether the up-regulation of RAB5A is sufficient to switch the mode of cell motility from individual to collective remains to be assessed and represents an interesting aspect to be investigated in future studies.

3.3. RAB5A sustains cell migration by modulating the protrusive activity of cells at the leading front.

Cell migration requires a tight coordination of protrusive and adhesive activities to generate forward migration of the epithelial sheet.

Actin polymerization drives the formation of thin sheet-like protrusion, the lamellipodium, by pushing the plasma membrane forward. This protrusive and migratory structure, observed in many different cell types, depends primarily on the small GTPase RAC1 and RAC1-mediated actin remodeling. We previously showed that RAB5A-dependent endocytic/exocytic cycles (EECs) of RAC1 is key to promote the spatial restriction of RAC1 signaling, leading to the formation of polarized migratory protrusions (Palamidessi,

Frittoli et al. 2008). More specifically, we showed that upon addition of motogenic stimuli, RAB5A mediates the concomitant recruitment of RAC1 and its GEF Tiam1 into early endosomes; endosomally- located, active RAC1 is then recycled back to the plasma membrane *via* an Arf6 mediated recycling route (Palamidessi, Frittoli et al. 2008). Thus, an endo/exocytic RAB5A-dependent flux of RAC1 appears to be required to spatially confine its activity and the acquisition of polarized actin remodeling, needed for directional migration. Hence, we tested whether RAB5A mediates RAC1 activation also in the context of epithelial collective locomotion. The majority of wound edge cells of collective migratory MCF-10A cell sheets showed a dramatic increase in protrusion area and persistence upon RAB5A expression. This suggests that cells at the leading front remodel actin and polarize the protrusive machinery along the advancing leading front, possibly in endo/exocytic and RAC1 dependent fashion. To explore this possibility, we will employ RAC1 FRET-biosensor that will allow us to obtain direct quantification of locally, activated RAC1 at the leading front.

It must be pointed out that the mechanism controlling RAC1 activation and localization in a group of collective migrating cells is likely more complex, since recent reports indicate that RAB5A/Tiam1/RAC1 is not the only circuitry responsible for RAC1 modulation. Studies performed on collective migration of border cells showed that RAB5 and RAB11 are important regulators of RAC activity and cell polarization during locomotion. In these cell system also, RAB5 is involved in RAC activation and the expression of its dominant negative form (RAB5S34N) abolished RAC-mediated protrusion formation. Conversely the small GTPase RAB11, involved in vesicles recycling, has been shown to be a key regulator of cell-cell communication critical to achieve spatiotemporal restriction of RAC activity in the entire cluster, preventing it from becoming uniformily distributed and thus inefficient for migration (Ramel, Wang et al. 2013). Similarly, in our system RAB5A may be involved in a more complex mechanism controlling RAC1 activation, thus cooperating

with other endocytic protein in the activation and localization of RAC1 in specific regions of the epithelial migrating sheet.

3.4. RAB5A expression affects cell to ECM adhesions of migrating cells at the wound edge.

Migrating cells need to establish dynamic contact with the ECM to anchor actin cytoskeleton to the substrate and exert motile forces. The main anchor structures are integrin-based focal adhesions (FAs). FAs are dynamic multiprotein assemblies that physically link the ECM with the actin cytoskeletal network of a cell protrusion, serving as a clutch that translates the pushing forces of actin polymerization into net traction forces (Nobes and Hall 1995). FAs undergo a constant turnover, particularly in migrating cells. These structures form at the leading edge of the migrating cell as focal contacts, mature and become enlarged, establishing more stable, yet dynamic attachment to the ECM. The subsequent disassembly of FAs allows detachment and forward locomotion (Ridley, Schwartz et al. 2003). Increasing evidences demonstrates the involvement of RAB5 in promoting migration of normal or transformed cells, in the latter case promoting an essential step in metastasis formation (Palamidessi, Frittoli et al. 2008; Mendoza, Ortiz et al. 2013; Palamidessi, Frittoli et al. 2013). Different groups collected evidences showing that RAB5 expression leads to an increased integrin trafficking and focal adhesion turnover (Palamidessi, Frittoli et al. 2008; Mendoza, Ortiz et al. 2013; Palamidessi, Frittoli et al. 2013). Indeed, RAB5 positive endosomes, particularly the active pool of RAB5, accumulates at the leading edge of cells undergoing directional migration [(Mendoza, Ortiz et al. 2013) and this work]. In particular, RAB5 was shown to transiently localize and associate in a complex with FAs components and to promote FAs disassembly, thereby affecting cell locomotion. FAs turnover, modulated by focal adhesion kinase (FAK) phosphorylation/dephosphorylation circuitry, was accelerated by RAB5 in migrating and

invasive cells. Hence, RAB5 is proposed as regulator of FAs disassembly thus promoting coordinated cell locomotion (Mendoza, Ortiz et al. 2013). In agreement with this notion, RN-tre, a GAP of RAB5A has been shown to be involved in FAs turnover during chemotactic cell migration. In RN-tre KO fibroblast, FAs turnover was indeed accelerated and cells were highly motile compared with controls, thus pointing to a role of RN-tre in the control of integrin endocytosis and FA stability, by turning off RAB5A (Palamidessi, Frittoli et al. 2013).

In our study, we show a reduction of FAs size in cells at the leading front of the collective migrating sheet when RAB5A is overexpressed. Vinculin and paxillin staining, typical component of FAs, evidenced smaller structures at the leading edge of RAB5A-MCF-10A cells after wounding, suggesting a faster turnover of FAs that shifts the balance between adhesion and motility toward a more motile phenotype. Although further investigation on the kinetic of FAs assembly/disassembly in our model system would be required to definitely prove the hypothesis we postulated, our observation are in agreement with previous work that demonstrate the involvement of RAB5A in FAs dynamics, through FAK activity (Mendoza, Ortiz et al. 2013) or RN-tre modulation (Palamidessi, Frittoli et al. 2013). Thus, we may hypothesize a signaling cascade where RAB5A activity is controlled by its GAP RN-tre, and sequentially controls FAK phosphorylation/dephosphorylation rate, thus promoting FAs disassembly and migration and invasiveness of cancer cells.

4. RAB5A functional perturbation abrogates the generation of invasive outgrowth in MCF-10.DCIS.com cells.

To further dissect the potential dual role of RAB5A as suppressor of tumor initiation and promoter of tumor progression, MCF-10.DCIS.com cells represent an optimal model since they allow us to recapitulate the transition from pre-invasive to invasive breast carcinoma that is frequently observed in human breast cancer (Miller, Santner et al. 2000). Three dimensional culture on reconstituted basement membrane has been used to mimic DCIS growth and progression to IDC occurring *in vivo*. Under these conditions, activation of c-Met by conditioned media from infiltrating fibroblasts secreting HGF or by recombinant HGF induces the development of invasive outhgrowth from DCIS structures (Edakuni, Sasatomi et al. 2001; Jedeszko, Victor et al. 2009). Using this model system, we show that perturbation of endocytosis by RAB5AS34N expression in MCF-10.DCIS.com cell line impairs the formation of HGF-induced invasive outgrowth, when cultured in three-dimensional reconstituted basement membrane overlay assay in agreement with clinical data that correlates RAB5A expression and metastatic potential (Frittoli, Palamidessi et al. 2014). This phenotype was also confirmed *in vivo* by subcutaneous injection of RAB5AS34N-expressing MCF-10.DCIS.com cells in immunodeficient mice; the myoepithelial organization was used as readout of cancer progression (Hu, Yao et al. 2008). One week after RAB5S34N induction, control and RAB5AS34N tumors were comparable in size and presented the typical DCIS morphology, with a core of cancer cells delimited by a smooth muscle actin (SMA)-positive myoepithelial layer. However, although MCF10.DCIS.com control lesions lost the myoepithelial layer and progressed to become invasive tumors after 3 weeks, RAB5AS34N-expressing cells maintained the typical DCIS histology and their invasiveness was significantly impaired. Furthermore, to assess whether the elevation of RAB5A expression was sufficient to promote lung dissemination, control and RAB5A

WT-expressing MCF10.DCIS.com were injected into mice tail vein and monitored for their ability to colonize the host lung. After 96 hours, the number of RAB5A-expressing MCF10.DCIS.com cells was significantly higher than that of control cells. Hence, RAB5A was sufficient to enhance the ability of these cells to extravasate and adhere to lung tissue (Frittoli, Palamidessi et al. 2014).

Collectively, *in vitro* and *in vivo* observations indicate that RAB5A promotes, at least in this model system, local and distal invasiveness of breast cancer cells, typical hallmarks of tumor aggressiveness.

Concluding remarks

Taken together, our evidences are consistent with a dual, temporally, distinct function of RAB5A in tumor development. RAB5A may act as a tumor suppressor gene, critical for the control of the morphogenetic processes and homeostasis of epithelial tissues, with a major impact on initiation of tumorigenesis in pathological conditions. On the other hand, clinical data together with *in vitro* and *in vivo* studies demonstrate that RAB5A is sufficient to promote an invasive and metastatic phenotypes relevant for cancer progression, ultimately sustaining both an individual mesenchymal mode of cell locomotion as well as enhancing coordinated collective motility, thereby impacting on the early steps of tumor dissemination.

REFERENCES

Abercrombie, M. (1961). "The bases of the locomotory behaviour of fibroblasts." Experimental cell research **Suppl 8**: 188-198.

Albeck, J. G., G. B. Mills, et al. (2013). "Frequency-modulated pulses of ERK activity transmit quantitative proliferation signals." Molecular cell **49**(2): 249-261.

Aupperlee, M. D., J. R. Leipprandt, et al. (2013). "Amphiregulin mediates progesterone-induced mammary ductal development during puberty." Breast cancer research : BCR **15**(3): R44.

Ballesteros-Arias, L., V. Saavedra, et al. (2014). "Cell competition may function either as tumour-suppressing or as tumour-stimulating factor in Drosophila." Oncogene **33**(35): 4377-4384.

Basolo, F., J. Elliott, et al. (1991). "Transformation of human breast epithelial cells by c-Ha-ras oncogene." Molecular carcinogenesis **4**(1): 25-35.

Baum, B. and M. Georgiou (2011). "Dynamics of adherens junctions in epithelial establishment, maintenance, and remodeling." J Cell Biol **192**(6): 907-917.

Behbod, F., F. S. Kittrell, et al. (2009). "An intraductal human-in-mouse transplantation model mimics the subtypes of ductal carcinoma in situ." Breast Cancer Res **11**(5): R66.

Berasain, C. and M. A. Avila (2014). "Amphiregulin." Seminars in cell & developmental biology **28**: 31-41.

Bilder, D., M. Li, et al. (2000). "Cooperative regulation of cell polarity and growth by Drosophila tumor suppressors." Science **289**(5476): 113-116.

Bissell, M. J., A. Rizki, et al. (2003). "Tissue architecture: the ultimate regulator of breast epithelial function." Current opinion in cell biology **15**(6): 753-762.

Bordoli, M. R., D. P. Stiehl, et al. (2011). "Prolyl-4-hydroxylase PHD2- and hypoxia-inducible factor 2-dependent regulation of amphiregulin contributes to breast tumorigenesis." Oncogene **30**(5): 548-560.

Britton, D. J., I. R. Hutcheson, et al. (2006). "Bidirectional cross talk between ERalpha and EGFR signalling pathways regulates tamoxifen-resistant growth." Breast cancer research and treatment **96**(2): 131-146.

Brumby, A. M. and H. E. Richardson (2003). "scribble mutants cooperate with oncogenic Ras or Notch to cause neoplastic overgrowth in Drosophila." The EMBO journal **22**(21): 5769-5779.

Bucci, C., A. Lutcke, et al. (1995). "Co-operative regulation of endocytosis by three Rab5 isoforms." FEBS Lett **366**(1): 65-71.

Busser, B., L. Sancey, et al. (2011). "The multiple roles of amphiregulin in human cancer." Biochimica et biophysica acta **1816**(2): 119-131.

Cavey, M. and T. Lecuit (2009). "Molecular bases of cell-cell junctions stability and dynamics." Cold Spring Harbor perspectives in biology **1**(5): a002998.

Chambard, J. C., R. Lefloch, et al. (2007). "ERK implication in cell cycle regulation." Biochimica et biophysica acta **1773**(8): 1299-1310.
Chatterjee, S., L. Seifried, et al. (2012). "Dysregulation of cell polarity proteins synergize with oncogenes or the microenvironment to induce invasive behavior in epithelial cells." PloS one **7**(4): e34343.
Christoforidis, S., H. M. McBride, et al. (1999). "The Rab5 effector EEA1 is a core component of endosome docking." Nature **397**(6720): 621-625.
Ciarloni, L., S. Mallepell, et al. (2007). "Amphiregulin is an essential mediator of estrogen receptor alpha function in mammary gland development." Proceedings of the National Academy of Sciences of the United States of America **104**(13): 5455-5460.
Collins, N. L., M. J. Reginato, et al. (2005). "G1/S cell cycle arrest provides anoikis resistance through Erk-mediated Bim suppression." Molecular and cellular biology **25**(12): 5282-5291.
Czirok, A., K. Varga, et al. (2013). "Collective cell streams in epithelial monolayers depend on cell adhesion." New journal of physics **15**.
de Beco, S., C. Gueudry, et al. (2009). "Endocytosis is required for E-cadherin redistribution at mature adherens junctions." Proceedings of the National Academy of Sciences of the United States of America **106**(17): 7010-7015.
Debnath, J. and J. S. Brugge (2005). "Modelling glandular epithelial cancers in three-dimensional cultures." Nature reviews. Cancer **5**(9): 675-688.
Debnath, J., K. R. Mills, et al. (2002). "The role of apoptosis in creating and maintaining luminal space within normal and oncogene-expressing mammary acini." Cell **111**(1): 29-40.
Debnath, J., S. K. Muthuswamy, et al. (2003). "Morphogenesis and oncogenesis of MCF-10A mammary epithelial acini grown in three-dimensional basement membrane cultures." Methods **30**(3): 256-268.
Deneka, M. and P. van der Sluijs (2002). "'Rab'ing up endosomal membrane transport." Nature cell biology **4**(2): E33-35.
Disanza, A., E. Frittoli, et al. (2009). "Endocytosis and spatial restriction of cell signaling." Mol Oncol **3**(4): 280-296.
Edakuni, G., E. Sasatomi, et al. (2001). "Expression of the hepatocyte growth factor/c-Met pathway is increased at the cancer front in breast carcinoma." Pathology international **51**(3): 172-178.
Egeblad, M., E. S. Nakasone, et al. (2010). "Tumors as organs: complex tissues that interface with the entire organism." Dev Cell **18**(6): 884-901.
Franco, D., F. Milde, et al. (2013). "Accelerated endothelial wound healing on microstructured substrates under flow." Biomaterials **34**(5): 1488-1497.
Friedl, P. (2004). "Prespecification and plasticity: shifting mechanisms of cell migration." Current opinion in cell biology **16**(1): 14-23.
Friedl, P. and S. Alexander (2011). "Cancer invasion and the microenvironment: plasticity and reciprocity." Cell **147**(5): 992-1009.
Friedl, P. and D. Gilmour (2009). "Collective cell migration in morphogenesis, regeneration and cancer." Nature reviews. Molecular cell biology **10**(7): 445-457.
Friedl, P. and K. Wolf (2010). "Plasticity of cell migration: a multiscale tuning model." J Cell Biol **188**(1): 11-19.
Frittoli, E., A. Palamidessi, et al. (2014). "A RAB5/RAB4 recycling circuitry induces a proteolytic invasive program and promotes tumor dissemination." The Journal of cell biology **206**(2): 307-328.
Fukui, K., S. Tamura, et al. (2007). "Expression of Rab5a in hepatocellular carcinoma: Possible involvement in epidermal growth factor signaling." Hepatology

research : the official journal of the Japan Society of Hepatology **37**(11): 957-965.
Giampieri, S., C. Manning, et al. (2009). "Localized and reversible TGFbeta signalling switches breast cancer cells from cohesive to single cell motility." Nat Cell Biol **11**(11): 1287-1296.
Giusti, C., S. Desruisseau, et al. (2003). "Transforming growth factor beta-1 and amphiregulin act in synergy to increase the production of urokinase-type plasminogen activator in transformed breast epithelial cells." International journal of cancer. Journal international du cancer **105**(6): 769-778.
Hanahan, D. and R. A. Weinberg (2000). "The hallmarks of cancer." Cell **100**(1): 57-70.
Hanahan, D. and R. A. Weinberg (2011). "Hallmarks of cancer: the next generation." Cell **144**(5): 646-674.
Hegerfeldt, Y., M. Tusch, et al. (2002). "Collective cell movement in primary melanoma explants: plasticity of cell-cell interaction, beta1-integrin function, and migration strategies." Cancer research **62**(7): 2125-2130.
Herr, R., F. U. Wohrle, et al. (2011). "A novel MCF-10A line allowing conditional oncogene expression in 3D culture." Cell communication and signaling : CCS **9**: 17.
Hills, S. A. and J. F. Diffley (2014). "DNA replication and oncogene-induced replicative stress." Current biology : CB **24**(10): R435-444.
Hogan, C., S. Dupre-Crochet, et al. (2009). "Characterization of the interface between normal and transformed epithelial cells." Nat Cell Biol **11**(4): 460-467.
Holbro, T. and N. E. Hynes (2004). "ErbB receptors: directing key signaling networks throughout life." Annu Rev Pharmacol Toxicol **44**: 195-217.
Hu, M., J. Yao, et al. (2008). "Regulation of in situ to invasive breast carcinoma transition." Cancer cell **13**(5): 394-406.
Itoh, T., K. S. Erdmann, et al. (2005). "Dynamin and the actin cytoskeleton cooperatively regulate plasma membrane invagination by BAR and F-BAR proteins." Dev Cell **9**(6): 791-804.
Jedeszko, C., B. C. Victor, et al. (2009). "Fibroblast hepatocyte growth factor promotes invasion of human mammary ductal carcinoma in situ." Cancer research **69**(23): 9148-9155.
Kessenbrock, K., V. Plaks, et al. (2010). "Matrix metalloproteinases: regulators of the tumor microenvironment." Cell **141**(1): 52-67.
Klijn, J. G., P. M. Berns, et al. (1992). "The clinical significance of epidermal growth factor receptor (EGF-R) in human breast cancer: a review on 5232 patients." Endocrine reviews **13**(1): 3-17.
Lammermann, T. and M. Sixt (2009). "Mechanical modes of 'amoeboid' cell migration." Curr Opin Cell Biol **21**(5): 636-644.
Lanzetti, L., A. Palamidessi, et al. (2004). "Rab5 is a signalling GTPase involved in actin remodelling by receptor tyrosine kinases." Nature **429**(6989): 309-314.
Leung, C. T. (2013). "Epithelial cell translocation: new insights into mechanisms of tumor initiation." BioEssays : news and reviews in molecular, cellular and developmental biology **35**(2): 80-83.
Leung, C. T. and J. S. Brugge (2012). "Outgrowth of single oncogene-expressing cells from suppressive epithelial environments." Nature **482**(7385): 410-413.
Li, B. and S. X. Sun (2014). "Coherent motions in confluent cell monolayer sheets." Biophysical journal **107**(7): 1532-1541.
Li, G. and P. D. Stahl (1993). "Structure-function relationship of the small GTPase rab5." J Biol Chem **268**(32): 24475-24480.

Li, M. L., J. Aggeler, et al. (1987). "Influence of a reconstituted basement membrane and its components on casein gene expression and secretion in mouse mammary epithelial cells." Proceedings of the National Academy of Sciences of the United States of America **84**(1): 136-140.

Li, Q. and R. R. Mattingly (2008). "Restoration of E-cadherin cell-cell junctions requires both expression of E-cadherin and suppression of ERK MAP kinase activation in Ras-transformed breast epithelial cells." Neoplasia **10**(12): 1444-1458.

Li, Y., H. Feng, et al. (1999). "[RAB5A, a gene possibly related to metastasis of human carcinoma of the lung and stomach]." Zhonghua zhong liu za zhi [Chinese journal of oncology] **21**(3): 178-181.

Liang, C. C., A. Y. Park, et al. (2007). "In vitro scratch assay: a convenient and inexpensive method for analysis of cell migration in vitro." Nature protocols **2**(2): 329-333.

Linardou, H., I. J. Dahabreh, et al. (2009). "Somatic EGFR mutations and efficacy of tyrosine kinase inhibitors in NSCLC." Nature reviews. Clinical oncology **6**(6): 352-366.

Liu, S. S., X. M. Chen, et al. (2011). "Knockdown of Rab5a expression decreases cancer cell motility and invasion through integrin-mediated signaling pathway." Journal of biomedical science **18**: 58.

Lu, H. and D. Bilder (2005). "Endocytic control of epithelial polarity and proliferation in Drosophila." Nature cell biology **7**(12): 1232-1239.

Ma, L., C. Gauville, et al. (1999). "Antisense expression for amphiregulin suppresses tumorigenicity of a transformed human breast epithelial cell line." Oncogene **18**(47): 6513-6520.

Madsen, C. D. and E. Sahai (2010). "Cancer dissemination--lessons from leukocytes." Dev Cell **19**(1): 13-26.

Martinez-Lacaci, I., M. Saceda, et al. (1995). "Estrogen and phorbol esters regulate amphiregulin expression by two separate mechanisms in human breast cancer cell lines." Endocrinology **136**(9): 3983-3992.

Maruthamuthu, V., Y. Aratyn-Schaus, et al. (2010). "Conserved F-actin dynamics and force transmission at cell adhesions." Current opinion in cell biology **22**(5): 583-588.

Mayor, S. and R. E. Pagano (2007). "Pathways of clathrin-independent endocytosis." Nat Rev Mol Cell Biol **8**(8): 603-612.

McBryan, J., J. Howlin, et al. (2008). "Amphiregulin: role in mammary gland development and breast cancer." Journal of mammary gland biology and neoplasia **13**(2): 159-169.

Mendoza, P., R. Ortiz, et al. (2013). "Rab5 activation promotes focal adhesion disassembly, migration and invasiveness in tumor cells." Journal of cell science **126**(Pt 17): 3835-3847.

Milde, F., D. Franco, et al. (2012). "Cell Image Velocimetry (CIV): boosting the automated quantification of cell migration in wound healing assays." Integrative biology : quantitative biosciences from nano to macro **4**(11): 1437-1447.

Miller, F. R., S. J. Santner, et al. (2000). "MCF10DCIS.com xenograft model of human comedo ductal carcinoma in situ." Journal of the National Cancer Institute **92**(14): 1185-1186.

Miller, F. R., H. D. Soule, et al. (1993). "Xenograft model of progressive human proliferative breast disease." Journal of the National Cancer Institute **85**(21): 1725-1732.

Morrison, H. A., H. Dionne, et al. (2008). "Regulation of early endosomal entry by the Drosophila tumor suppressors Rabenosyn and Vps45." Molecular biology of the cell **19**(10): 4167-4176.

Mosesson, Y., G. B. Mills, et al. (2008). "Derailed endocytosis: an emerging feature of cancer." Nat Rev Cancer **8**(11): 835-850.

Mosmann, T. (1983). "Rapid colorimetric assay for cellular growth and survival: application to proliferation and cytotoxicity assays." Journal of immunological methods **65**(1-2): 55-63.

Mottola, G., A. K. Classen, et al. (2010). "A novel function for the Rab5 effector Rabenosyn-5 in planar cell polarity." Development **137**(14): 2353-2364.

Muthuswamy, S. K., D. Li, et al. (2001). "ErbB2, but not ErbB1, reinitiates proliferation and induces luminal repopulation in epithelial acini." Nat Cell Biol **3**(9): 785-792.

Ng, M. R., A. Besser, et al. (2012). "Substrate stiffness regulates cadherin-dependent collective migration through myosin-II contractility." The Journal of cell biology **199**(3): 545-563.

Niessen, C. M. (2007). "Tight junctions/adherens junctions: basic structure and function." The Journal of investigative dermatology **127**(11): 2525-2532.

Nobes, C. D. and A. Hall (1995). "Rho, rac, and cdc42 GTPases regulate the assembly of multimolecular focal complexes associated with actin stress fibers, lamellipodia, and filopodia." Cell **81**(1): 53-62.

Nobes, C. D. and A. Hall (1999). "Rho GTPases control polarity, protrusion, and adhesion during cell movement." J Cell Biol **144**(6): 1235-1244.

Onodera, Y., J. M. Nam, et al. (2012). "Rab5c promotes AMAP1-PRKD2 complex formation to enhance beta1 integrin recycling in EGF-induced cancer invasion." The Journal of cell biology **197**(7): 983-996.

Pagliarini, R. A. and T. Xu (2003). "A genetic screen in Drosophila for metastatic behavior." Science **302**(5648): 1227-1231.

Palamidessi, A., E. Frittoli, et al. (2013). "The GTPase-activating protein RN-tre controls focal adhesion turnover and cell migration." Current biology : CB **23**(23): 2355-2364.

Palamidessi, A., E. Frittoli, et al. (2008). "Endocytic trafficking of Rac is required for the spatial restriction of signaling in cell migration." Cell **134**(1): 135-147.

Partanen, J. I., A. I. Nieminen, et al. (2007). "Suppression of oncogenic properties of c-Myc by LKB1-controlled epithelial organization." Proceedings of the National Academy of Sciences of the United States of America **104**(37): 14694-14699.

Partanen, J. I., T. A. Tervonen, et al. (2012). "Tumor suppressor function of Liver kinase B1 (Lkb1) is linked to regulation of epithelial integrity." Proceedings of the National Academy of Sciences of the United States of America **109**(7): E388-397.

Paterson, A. D., R. G. Parton, et al. (2003). "Characterization of E-cadherin endocytosis in isolated MCF-7 and chinese hamster ovary cells: the initial fate of unbound E-cadherin." J Biol Chem **278**(23): 21050-21057.

Petersen, O. W., L. Ronnov-Jessen, et al. (1992). "Interaction with basement membrane serves to rapidly distinguish growth and differentiation pattern of normal and malignant human breast epithelial cells." Proceedings of the National Academy of Sciences of the United States of America **89**(19): 9064-9068.

Ramel, D., X. Wang, et al. (2013). "Rab11 regulates cell-cell communication during collective cell movements." Nature cell biology **15**(3): 317-324.

Reginato, M. J., K. R. Mills, et al. (2005). "Bim regulation of lumen formation in cultured mammary epithelial acini is targeted by oncogenes." Molecular and cellular biology **25**(11): 4591-4601.
Reynolds, A. B. and A. Roczniak-Ferguson (2004). "Emerging roles for p120-catenin in cell adhesion and cancer." Oncogene **23**(48): 7947-7956.
Ridley, A. J., H. F. Paterson, et al. (1992). "The small GTP-binding protein rac regulates growth factor-induced membrane ruffling." Cell **70**(3): 401-410.
Ridley, A. J., M. A. Schwartz, et al. (2003). "Cell migration: integrating signals from front to back." Science **302**(5651): 1704-1709.
Roberts, M., S. Barry, et al. (2001). "PDGF-regulated rab4-dependent recycling of alphavbeta3 integrin from early endosomes is necessary for cell adhesion and spreading." Curr Biol **11**(18): 1392-1402.
Roberts, M. S., A. J. Woods, et al. (2003). "ERK1 associates with alpha(v)beta 3 integrin and regulates cell spreading on vitronectin." The Journal of biological chemistry **278**(3): 1975-1985.
Robinson, B. S. and K. H. Moberg (2011). "Drosophila endocytic neoplastic tumor suppressor genes regulate Sav/Wts/Hpo signaling and the c-Jun N-terminal kinase pathway." Cell cycle **10**(23): 4110-4118.
Rodahl, L. M., K. Haglund, et al. (2009). "Disruption of Vps4 and JNK function in Drosophila causes tumour growth." PloS one **4**(2): e4354.
Roeth, J. F., J. K. Sawyer, et al. (2009). "Rab11 helps maintain apical crumbs and adherens junctions in the Drosophila embryonic ectoderm." PloS one **4**(10): e7634.
Rolland, Y., P. Marighetti, et al. (2014). "The CDC42-Interacting Protein 4 Controls Epithelial Cell Cohesion and Tumor Dissemination." Developmental cell **30**(5): 553-568.
Russo, J., L. Tait, et al. (1991). "Morphological expression of cell transformation induced by c-Ha-ras oncogene in human breast epithelial cells." Journal of cell science **99 (Pt 2)**: 453-463.
Sahai, E. and C. J. Marshall (2003). "Differing modes of tumour cell invasion have distinct requirements for Rho/ROCK signalling and extracellular proteolysis." Nat Cell Biol **5**(8): 711-719.
Sanz-Moreno, V., G. Gadea, et al. (2008). "Rac activation and inactivation control plasticity of tumor cell movement." Cell **135**(3): 510-523.
Scaltriti, M. and J. Baselga (2006). "The epidermal growth factor receptor pathway: a model for targeted therapy." Clinical cancer research : an official journal of the American Association for Cancer Research **12**(18): 5268-5272.
Scholzen, T. and J. Gerdes (2000). "The Ki-67 protein: from the known and the unknown." Journal of cellular physiology **182**(3): 311-322.
Scita, G. and P. P. Di Fiore (2010). "The endocytic matrix." Nature **463**(7280): 464-473.
Shaw, K. R., C. N. Wrobel, et al. (2004). "Use of three-dimensional basement membrane cultures to model oncogene-induced changes in mammary epithelial morphogenesis." Journal of mammary gland biology and neoplasia **9**(4): 297-310.
Shoyab, M., V. L. McDonald, et al. (1988). "Amphiregulin: a bifunctional growth-modulating glycoprotein produced by the phorbol 12-myristate 13-acetate-treated human breast adenocarcinoma cell line MCF-7." Proceedings of the National Academy of Sciences of the United States of America **85**(17): 6528-6532.
Sigismund, S., S. Confalonieri, et al. (2012). "Endocytosis and signaling: cell logistics shape the eukaryotic cell plan." Physiological reviews **92**(1): 273-366.

Sigismund, S., T. Woelk, et al. (2005). "Clathrin-independent endocytosis of ubiquitinated cargos." Proc Natl Acad Sci U S A **102**(8): 2760-2765.
Simonsen, A., R. Lippe, et al. (1998). "EEA1 links PI(3)K function to Rab5 regulation of endosome fusion." Nature **394**(6692): 494-498.
Simpson, D. R., M. Yu, et al. (2011). "Epithelial cell organization suppresses Myc function by attenuating Myc expression." Cancer research **71**(11): 3822-3830.
Simpson, K. J., L. M. Selfors, et al. (2008). "Identification of genes that regulate epithelial cell migration using an siRNA screening approach." Nature cell biology **10**(9): 1027-1038.
Slamon, D. J., G. M. Clark, et al. (1987). "Human breast cancer: correlation of relapse and survival with amplification of the HER-2/neu oncogene." Science **235**(4785): 177-182.
Slamon, D. J., W. Godolphin, et al. (1989). "Studies of the HER-2/neu proto-oncogene in human breast and ovarian cancer." Science **244**(4905): 707-712.
Small, J. V., T. Stradal, et al. (2002). "The lamellipodium: where motility begins." Trends in cell biology **12**(3): 112-120.
Sorkin, A. and M. von Zastrow (2009). "Endocytosis and signaling: intertwining molecular networks." Nat Rev Mol Cell Biol **In press**.
Soule, H. D., T. M. Maloney, et al. (1990). "Isolation and characterization of a spontaneously immortalized human breast epithelial cell line, MCF-10." Cancer research **50**(18): 6075-6086.
Spancake, K. M., C. B. Anderson, et al. (1999). "E7-transduced human breast epithelial cells show partial differentiation in three-dimensional culture." Cancer research **59**(24): 6042-6045.
Stenmark, H. (2009). "Rab GTPases as coordinators of vesicle traffic." Nature reviews. Molecular cell biology **10**(8): 513-525.
Stenmark, H. and V. M. Olkkonen (2001). "The Rab GTPase family." Genome biology **2**(5): REVIEWS3007.
Stenmark, H., R. G. Parton, et al. (1994). "Inhibition of rab5 GTPase activity stimulates membrane fusion in endocytosis." The EMBO journal **13**(6): 1287-1296.
Stenmark, H., G. Vitale, et al. (1995). "Rabaptin-5 is a direct effector of the small GTPase Rab5 in endocytic membrane fusion." Cell **83**(3): 423-432.
Sternlicht, M. D., S. W. Sunnarborg, et al. (2005). "Mammary ductal morphogenesis requires paracrine activation of stromal EGFR via ADAM17-dependent shedding of epithelial amphiregulin." Development **132**(17): 3923-3933.
Stiehl, D. P., M. R. Bordoli, et al. (2012). "Non-canonical HIF-2alpha function drives autonomous breast cancer cell growth via an AREG-EGFR/ErbB4 autocrine loop." Oncogene **31**(18): 2283-2297.
Szabo, A., R. Unnep, et al. (2010). "Collective cell motion in endothelial monolayers." Physical biology **7**(4): 046007.
Takino, K., S. Ohsawa, et al. (2014). "Loss of Rab5 drives non-autonomous cell proliferation through TNF and Ras signaling in Drosophila." Developmental biology **395**(1): 19-28.
Teddy, J. M. and P. M. Kulesa (2004). "In vivo evidence for short- and long-range cell communication in cranial neural crest cells." Development **131**(24): 6141-6151.
Theveneau, E. and R. Mayor (2013). "Collective cell migration of epithelial and mesenchymal cells." Cellular and molecular life sciences : CMLS.
Thiery, J. P., H. Acloque, et al. (2009). "Epithelial-mesenchymal transitions in development and disease." Cell **139**(5): 871-890.

Thomas, C. and D. Strutt (2014). "Rabaptin-5 and Rabex-5 are neoplastic tumour suppressor genes that interact to modulate Rab5 dynamics in Drosophila melanogaster." Developmental biology **385**(1): 107-121.

Torres, V. A., A. Mielgo, et al. (2010). "Rab5 mediates caspase-8-promoted cell motility and metastasis." Molecular biology of the cell **21**(2): 369-376.

Torres, V. A. and D. G. Stupack (2011). "Rab5 in the regulation of cell motility and invasion." Current protein & peptide science **12**(1): 43-51.

Vaccari, T. and D. Bilder (2005). "The Drosophila tumor suppressor vps25 prevents nonautonomous overproliferation by regulating notch trafficking." Developmental cell **9**(5): 687-698.

Vitale, G., V. Rybin, et al. (1998). "Distinct Rab-binding domains mediate the interaction of Rabaptin-5 with GTP-bound Rab4 and Rab5." Embo J **17**(7): 1941-1951.

Vitorino, P., M. Hammer, et al. (2011). "A steering model of endothelial sheet migration recapitulates monolayer integrity and directed collective migration." Molecular and cellular biology **31**(2): 342-350.

Vitorino, P. and T. Meyer (2008). "Modular control of endothelial sheet migration." Genes & development **22**(23): 3268-3281.

Wang, Y., O. Roche, et al. (2009). "Regulation of endocytosis via the oxygen-sensing pathway." Nat Med **15**(3): 319-324.

Weaver, V. M., A. R. Howlett, et al. (1995). "The development of a functionally relevant cell culture model of progressive human breast cancer." Seminars in cancer biology **6**(3): 175-184.

Willmarth, N. E. and S. P. Ethier (2006). "Autocrine and juxtacrine effects of amphiregulin on the proliferative, invasive, and migratory properties of normal and neoplastic human mammary epithelial cells." The Journal of biological chemistry **281**(49): 37728-37737.

Wodarz, A. (2000). "Tumor suppressors: linking cell polarity and growth control." Current biology : CB **10**(17): R624-626.

Wolf, K. and P. Friedl (2006). "Molecular mechanisms of cancer cell invasion and plasticity." Br J Dermatol **154 Suppl 1**: 11-15.

Wolf, K., I. Mazo, et al. (2003). "Compensation mechanism in tumor cell migration: mesenchymal-amoeboid transition after blocking of pericellular proteolysis." J Cell Biol **160**(2): 267-277.

Xiang, B. and S. K. Muthuswamy (2006). "Using three-dimensional acinar structures for molecular and cell biological assays." Methods in enzymology **406**: 692-701.

Xue, B., K. Krishnamurthy, et al. (2013). "Loss of Par3 promotes breast cancer metastasis by compromising cell-cell cohesion." Nature cell biology **15**(2): 189-200.

Yang, N., C. D. Morrison, et al. (2012). "TAZ induces growth factor-independent proliferation through activation of EGFR ligand amphiregulin." Cell cycle **11**(15): 2922-2930.

Yang, P. S., P. H. Yin, et al. (2011). "Rab5A is associated with axillary lymph node metastasis in breast cancer patients." Cancer science **102**(12): 2172-2178.

Yarar, D., C. M. Waterman-Storer, et al. (2005). "A dynamic actin cytoskeleton functions at multiple stages of clathrin-mediated endocytosis." Mol Biol Cell **16**(2): 964-975.

Yarden, Y. (2001). "The EGFR family and its ligands in human cancer. signalling mechanisms and therapeutic opportunities." European journal of cancer **37 Suppl 4**: S3-8.

Yarden, Y. and M. X. Sliwkowski (2001). "Untangling the ErbB signalling network." Nature reviews. Molecular cell biology **2**(2): 127-137.
Yonemura, S. (2011). "Cadherin-actin interactions at adherens junctions." Current opinion in cell biology **23**(5): 515-522.
Yu, F. X. and K. L. Guan (2013). "The Hippo pathway: regulators and regulations." Genes & development **27**(4): 355-371.
Yu, L., F. Hui-chen, et al. (1999). "Differential expression of RAB5A in human lung adenocarcinoma cells with different metastasis potential." Clinical & experimental metastasis **17**(3): 213-219.
Zaczek, A., B. Brandt, et al. (2005). "The diverse signaling network of EGFR, HER2, HER3 and HER4 tyrosine kinase receptors and the consequences for therapeutic approaches." Histology and histopathology **20**(3): 1005-1015.
Zeigerer, A., J. Gilleron, et al. (2012). "Rab5 is necessary for the biogenesis of the endolysosomal system in vivo." Nature **485**(7399): 465-470.
Zerial, M. and H. McBride (2001). "Rab proteins as membrane organizers." Nature reviews. Molecular cell biology **2**(2): 107-117.
Zhang, J., J. Y. Ji, et al. (2009). "YAP-dependent induction of amphiregulin identifies a non-cell-autonomous component of the Hippo pathway." Nature cell biology **11**(12): 1444-1450.
Zhao, Z., X. F. Liu, et al. (2010). "Rab5a overexpression promoting ovarian cancer cell proliferation may be associated with APPL1-related epidermal growth factor signaling pathway." Cancer science **101**(6): 1454-1462.

ACKNOWLEDGEMENTS

I thank Drs Aldo Ferrari and Martin Bergert from ETH in Zurich for CIV analysis and helpful suggestions; all the facilities at IFOM, in particular Sara Barozzi and Emanuele Martini for MatLab analysis and technical support; I also thank Fondazione Umberto Veronesi for financial support over the four years of the PhD program.

I thank my external advisor Prof. Miguel A. del Pozo from CNIC in Madrid and my internal advisor Dr. Nicolai Sidenius from IFOM in Milan, for the scientific discussions and feedbacks about my PhD project.

I would also like to thank my external examiner Dr. Anne Blangy from CRBM in Montpellier, and my internal examiner Prof. Giuliana Pelicci from IEO in Milan, for having accepted to be my examination committee.

I wish to thank Prof. Pier Paolo di Fiore from IFOM in Milan, for advices and scientific discussions that helped me in improving my research.

I would like to express my special thanks to my advisor Prof. Giorgio Scita, from IFOM in Milan, for being a great mentor for me and for all the aspiring suggestions, I would like to thank him for encouraging my research and for helping me to grow as a research scientist, his advices have been priceless.

I warmly thank all the people of Scita's group, present and past members, who supported me throughout the course of the PhD. I am thankful for the constructive criticism and scientific advices during these four years. I am sincerely grateful to them for sharing their knowledge, as well as for all the enjoyable moments in our everyday life in the lab, especially in the last months.

A big thank to all the people, colleagues and friends, that shared with me this exciting and challenging journey over the last few years.

I huge thank to my family, my biggest supporter, who has brought great joy to my life, a big thank for their love, support and understanding that helped me in completing this work.